General Disclaimer

One or more of the Following Statements may affect this Document

- This document has been reproduced from the best copy furnished by the organizational source. It is being released in the interest of making available as much information as possible.

- This document may contain data, which exceeds the sheet parameters. It was furnished in this condition by the organizational source and is the best copy available.

- This document may contain tone-on-tone or color graphs, charts and/or pictures, which have been reproduced in black and white.

- This document is paginated as submitted by the original source.

- Portions of this document are not fully legible due to the historical nature of some of the material. However, it is the best reproduction available from the original submission.

BOLT   BERANEK   AND   NEWMAN   INC

CONSULTING   ·   DEVELOPMENT   ·   RESEARCH

EVALUATION OF THE NASA AMES #1 7×10 FOOT WIND TUNNEL AS AN ACOUSTIC TEST FACILITY

John F. Wilby
Terry D. Scharton

30 June 1975

TABLE OF CONTENTS

TABLE OF CONTENTS (Con't)

SUMMARY

   Measurements have been made in the #1 7'x10' wind tunnel
at NASA Ames Research Center, with the objectives of defining
the acoustic characteristics and recommending minimum cost
treatments so that the tunnel can be converted into an acoustic
research facility. The results indicate that the noise levels
in the test section are due to (a) noise generation in the test
section, associated with the presence of solid bodies such as the
pitot tube, and (b) propagation of acoustic energy from the
fan.

   A criterion for noise levels in the test section is
recommended, based on low-noise microphone support systems
currently available. The criterion appears to be adequate
for most test programs envisaged for the tunnel. Noise control
methods required to meet the criterion include removal of hard-
ware items for the test section and diffuser, improved design
of microphone supports, and installation of acoustic treat-
ment in the settling chamber and diffuser.

   Discussion of the design of an open test section for the
7'x10' wind tunnel is contained in a separate report.

1. INTRODUCTION

The aeroacoustics program at NASA Ames Research Center
is creating a demand for facilities in which the effects of
flight speed on noise generation can be studied. As a con-
sequence, NASA Ames are considering the use of the #1 7'x10'
tunnel as an acoustic facility. Three alternative configura-
tions have been proposed for the test section. These are
hardwall, treated wall, and partially open (three sides removed).
Under Task III of Master Agreement Contract NAS2-8382, Bolt
Beranek and Newman Inc. have performed an investigation of the
acoustical characteristics of the #1 7'x10' wind tunnel and
the results of the investigation are presented in this report.

An increasing interest in the use of wind tunnels as aero-
acoustic test facilities is evident from the number of recent
studies [1-9] of tunnel characteristics. In general the
investigations have measured the acoustical properties of
a tunnel, with and without flow, in its existing configuration.
There has been little work done to modify tunnel designs so
that the test section can be used as a satisfactory acoustic
environment. The objective of the present investigation is
to recommend changes to the 7'x10' wind tunnel which would
provide an acoustic environment adequate for future test programs.
As is the case for most wind tunnels in current operation,
the 7'x10' tunnel at NASA Ames Research Center was designed
without consideration of acoustic criteria. Thus acoustic
measurements are very limited in the present configuration.

Under the present study, the acoustical characteristics
of the tunnel, with a hardwall test section, were measured
in the Ames #1 7'x10' tunnel with zero flow. Reverberation
tests were made in the test section, diffuser and settling
chamber, and acoustic propagation around the tunnel circuit
was measured using a horn driver as a noise source. The data
were supplemented with existing NASA Ames data for hardwall
and treated wall test sections for both #1 and #2 tunnels.
The results are presented in Section 3.

Noise levels in the tunnel were measured in the test
section, diffuser and setting chamber with no airflow in
order to determine ambient levels. Then, with airflow, the
noise levels were measured to determine contributions from
the fan and other noise sources. These measurements are dis-
cussed in Section 4. Acoustic characteristics of the test
chamber surrounding the test section are given in Section 5,
and acoustic criteria for the tunnel are discussed in Section 6.

Section 7 presents noise control methods designed to meet
the criterion for noise levels in the tunnel test sections. The
methods involve reducing noise generation in the test section
itself, and attenuating fan noise as it propagates around the
tunnel. Section 8 summarizes the findings of the investigation,
recommends further testing to improve the understanding of
noise generation in the test section, and recommends instrumenta-
tion for the noise research facility.

2. DESCRIPTION OF TUNNEL

The #1 7'x10' wind tunnel at the NASA Ames Research Center is one of two identical tunnels. It is a subsonic, closed circuit, tunnel with a single drive fan, and a maximum operating dynamic pressure of about 4,790 N/m² (100 lb/ft²) in the test section. A diagram of the tunnel is shown in Figure 1. The test section is about 7.6 m (25 feet) in length and the contraction ratio from settling chamber to test section is approximately 14.

The section of tunnel circuit between the fan and settling chamber is vented to atmosphere. Hence the total pressure in the tunnel is essentially atmospheric and the static pressure in the test section is below atmospheric. The test section is vented to the test chamber, so that the chamber pressure is also below atmospheric when the tunnel is operating.

Tunnel walls are constructed from steel plates except in the settling chamber where the floor is concrete and part of the wall is made from panels of corrugated transite.

Operating conditions during the acoustic investigation are shown in Figure 2. These conditions are appropriate to a tunnel with a hardwall test section and no model. Any other configuration would probably require a higher fan speed in order to achieve a given dynamic pressure or flow speed.

No aerodynamic measurements were made during the investigation, with the exception of a pitot-static tube which was used to indicate tunnel operating condition. The pitot traverse system was present at the downstream end of the test section and was retracted as far as possible, so that the horizontal airfoil was about 38 cm (15 inches) below the roof of the tunnel. The flow characteristics in the diffuser are reputed to be marginal - flow entry into the diffuser is aided by two horizontal airfoils situated at the junction between test

section and diffuser.   An indication of the flow problems in
the diffuser was encountered during the noise measurements
when strong, low frequency, fluctuations occurred in the
microphone signal from the south leg of the diffuser.

3. ACOUSTIC CHARACTERISTICS OF TUNNEL SPACE

3.1 Measurement Program

Prior to the present noise investigation of the #1 7'x10' wind tunnel, a limited amount of acoustic data was available from previous tests in the #1 and #2 tunnels. These tests were conducted by NASA Ames and other personnel [3, 4, 10, 11]. Measurements were made in the test sections of the two tunnels using impulsive and steady-state noise sources to determine reverberation times and hall radius. The hall radius for a given frequency and direction is the distance from a noise source at which the direct and reverberant sound fields have equal values of the mean square sound pressure.

During the present program, acoustic characteristics were measured in the diffuser and settling chamber as well as in the test section. Microphone locations 1-6 are identified in Figure 1. Reverberation times were measured using an impulsive noise source (pistol shot) at several locations in the tunnel. In addition, steady state noise sources were used to measure sound pressure distributions around the tunnel circuit and to obtain further data on the hall radius of the test section. The sound source was a horn driver, without the horn, in the first case and an ILG noise source for the hall radius measurements.

Microphones in the diffuser and setting chamber were B and K ½ inch microphones with nose cones. They were mounted at a height of 1.8 m (6 feet) above the tunnel floor, pointing in the upstream direction. Several microphone configurations were used in the test section but most of the data were obtained using a B and K ¼ inch microphone with nose cone. The microphone height was about 0.6 m (2 feet).

For the tunnel flow conditions, data were obtained at five
values of the test section dynamic pressure i.e. 239, 479, 958,
1915 and 3830 N/m² (5, 10, 20, 40 and 80 lb/ft²). Correspond-
ing fan speeds can be obtained from Figure 2. Typical tempera-
ture and humidity data measured in the test section are shown
in Table I. During the first five days (December 9-13) the
relative humidity remained high and fairly constant. On the
sixth test day (December 17) the humidity was lower.

3.2 Tunnel Reverberation

Reverberation times were measured at the six microphone
locations in the tunnel, with the pistol noise source approxi-
mately 0.9 m (3 feet) from the microphone. Additional measure-
ments of the reverberation in the test section were obtained
with the noise source located between the drive fan and
microphone location #4, and with the source adjacent to
microphone #6. In all cases frequency-dependent reverberation
times were obtained by replaying the recorded signal through
octave band filters.

Reverberation decay signatures measured in the diffuser
and settling chamber show a single average decay rate typical
of a diffuse sound field. Figure 3 shows example decay
signatures, for the octave band centered at 1000 Hz, measured
in the diffuser (#3) and settling chamber (#5). Reverbera-
tion times for the diffuser and settling chamber are listed in
Table II and plotted in Figure 4.

The reverberation characteristics of the test section are
more complicated than those of other regions of the tunnel.
The reverberation decay signature exhibits the two or three
stages observed in other tunnel test section studies [3-6].
Figure 5 shows typical decay signatures measured in the test
section for frequencies of 1000 and 4000 Hz. At 1000 Hz the
signature shows an initial series of several strong peaks

TABLE I

Temperature and Humidity During Tests

Date	Temperature °F	Relative Humidity %	Barometric Pressure Inch Hg.
12/9/74	53	78	30.21
12/10/74	48	82	30.31
12/12/74	61	84	30.37
Average	54	81	30.30
12/17/74	63	61·	-

TABLE II

Reverberation Times for Diffuser and Settling Chamber

Frequency (Hz)	250	500	1000	2000	4000	8000
			T_R (sec)			
Diffuser: #2	5.0	5.8	5.0	3.5	2.8	2.0
#3	7.1	6.8	5.6	5.0	3.8	2.2
Average	6.0	6.3	5.3	4.2	3.3	2.1
Settling Chamber:						
#4	6.5	6.9	7.0	6.4	4.6	2.4
#5	6.7	7.0	6.8	5.1	4.0	2.1
#6	8.4	8.2	6.4	5.5	4.0	2.5
Average	7.2	7.4	6.7	5.7	4.2	2.3

which form the first stage of the decay. These are followed
by a two stage general decay with reverberation times of 4.0
and 8.4 seconds respectively. From an analysis of the time
separation between the peaks in the first stage of the decay
pattern, the peaks can be associated with individual reflections
from the end walls of the tunnel in the diffuser and settling
chamber. Based on steady-state data, to be discussed later,
the stronger reflections probably come from the diffuser.
Gradually the reflections merge and the second stage of the
decay signature represents subsequent decay of the sound
propagating along the tunnel axis. Finally, the third stage,
with longer reverberation times, represents the slower decay
of transverse waves which do not propagate, or propagate
only slowly, along the tunnel.

At 4000 Hz the individual reflections from the diffuser
and settling chamber walls are no longer evident and the
decay signature shows only the second and third stages, with
associated reverberation times of 1.0 and 4.4 seconds
respectively.

Reverberation times measured in the test section, with
noise source in the test section, are shown in Table III and
compared with data for other regions in Figure 4. It is seen
that the test section reverberation times associated with the
third stage of the decay are similar in value to those measured
elsewhere in the tunnel. They are also similar to values
measured in the test section when the source is elsewhere
(Table III, Figure 4).

However, if the data are non-dimensionalized with respect
to an equivalent cross-sectional diameter [4]

$$d = \frac{4A}{\pi}$$ (1)

TABLE III

Reverberation Times for 7'x10' Test Section

Frequency (Hz)	250	500	1000	2000	4000	8000
	T_R (sec)					
Noise Source in Test Section:						
Decay Stage 2 Run 1	5.3	5.0	4.0	1.1	1.0	1.3
2	3.6	3.8	3.6	2.9	1.6	1.6
3	4.3	4.4	3.8	1.8	2.2	1.6
4	5.9	5.1	5.4	2.1	2.6	0.8
Average	4.8	4.6	4.2	2.0	1.9	1.3
Decay Stage 3 Run 1	–	7.0	8.4	4.4	4.4	3.2
2	–	4.4	4.6	4.2	3.0	5.4
3	–	–	5.4	4.0	3.4	3.0
4	–	8.0	10.0	4.3	4.0	2.0
Average	–	6.5	7.1	4.2	3.7	3.4
Noise Source Not in Test Section:						
Source at fan	8.5	8.0	8.5	6.2	4.0	2.2
Source at #6	6.9	6.8	6.0	5.2	4.4	1.3
Average	7.7	7.4	6.8	5.7	4.2	1.8

where A is the cross-sectional area, data for the diffuser and settling chamber collapse with test section data associated with the second stage of reverberation decay (Figure 6).

3.3 Hall Radius

The hall radius for a noise source in an enclosure is the distance from the source at which the direct and reverberant fields have equal sound pressure level. Thus, the equation for the hall radius r_H can be written as [5]

$$r_H \simeq \left[\frac{Q(S\alpha + 4mV)}{16\pi} \right]^{1/2} e^{-(r_H m/2)} \tag{2}$$

where Q is the source directivity factor, m is the air absorption factor, V is the enclosure volume and S is the surface area with mean absorption α. In practice

$$e^{-(r_H m/2)} \simeq 1,$$

and the term $(S\alpha + 4mV)$ can be replaced by the measured reverberation time

$$(S\alpha + 4mV) = \frac{55.2V}{C_o T_R} \tag{3}$$

where C_o is the speed of sound. Then

$$r_H \simeq \left[\frac{55.2 \; QV}{16\pi \; C_o T_R} \right]^{1/2} \tag{4}$$

For a given enclosure the hall radius can be determined directly with a steady-state acoustic source, or indirectly by means of equation (4) and reverberation data. Vér et al [5] have found that for wind tunnel test sections there can be large differences between direct and indirect estimates of the hall radius, with the indirect values being greater by factors of up to 2.

In the present case of the 7'x10' tunnel there is some ambiguity in the choice of volume V since there is no well-defined separation between test section and diffuser. A lower bound on the calculated hall radius can be obtained when V is given the value associated with a 7.6 m (25 feet) long test section. An upper bound has been calculated with V equal to the total volume of the southern leg of the tunnel i.e. including part of the diffuser and settling chamber. Values of hall radius calculated for the second stage reverberation times (Table III) are shown in Figure 7(a).

Direct measurement of the hall radius was made using an ILG noise source. A single microphone traverse was made along the tunnel centerline, in the downstream direction. The resulting values of hall radius lie in the lower half of the range of calculated values (Figure 7(a)), as might be expected from the results of Ver et al [5].

Comparison of the present results with data from previous investigations in the #1 and #2 7'x10' tunnels is difficult. Arndt and Boxwell [3] measure the hall radius along the centerline of an unlined test section but, except at 800 Hz, all the measuring locations appear to be in the reverberant field. Consequently, values of the hall radius cannot be determined. Data for a lined test section have been obtained by Claes [10] and Soderman [11]. In both cases a 7.6 cm (3 inch) thick layer of Scottfelt was used, but Claes covered the Scottfelt with a 0.64 cm (¼ inch) thick perforated plate. Typical results are shown in Figure 7(b) and, as expected, the radii are larger than those in Figure 7(a) for an unlined test section.

3.4 Tunnel Absorption

Estimates of the mean acoustic absorption coefficients for the tunnel can be obtained from measured reverberation times, provided that appropriate values can be determined

for the volume and surface area of the tunnel space. If $\bar{\alpha}$
is the mean absorption coefficient, including the effects of
atmospheric absorption, then, from equation (3)

$$\bar{\alpha} = \frac{0.049V}{ST_R} \quad \text{in English units}$$

$$= \frac{0.161V}{ST_R} \quad \text{in mks units}$$

$$\left.\begin{array}{c}\\\\\\\\\end{array}\right\} \quad (5)$$

If the tunnel is considered as a single unit, the total
volume is approximately 9,060 m³ (3.2 x 10⁵ ft³) and the
surface area is about 409 m² (4.4 x 10³ ft²). The resulting
values of $\bar{\alpha}$ and $S\bar{\alpha}$ are shown in Table IV. When atmospheric
absorption is taken into account, the estimated wall absorption
coefficient is 0.05. This value is consistent with absorption
coefficients for metal plates, indicating that the tunnel
can be considered as a coherent volume.

However it is convenient to consider the tunnel as
being formed of two volumes which are the diffuser and
settling chamber. These volumes are coupled by the tunnel
section containing the fan and, to a lesser degree, by
the test section. The idealized tunnel is shown in Figure 8.
Approximate volumes of the two spaces are 1.6x10³m³(5.5x10⁴ft³)
for the diffuser and 4.7x10³m³(1.67x10⁵ft³) for the settling
chamber. Corresponding estimates of the absorption $S\bar{\alpha}$ are
shown in Table IV.

The sound absorption data in Table IV can be used to
estimate sound power levels, using measured sound pressure
levels as the reference. For the reverberant field in a
large enclosure, the sound power level PWL is given by

$$\text{PWL} = \text{SPL} + 10 \log \left(\frac{S\bar{\alpha}}{4}\right) \quad \text{dB re } 10^{-12} \text{ W} \quad (6)$$

TABLE IV

Absorption in Tunnel, Diffuser and Settling Chamber

Frequency (Hz)	250	500	1000	2000	4000	8000
Total Tunnel:						
T_R (sec)	6.4	6.5	6.0	4.5	3.5	2.3
$\bar{\alpha}$	0.05	0.05	0.05	0.07	0.09	0.14
$S\bar{\alpha}$ (ft^2)	2450	2410	2610	3480	4480	6820
(m^2)	228	224	243	324	417	634
α_A	0	0	0	0.01	0.04	0.09
α	0.05	0.05	0.05	0.06	0.05	0.05
Diffuser:						
T_R (sec)	6.0	6.3	5.3	4.2	3.3	2.1
$S\bar{\alpha}$ (ft^2)	450	430	510	640	820	1280
(m^2)	41.7	39.7	47.2	59.6	75.9	119
PWL-SPL (dB)	10	10	11	12	13	15
Settling Chamber:						
T_R (sec)	7.2	7.4	6.7	5.7	4.2	2.3
$S\bar{\alpha}$ (ft^2)	1140	1110	1220	1440	1950	3560
(m^2)	106	103	113	133	181	331
PWL-SPL (dB)	14	14	15	16	17	19

where S is in m^2 and the SPL is in dB re 2×10^{-5} N/m^2.
Estimated differences between PWL and SPL in the diffuser
and settling chamber are contained in Table IV. The values
are plotted in Figure 9 for comparison with similar data
from the NASA Ames 40'x80' tunnel and the NASA Lewis 9'x15'
V/STOL wind tunnel.

Similar estimates can be made for the test section
although, as indicated earlier, the situation is complicated
by the multi-stage reverberation decay and the ambiguity
in the choice of an appropriate volume. Table V contains
values of PWL-SPL calculated for the three average rever-
beration times listed in Table III. The table also contains
estimates for two volumes, the smaller volume being the
test section alone and the larger volume including the
southern leg of the diffuser. The settling chamber was
excluded because of poor coupling from settling chamber
to test section (see section 3.5). The results show a
difference of about 10 dB between estimates based on the
two volumes.

When the estimates are plotted in Figure 9, they are
seen to lie below values in other parts of the tunnel and
in other tunnels.

It should be noted that there are alternative ways
of determining the difference between sound power level
and sound pressure level. The direct method, using a
noise source of known power level, was used to obtain
the data in Figure 9 for the NASA Lewis tunnel and performs
essentially the same averaging as is done in Table V.

3.5 Noise Source Without Flow

Acoustic losses around the tunnel were measured when
a noise source was located between the drive fan and micro-
phone #4, approximately 9.1 m (30 feet) upstream of the

TABLE V

Relationship Between Sound Power Level and Pressure Level
in Test Section (from Reverberation Data)

Frequency (Hz)	250	500	1000	2000	4000	8000
			PWL–SPL dB re 10^{-12} W			
Test Section $V = 49.6\ m^3\ (1750\ ft^3)$						
Decay Stage 2	-3.5	-3.3	-2.9	+0.3	+0.5	+2.2
Decay Stage 3	-	-4.8	-5.2	-2.9	-2.4	-2.0
Source Elsewhere	-5.6	-5.4	-5.0	-4.3	-2.9	+0.8
Average	-4.6	-4.5	-4.4	-2.3	-1.6	0.3
Test Section Plus Diffuser (South Leg) $V = 627\ m^3\ (22156\ ft^3)$						
Decay Stage 2	7.5	7.7	8.1	11.3	11.5	13.2
Decay Stage 3	-	6.2	5.8	8.1	8.7	9.0
Source Elsewhere	5.5	5.6	6.0	6.8	8.1	11.8
Average	6.5	6.5	6.6	8.7	9.4	11.3

microphone, and in the test section approximately 2.4 m
(8 feet) upstream of microphone #1. The source was an
electro-magnetic driver which was pointed in the downstream
direction. However, because the driver was not coupled
to a horn there was some acoustic energy propagated in
the upstream direction. This upstream propagation is evident
in measurements at adjacent upstream microphones.

Ambient noise levels and frequency limitations of the
driver restricted data acquisition to the frequency range
of 630-20,000 Hz. Acoustic spectra measured at the six
microphone locations in the tunnel are plotted in Figures
10 and 11.

The spatial variation of sound pressure levels around
the tunnel is shown at several frequencies in Figures 12
and 13, for the source location near to the fan and in the
test section, respectively. In each figure the upper set
of curves represent the measured sound pressure levels,
whereas the lower set of curves show sound levels normalized
with respect to tunnel cross-sectional area, using the
test section area A_t as reference. The second set of
curves represent the acoustic energy distribution around
the tunnel. The results show that the largest reduction
in energy occurs between the settling chamber and test
section. Table VI lists the energy reductions measured
between microphone locations for the two noise source
positions.

The data indicate that acoustic energy passes easily
from the test section to the lower speed sections, but it
does not pass easily from a region of large cross-sectional
area (settling chamber) to a region of small area (test
section). This result is consistent with comments by
Bies [2] regarding the acoustic characteristics of the
NASA Ames 40'x80' wind tunnel. Bies also showed that

TABLE VI

Acoustic Energy Reductions Between Microphone Locations
(No Tunnel Flow)

(a)   Source between fan and microphone #4

Microphone Location	4 —— 5 —— 6 —— 1 —— 2 —— 3				
Frequency (Hz)	Energy Reduction (dB)				
630-5000	4	0	13	0	0
5000 and above	12	2	13	3	0

(b)   Source in test section

Microphone Location	1 —— 2 —— 3 —— 4 —— 5 —— 6				
Frequency (Hz)	Energy Reduction (dB)				
630-5000	4	1	2	0	0
5000 and above	10	2	10	0	0

the acoustic field around a source in the 40'x80' tunnel fell off with distance r as r^{-2} close to the source and as r^{-1} in the reverberant field. Measurements in the 7'x10' tunnel indicate a spatial decay which is slower than r^{-1}.

No tests were performed with the noise source pointing in the upstream direction. However since there is no rapid contraction in the upstream direction, i.e. there is no counterpart of the transition from settling chamber to test section, there will probably be no large differences in energy between any two adjacent microphone locations.

4. SOUND LEVELS IN TUNNEL

4.1 Ambient Noise Levels

The #1 7'x10' wind tunnel is located close to other wind tunnels, and the NASA Ames Research Center is adjacent to Moffett Field Naval Air Station. Consequently, ambient noise levels can vary considerably from hour to hour. These ambient levels are out of the control of the operator of the 7'x10' tunnel.

During the present investigation of the 7'x10' tunnel noise, ambient noise levels were measured on several occasions. Conditions ranged from a foggy morning, when there were no tunnel or aircraft operations, to operation of the adjacent 14-foot Transonic Tunnel. Only two tunnels were operated during the period of the noise measurements. Thus it was not possible to determine the ambient noise levels associated with operation of all the wind tunnels.

The range of ambient noise levels encountered in the test section during the survey is shown by the spectra in Figure 14. Checks with a sound level meter indicated that, at frequencies above about 8000 Hz, the ambient signal levels were dictated by system electronic noise rather than by acoustic noise. The ambient noise levels show a range of up to 40 dB, depending on the operating condition of the 14-foot Transonic Tunnel.

Noise from the 2'x2' Transonic Tunnel was detected at discrete frequencies, as indicated by measurements in the settling chamber (Figure 15). Peaks were observed in the 1000 Hz and 1600 Hz one-third octave bands. Some variations in these frequencies were recorded during operation of the 2'x2' tunnel.

A comparison of ambient noise levels at measuring loca-
tions around the tunnel is shown in Figure 16. The spectra
were measured during a relatively quiet period. Highest
sound pressure levels were recorded in the test section.
A similar comparison during operation of the 14-foot Transonic
Tunnel is shown in Figure 17. In this case the sound levels
in the settling chamber, which is the tunnel region closest
to the 14-foot tunnel, are up to 5 dB higher than elsewhere.
Measurements with a sound level meter indicated that the
sound pressure levels in the settling chamber were 10 to
15 dB lower than the corresponding external levels, as shown
in Figure 18.

4.2 Noise Levels with Flow

Noise levels in the tunnel were measured at five flow
conditions corresponding to dynamic pressures (q_t) of 239, 479,
958, 1915 and 3830 N/m² (5,10,20,40 and 80 lb/ft²) in the
test section. Sound pressure spectra for the six microphone
locations (Figure 1) are presented in Figures 19-24. The
one-third octave band spectra indicate that the sound field
is composed of broadband and discrete frequency components.
The presence of tones is confirmed by narrowband analyses,
examples of which are shown in Figure 25.

Published studies of wind tunnel noise [4,5,6,9] have
shown that the spectral levels varied as the sixth power
of tunnel speed (U^6) or third power of dynamic pressure
(q^3). This is true of the present data for the 7'x10' tunnel.
Figures 26-28 contain data for microphone locations in the
test section (#1), diffuser (#3) and settling chamber (#5),
normalized on the basis of test section dynamic pressure
q_t with q_{ref} = 1197 N/m² (25 lb/ft²) as the reference value.
The spectra show good collapse except at frequencies where
discrete fequency tones are present. Noise levels in the
test section are particularly influenced by the presence

of tones or narrowband components. Bies [1] observed peaks
in the noise spectra of the 40'x80' tunnel which he was unable
to identify.

Since the microphones are immersed in the airflow, there
is a potential for flow-induced self noise on the microphones.
Such noise would be dipole in character and vary as the
third power of the local dynamic pressure q_ℓ. For the low
Mach numbers encountered in the tunnel, the local dynamic
pressure can be related to the test section dynamic pressure
by the simple approximation

$$A_t^2 q_t = A_\ell^2 q_\ell \qquad\qquad (7)$$

where A_t, A_ℓ are the tunnel cross-sectional areas in the test
section and at the microphone location. Sound pressures
normalized with respect to local dynamic pressure are compared
at different measuring locations in Figures 29 and 30 for
$q_t = 479$ N/m^2 (10 lb/ft^2) and 3830 N/m^2 (80 lb/ft^2) respectively.
The data show a wide variation in level, which indicates that,
at least for microphones #2 through #6, self noise does not
make a significant contribution to the measurements. Micro-
phone #1 requires further investigation.

In Section 3.5, propagation of acoustical energy around
the tunnel was studied using a noise source in a zero flow
condition. The data indicated that there were no large
differences in acoustical energy between adjacent measuring
locations except in the case of propagation in the downstream
direction from settling chamber to test section. If it is
assumed that the noise levels measured in the presence of
flow are generated by a localized source such as the drive
fan, the distribution of acoustical energy should be similar
to that for the zero flow case. To test this assumption,
sound pressure spectra measured at the six microphone locations

at $q_t = 479$ N/m^2 (10 lb/ft^2) and 3830 N/m^2 (80 lb/ft^2) are
compared in an un-normalized form in Figures 31 and 32.
The same data, normalized with respect to cross-sectional
area, are compared in Figures 33 and 34.

The comparison shows that spectra for measurement
locations #2-#6 show a better collapse onto a single curve
when normalized with respect to area, although the un-normalized
spectra do not show a large variation with location. Nor-
malized data for microphone #1 show little agreement with
spectra for the other locations. The results indicate
an apparent loss of acoustical energy at low frequencies
and a gain at high frequencies. An energy loss at low
frequencies is consistent with the results for the no-flow
case, particularly if the energy is propagated from fan
to test section in the flow direction. If some energy
propagates in the upstream direction, the energy loss effect
would be weaker than that indicated by the zero flow data.
Again this is consistent with the measurements since the
apparent low frequency energy loss in Figures 33 and 34
is less than that listed in Table VI between microphones
#6 and #1.

The increase in acoustic energy at high frequencies
requires further discussion, which is reserved for the follow-
ing section.

4.3 Discrete Frequency Sound in Test Section

It has been shown (Figure 25) that the acoustic field
in the test section contains several prominent discrete
frequency components. Since these occur at frequencies
well above the blade passage frequencies (see Section 4.5)
one possible source is that of vortex shedding from obstruc-
tions in the flow.

Prediction of the frequency of tones associated with
vortex shedding from a circular cylinder is well established.
The Strouhal number is defined in terms of cylinder diameter D
and flow velocity U. For Reynolds numbers (based on diameter)
in the range

$$10^3 < R_e < 10^4$$

the Strouhal number is

$$S_D = \frac{fD}{U} = 0.2 \quad . \tag{8}$$

As Reynolds number decreases below a value of 10^3, the value
of the Strouhal number decreases until no sound is produced
when $R_e < 30$. Alternatively the Strouhal number can be based
on the width h of the vortex street

$$S_h = \frac{fh}{U} = 0.281 \quad , \tag{9}$$

where the larger value occurs because the vortex street
spreads out behind the cylinder.

The case of an airfoil is more difficult because of the
uncertainty in defining the appropriate length scale. The
maximum width of the body is no longer the appropriate dimen-
sion. For example Bauer [12] shows a wide variation in
Strouhal number, $0.015 < S < 0.6$, when the thickness of
a plate or airfoil is used as the length scale. As an
alternative boundary layer thickness δ, displacement thickness
δ^* or momentum thickness θ, evaluated at the trailing edge
of the plate or airfoil, have been introduced as length
scales.

Bauer [12] defines a Strouhal number for a plate of
thickness d as

$$S_w = \frac{f(d+2\delta^*)}{U_s} = 0.20 \text{ to } 0.26 \tag{10}$$

for Reynolds number, based on distance x in flow direction, of $3 \times 10^4 \lesssim R_{e_x} \lesssim 3 \times 10^5$. In equation (10)

$$U_S = \sqrt{1 - C_p}\, U$$

where C_p is the pressure coefficient. A similar form is proposed by Hayden [13]

$$\text{i.e.} \quad S_W = \frac{f\delta_W}{U} = 0.25 \tag{11}$$

where U is the free stream velocity and δ_W is the wake thickness which can be measured, or calculated from

$$\delta_W = d_t + 2\delta^* \tag{12}$$

where d_t is the thickness of the airfoil at the trailing edge.

Hersh, Soderman and Hayden [14] define a Strouhal number based on the boundary layer thicknesses δ_u, δ_ℓ, on the upper and lower surfaces at the trailing edge.

$$S_\delta = \frac{0.6f(\delta_u + \delta_\ell)}{U} \simeq 0.281 \tag{13}$$

Finally Hanson [15] relates Strouhal number and Reynolds number for airfoils with different trailing edge shapes

$$S_\theta = 0.0728 \left[1 - \frac{1038}{R_{e_\theta}} \right] \tag{14}$$

where

$$S_\theta = \frac{f\theta}{U_s} \quad , \quad R_{e_\theta} = \frac{U_s \theta}{\nu}$$

θ is the total wake momentum thickness measured near the trailing edge and U_s is the velocity at the separation point in free streamline theory.

There were several potential generators of vortex
noise in the test section when the acoustic measurements
were being made.   They included:-

   (a)   pitot tube and support strut used to measure
         tunnel flow.   (The strut was mounted through the
         roof of the test section at a distance of 36 cm
         [14 inches] from the side wall.

   (b)   a trapeze-like traverse support system composed
         of three airfoils, one horizontal and two vertical.
         (The system was not used during the survey and
         was retracted as far as possible, such that the
         horizontal airfoil was about 38 cm [15 inches]
         from the roof of the test section.)

   (c)   two airfoils used to turn the airflow into the
         diffuser.

   (d)   support struts for the microphones, plus the
         microphone cables taped to the strut trailing
         edge.

In addition the fan blades, support struts and guide vanes,
and the turning vanes at the four corners of the tunnel
circuit may generate vortices in the low speed sections
of the tunnel.

Items (a), (b) and (d) above are symmetrical airfoils,
whereas airfoils (c) have a slight camber. Typical dimensions
are shown in Figure 35. The majority of the acoustic measure-
ments were made with the pitot tube in the "extended" position,
but some measurements were obtained when the pitot was
"retracted."

Narrowband spectra of the sound in the test section
are shown in Figure 25. Using data of this type, frequencies
of the spectral peaks have been plotted in Figure 36 with

the associated flow speed in the test section. A series
of straight-line curves have been constructed to fit some
of the data points and, assuming a Strouhal number

$$S = \frac{fd}{U} = 0.25 \quad , \tag{15}$$

associated values of d are identified on the curves.

Only one family of discrete frequency peaks was identified
positively during the measurement program. When the pitot
tube was adjusted from the "extended" to the "retracted"
position the family of tones, associated with dimension
d = 0.62 cm (0.245 inch) in Figure 36, was eliminated.
This is demonstrated by the narrow-band spectra in Figure
37, where peaks at frequencies 1600 Hz (q = 958 N/m²)
and 3200 Hz (q = 3830 N/m²) disappear when the pitot is
"retracted."

The value of d predicted in Figure 36 is very close
to the thickness of 0.64 cm (0.25 inch) of the parallel-
sided lower section of the support strut of the pitot tube.
This agreement supports the use of equation (15).

Spatial distributions of the discrete frequency peaks
around the tunnel circuit have been plotted for comparison
with acoustic distributions measured with zero flow (Figures
12 and 13). For the tones associated with the pitot tube
strut, the distribution (Figure 38(a)) is similar to that
in Figure 13 for a noise source in the test section, the
sound pressure levels at microphone #4 being 15-20 dB
lower than those in the test section. This agreement
provides validation of the method of comparison.

Using the above approach, data for the spectral peaks
associated with dimension d = 1.5 cm (0.6 inch) in Figure 36,
are plotted in Figure 38(b) and indicate that the noise source

is located in the test section. In contrast, spatial
distributions associated with dimension d = 4.0 cm (1.58 inch)
are plotted in Figure 39 and by comparison with Figure 12,
indicate that the noise source is located in the neighborhood
of the fan rather than in the test section. If this inter-
pretation is correct then the appropriate length scale will
be smaller than 4.0 cm (1.58 inch), because the velocity
at the fan is lower than the value of the test section
velocity used in Figure 36.

In the absence of reliable estimates of the wake thicknesses
for the pitot traverse and diffuser entry airfoils, it is
difficult to predict the vortex street-frequencies. However
estimates have been made for the wake of the diffuser-entry
airfoils, using simplifying assumptions. The methods assume
either (1) that the boundary layer growth is the same as
for a flat plate with zero pressure gradient and that the
trailing edge thickness is 0.48 cm (3/16 inch) or (2) that
the aerodynamic data can be scaled from that for a NACA
0012 airfoil [13] with a chord of 15.5 cm (6 inches). The
results show a wide range of wake thicknesses

(a) $\delta_w = d_t + 2\delta^*$ i.e. 0.74 cm $< \delta_w$ 0.85 cm

$\quad\quad\quad\quad\quad$ or   0.29" $< \delta_w <$ 0.33"

(b) $\delta_w = 0.6 (\delta_u + \delta_\ell)$ i.e 1.3 cm $< \delta_w$ 1.8 cm

$\quad\quad\quad\quad\quad$ or 0.51" $< \delta_w <$ 0.70"

(c) δ_w (NACA 0012)   = 2.3 cm

$\quad\quad\quad\quad\quad\quad\quad\quad$ = 0.8 inch

The range of values for a given method is associated with
the range of flow speeds encountered during the measurements.
The total range of the estimates, 0.74 cm to 2.3 cm (0.29
to 0.8 inch) encompasses the values d = 1.37, 1.55 and 1.95 cm
(.54, 0.60 and 0.77 inch) which are associated with three
curves of Figure 36. Thus there is evidence that the diffuser-
entry airfoils are contributing to the noise levels in the
test section. The same is probably true for the pitot traverse
system and for the microphone support struts.

4.4 Broadband Sound in Test Section

In an attempt to identify the source(s) of the broadband
noise measured by the microphone in the test section, several
diagnostic tests were performed. The results of these tests
will be discussed in this section. Broadband noise generated
by the fan is discussed in Section 4.5.

During the diagnostic tests, the #1 microphone was
moved to various locations in the test section, a B and K
1/4 inch microphone was used with and without a nose cone,
a BBN 15.5 cm (6 inch) long porous pipe microphone was used,
and a B and K 1/4 inch microphone was flush-mounted in the
tunnel wall.

4.4.1 Sound Level Distribution in Test Section

Six microphone locations in the test section are shown
in Figure 40. Location 1 was used during most of the measure-
ment program, and location 1A was used as a position close
to location 1 for comparative purposes such as calibration
of the porous pipe microphone. Locations 1B, 1C, 1D and 1E
were used to determine the variation of sound levels in the
test section, locations B, C and D being used when the
pitot tube was in the extended position, and locations C
and E when the pitot was retracted.

Figure 41 compares spectra measured at locations 1, 1B, 1C and 1D for test section dynamic pressures of 239 N/m² (5 lb/ft²) and 1915 N/m² (40 lb/ft²). At the lower tunnel speed the low frequency sound level changes with microphone location but there is no well defined trend. As tunnel speed increases, the data variation, as a function of microphone position, decreases and at q = 1915 N/m² (40 lb/ft²) the spectra are essentially the same at all positions. Thus for all practical purposes the measured sound levels can be considered fairly uniform in the test section.

4.4.2 Fluctuating Total Pressure

When the 1/4 inch microphone is used without a nose cone or protective grid, and is pointed in the upstream direction, it measures the fluctuating component of the total pressure. Thus the mean square pressure $\overline{p_t^2}$ is given by

$$\overline{p_t^2} \simeq (\rho U u')^2 \tag{16}$$

where U is the mean flow velocity and u' is the fluctuating component of velocity in the direction parallel to the tunnel centerline.

Figure 42 shows that removal of the nose cone produces an increase in the microphone signal. On the average, the increase is about 5 dB at frequencies in the range 100-10,000 Hz. However there are two exceptions to the general trend. At frequencies where discrete tones dominate the spectrum, the measured sound levels are the same, with or without the nose cone. In this case the acoustic pressures in the test section dominate the aerodynamic total pressure fluctuations. The second exception occurs at high frequencies, where the microphone signal is higher when the nose cone is present than when it is not.

The measured total pressure spectra can be compared
with estimated values, using existing turbulence data as
a basis. Hodder [16] has measured turbulence levels in the
#1 7'x10' tunnel test section, prior to installation of the
screens which are now present at the turning vanes in the
settling chamber. The reference indicates that the overall
turbulence intensity is 0.34% to 0.56%, with an average
value of 0.45%, when the air speed in the test section is
5.5-38.6 m/s (18-98 ft/sec). Figure 6 of the reference
presents a turbulence intensity spectrum for a constant
bandwidth of 25 Hz. This spectrum can be converted in a
one-third octave band pressure spectrum, using equation (16),
for comparison with the microphone measurements (Figure 43).

Figure 43 shows that in the mid-frequency range, 315-
3150 Hz, there is reasonably good agreement between measured
and estimated spectra. At low and high frequencies the
spectra deviate, with the calculated values being the higher.
The high frequency derivation is similar to that observed
by Nakamura et al [17,18], where the effect was found to
depend on microphone diameter. An explanation for the low
frequency deviation has not been found.

There is one other discrepancy between the estimated
and measured total pressure spectra. The assumption that
u´/U is constant and does not vary with U results in the
relationship

$$\overline{p_t^2} \propto U^4$$

In contrast the experimental data varies as U^6 rather than
U^4. Thus it is possible that the assumption of constant
u´/U is incorrect, but further turbulence measurements
are required to solve this inconsistency. However there
is sufficient agreement between the measured and calculated
levels in Figure 43 to justify application of the existing
turbulence data [16] to the case of a microphone with nose
cone.

4.4.3 Aerodynamic Noise on Microphone

A precise mathematical formulation for the aerodynamic pressure fluctuations measured by a microphone with nose cone is difficult to establish. For homogeneous turbulence, which is probably the closest representation of tunnel conditions, the static pressure fluctuations are determined by the fluctuating dynamic pressure

$$\text{i.e. } \sqrt{\overline{p_s^2}} = \frac{1}{2}\,\rho(u')^2 \tag{17}$$

However, Fuchs [19] has shown that in the case of inhomogeneous turbulence, the relationships depends on the type of flow field. Thus, for the core region of a circular jet he shows

$$\sqrt{\overline{p_s^2}} \simeq \frac{1}{2}\,\rho U u' \tag{18}$$

whereas in a plane turbulent boundary layer

$$\sqrt{\overline{p_s^2}} = \frac{1}{63}\,\rho U^{1.5}(u')^{0.5} \tag{19}$$

When equations (17)-(19) are compared with equation (16), and a turbulence intensity value $u'/U = 0.45\%$ is substituted, the possible range of overall pressure levels is found to be large. Equation (19) predicts a level 5.5 dB greater than the pressure level given by equation (16), whereas equation (18) gives a level 6 dB below that of equation (16) and equation (17) predicts a level 53 dB lower. The aerodynamic self-noise level for the B and K 1/4 inch microphone with nose cone, neglecting the influence of support struts, will lie somewhere within the above range, probably close to the lower limit set by homogeneous turbulence.

Available data on microphone self-noise is of little help
because the range of experimental data is almost as large as
that predicted above. Figure 44 compares normalized self-
noise spectra measured by Bruel and Kjaer [20,21], and by
Noiseux [22,23]. The lowest levels in the figure, reported
by Noiseux [23], were measured in a BBN wind tunnel with
tubulence intensity levels similar to those in the #1
7'x10' wind tunnel. The microphone support was carefully
designed to provide a clean aerodynamic profile. An aero-
dynamic body was fitted to the microphone preamplifier which
was attached to an aerodynamic strut. Thus, these levels
probably represent the aerodynamic noise floor which can be
achieved in the 7'x10' tunnel within the current state of
the art.

An average curve for the aerodynamic noise measured by
Noiseux [23] is compared in Figure 45 with spectra measured
in the 7'x10' test section using different microphone systems.
The levels in the 7'x10' tunnel are 10 to 30 dB higher than
those measured by Noiseux [23], but are similar to those
measured by Scharton [24] in a BBN aerodynamic test facility,
when no special precautions were taken in the design of the
microphone supports. Measured total pressure levels, discussed
in Section 4.4.2, are 20 to 35 dB higher than the levels
measured by Noiseux, which is within the wide range predicted
by equations (16)-(19).

It is interesting to note that the noise levels measured
by the 6-inch porous pipe microphone are not significantly
lower than those measured using microphones with nose cones.
Measurements by Noiseux [22] indicate that the aerodynamic
noise of a porous pipe microphone is lower than that of a
B and K microphone with nose cone. Based on data from

Reference 22, the noise spectrum for a porous pipe microphone
has been estimated for a dynamic pressure of 958 N/m^2
(20 lb/ft^2). The spectrum is shown in Figure 45 for the
case where the porous pipe is parallel to the flow direction.

4.4.4 Acoustic Radiation from Boundary Layer

The pressure fluctuations in the turbulent boundary
formed on the wall of the test section will radiate noise
into the test section. The radiation is associated with the
low wave number components of the boundary layer pressure
field but, unfortunately, little is known about these components.
Consequently, prediction of the acoustic radiation is a very
inexact procedure, with estimated levels differing by up to
40 dB, depending on assumptions made regarding the low wave
number spectrum for the boundary layer.

Fluctuating pressures measured at the wall of the test
section in the 7x10 foot tunnel are typical of those beneath a
fully developed turbulent boundary layer (Fig. 46). .Thus estimates
of the radiated sound can be based on available data for boundary
layers. Estimates of the radiated sound are found to be within
a range of 40 to 80 dB re $2x10^{-5}$ N/m^2, with the acoustic power
following a U^7 to U^8 law. Comparison with measured sound
levels in the test section shows that the measured values lie
at, or above, the upper bourd of the predictions and follow a
U^6 law. Thus it is concluded that sound radiated by the
turbulent boundary layer is not a significant component of
the noise measured in the test section but may become impor-
tant if noise from other sources is reduced.

4.4.5 Comparison with Other Measurements

Noise levels measured in the test section of the 7'x10'
wind tunnel are compared with data from other tunnels in
Figure 47. Data for the tunnels are listed in Table VII.

TABLE VII

Tunnel Data

Tunnel	Ref.	Speed Range m/s	ft/sec	Test Section	
NASA Ames 7x10	–	20–79	65–260	Closed,	Untreated
NASA Ames 40x80	1	40–79	130–260	Closed,	Untreated
NASA Langley 15x22	6	28–70	90–230	Open,	Untreated
NASA Langley 30x60	5	11–28	35–95	Open,	Untreated
NRDC 8x8	–	40–61	130–200	Open, .	Anechoic
Penn State 4x5	4	18–46	60–150	Closed,	Untreated
RAE 24 ft	7	37	120	Open,	Untreated
UARL 3.5 ft	8	31	100	Open,	Anechoic
Von Karman Test 10 ft	8	16–52	52–170	Open,	Untreated

Data for the 7'x10' tunnel is presented in the form of an average curve for the normalized spectra. All spectra are normalized with respect to test section dynamic pressure, with a reference of 1197 N/m² (25 lb/ft²). The comparison shows that the levels measured in the 7'x10' tunnel lie in about the middle of the range of data for all the tunnels. However, the data for the 7'x10' tunnel have a greater proportion of the energy at high frequencies than do most other tunnels. One point has to be borne in mind for this comparison - there is no information on the microphone installations used in the acquisition of the noise data.

Noise levels in the #1 7'x10' tunnel have been measured by NASA Ames when the test section was lined with 7.6 cm (3 inches) of Scottfelt 3-900 material. The data were obtained during a joint NASA Ames - BBN investigation of the noise from a model-scale augmentor wing, and microphone installations were similar to those used in the present investigation. A comparison of the normalized spectra obtained in the lined and unlined test sections is shown in Figure 48, where the presence of the lining appears to provide some reduction in high frequency noise. However at least part of the observed reduction may be due to differences in the length of the pitot tube strut, since the strut is the dominant noise source in the high frequency region.

4.5 Fan Noise

4.5.1 Measured Levels

Sound pressure levels measured in the diffuser and settling chamber are shown in Figures 20 to 24, and spectra for two locations have been normalized with respect to test section dynamic pressure in Figures 27 and 28. Preliminary analysis in Section 4.2 attributed the sound levels in the diffuser and

settling chamber to the drive fan. Further analysis of the
fan noise will be performed in this section. Relevant
geometric data for the fan is listed in Table VIII.

TABLE VIII
Fan Geometry Data

Blade tip diameter	D_T = 9.1 m	(30 feet)
Hub diameter	D_H = 2.4 m	(8 feet)
Number of blades	B = 8	
Tip chord	0.51 m	(20 inches)
Root chord	0.74 m	(29.2 inches)
Mean solidity	s = 0.27	

4.5.2 Fan Tones

Typical of all fans, the noise generated by the tunnel
drive fan will contain broadband and discrete frequency
components. The main discrete frequency contributions will
occur at the fan blade passage frequency and its low order
harmonics. For most operating conditions, the blade passage
tones occur at frequencies below 100 Hz and thus are below
the frequency range of interest in most wind tunnel tests.

The sound pressure levels associated with blade passage
components, and the number of prominent harmonics encountered
in the 7'x10' tunnel, are indicated in Figure 49. The figure
contains power spectral density curves for microphone locations
in the test section (#1) and downstream of the fan (#4) over a
range of test section dynamic pressures from 239 N/m²
(5 lb/ft²) to 3830 N/m² (80 lb/ft²).

Spatial distributions of the tone sound pressure levels
are shown in Figures 50 and 51 for test section dynamic
pressures of 479 N/m² (10 lb/ft²) and 1915 N/m² (40 lb/ft²)
respectively. Curves are presented for the blade passage
frequency fundamental f_B and the next three harmonics, $2f_B$,
$3f_B$ and $4f_B$. In general the distribution patterns are similar
to those in Figure 12 for a noise source near the fan, and
in Figure 39 where the data are interpreted as indicating
the noise source is near the fan.

In some cases the data in Figures 50 and 51 indicate
that the noise propagates into the test section via the diffuser
rather than via the settling chamber. This is particularly
true of the blade passage fundamental frequency at $q = 479$ N/m²
(10 lb/ft²) where the normalized levels in the test section
exceed those in the settling chamber. Acoustic tests with zero
flow showed an energy decrease when sound was transmitted from
settling chamber to test section.

4.5.3 Broadband Noise

To obtain further confirmation that the broadband noise
in the diffuser and settling chamber is generated mainly by
the fan, the measured levels have been compared with predicted
values.

Several methods of predicting fan noise have been developed
by different authors. Scharton et al [25] have used some of
the methods, which are suitable for large scale fans, to predict
noise in the modified 40'x80' wind tunnel proposed for NASA
Ames Research Center. The methods require geometric and/or

aerodynamic information for the fan. Some of the aerodynamic
data are not readily available for the drive fan of the 7'x10'
tunnel. Consequently only rough estimates can be made and the
resulting estimates of sound power level will contain possible
errors.

Scharton et al [25] list the following fan prediction
methods

(a) General Electric Company Method:
     The octave band power level, OBPWL (f), for the octave
     band centered at frequency f, is given by

$$OBPWL(f) = 40 \log \Omega + 70 \log D_T + 10 \log \left[1 - \left(\frac{D_H}{D_T}\right)^3 \right] +$$

$$+ 10 \log f - 10 \log [1+(4.4\Phi)^2] - 79.5 \text{ dB re } 10^{-12} \text{ W} \quad (20)$$

where Ω = fan r.p.m.

and $\Phi = \frac{f}{\Omega} \left[1 - \left(\frac{D_H}{D_T}\right)^3 \right]$

Other symbols are identified in Table VIII.

(b) BBN Modified Ventilating Fan Method:
     The overall sound power level, OAPWL, is given by

$$OAPWL = 50 \log \Omega + 70 \log D_T - 85 \quad \text{dB re } 10^{-12} \text{ W} \quad (21)$$

The octave band levels are obtained from Table IX.

TABLE IX
Normalized Fan Noise Spectrum

f/f_B	0.25	0.5	1	2	4	8	16	32	64	128
OBPWL(f)-OAPWL	-9	-6	-5	-7	-10	-13	-16	-19	-21	-24

The frequency f_B is the blade passage frequency,

$$f_B = \frac{\Omega B}{60}$$

(c) BBN Single Stage Compressor Method:

$$\text{OAPWL} = 50 \log\left(\frac{V_{rel}}{1000}\right) + 10 \log\left(\frac{V_a}{V_{rel}}\right) + 10 \log w + 10 \log s$$

$$- 15 \log\left(\frac{T}{T_{ref}}\right) + \alpha + 126.5 \text{ dB re } 10^{-12} \text{W} \qquad (22)$$

where V_{rel} = relative tip speed (ft/sec)

V_a = mean axial flow speed (ft/sec)

w   = weight flow (lb/sec)

T   = static inlet temperature

T_{ref} = reference temperature

α = mean incidence deviation

The octave band spectrum is obtained from Table IX.

(d) BBN Low Tip Speed Fan Method:

$$\text{OAPWL} = 14 \log (P_r - 1) + 10 \log F + 10 \log B + 122 \text{ dB}$$

$$\text{re } 10^{-12} \text{W} \qquad (25)$$

where P_r = fan pressure ratio

and F = fan thrust

Again the octave band spectrum is obtained from Table IX.

It is seen that methods (a), (b) and (c) all result in a V^6 relationship for the octave band sound pressure levels at frequencies above the blade passage frequency.

Methods (a)-(c) were used to estimate fan acoustic power levels for the 7'x10' tunnel; the spectra are shown in Figure 52. Method (d) was not used because of the unavailability

of aerodynamic data. The spectra were calculated for operating conditions associated with a dynamic pressure of 1197 N/m² (25 lb/ft²) in the test section.

Measured values for the fan sound power level were obtained from sound pressure levels averaged in the diffuser and settling chambers. Before averaging, the data were normalized with respect to test section dynamic pressure, with q_t= 1197 N/m² (25 lb/ft²) as reference. Sound pressure levels were converted to power levels using absorption data in Table IV. The calculated octave band sound power levels are contained in Table X, where it is evident that the fan sound power is distributed equally in the upstream and downstream directions.

Measured and predicted power levels are compared in Figure 52. The measured values lie within the range predicted by the three methods, but are closer to the two methods which use only geometric parameters. This may be due to uncertainties in the aerodynamic properties creating errors in the estimate.

TABLE X

Measured Sound Power Level for Drive Fan

Frequency (Hz)	125	250	500	1000	2000	4000	8000	16000
Diffuser:								
PWL–SPL (Table IV)	(10)	10	10	11	12	13	15	(17)
Average SPL (dB)**	96	94	90	85	79	72	67	57
OBPWL (dB)*	(106)	104	100	96	91	85	82	(74)
Settling Chamber:								
PWL–SPL (Table IV)	(14)	14	14	15	16	17	19	(21)
Average SPL (dB)**	92	91	87	82	77	68	61	45
OBPWL (dB)*	(106)	105	101	97	93	85	80	(66)
Total OBPWL (dB)*	(109)	108	104	100	95	88	85	(75)

* dB re 10^{-12}W

** dB re 2×10^{-5}N/m^2

5. ACOUSTIC CHARACTERISTICS OF TEST CHAMBER

The acoustic characteristics of the test chamber are of
no importance when the tunnel is operated with the test section
closed, as is the case at present. However, if the test
section is redesigned to permit an open configuration, the
acoustic properties of the chamber will influence the sound
measurements. Thus reverberation measurements were made in
the chamber.

The test chamber surrounds the test section and the first
part of the diffuser. The walls and roof are made of steel
plates, with supporting steel I beams, and are covered with
1-inch thick fiber-board panels. In one quadrant of the chamber
there is a high bay area which extends from floor to ceiling.
In the remaining three quadrants the chamber has a wooden platform
at a height of about 3.4m (11 feet) above the floor. Dimensions
of the chamber are approximately 13.7x16.8 x9.1m (45'x55'x30').

Reverberation time measurements were made at four locations
in the chamber, using a pistol as the noise source. Average
absorption data calculated from the measurements are shown in
Table XI.

TABLE XI
Absorption Data for Test Chamber

Frequency (Hz)	250	500	1000	2000	4000	8000
T_R (sec)	0.7	0.6	0.5	0.6	0.5	0.6
$\bar{\alpha}$	0.47	0.55	0.66	0.55	0.66	0.55
$S\bar{\alpha}$ (ft^2)	5200	6060	7280	6060	7280	6060
(m^2)	480	560	680	560	680	560

6. ACOUSTIC CRITERIA

Modification of a wind tunnel to provide an acoustic test facility must satisfy two acoustic conditions. Firstly, the tunnel ambient noise levels, with and without flow, must be lower than those generated by the model. Ideally a signal-to-noise ratio greater than 10 dB is desired. Secondly, the reverberation characteristics of the test section should be such that free field measurements can be made without having to locate the microphones too close to the model.

In the present case, where there are three optional configurations for the test section, criteria for ambient noise levels must be satisfied in all three designs. Reverberation criteria however may change from configuration to configuration. For example, in the unlined configuration the test section may be used only for sound power measurements without reference to directivity properties. Directivity measurements can then be performed in a lined test section.

6.1 Typical Model Noise Levels

Before establishing acoustic criteria it is necessary to determine the type of model tests to be conducted in the wind tunnel. The main reason for using a wind tunnel as an acoustic facility is to study the effects of forward velocity on noise generation. The noise source may be a propulsion system such as a jet, rotor, or propulsive high-lift device. Alternatively, the noise may be generated by airflow over an airfoil, flap, wheel strut, etc. In general the noise levels generated by a propulsion system will be higher than those associated with aerodynamic noise from the airframe. Thus the latter case will probably determine acceptable levels for tunnel noise when the tunnel is operating.

Estimates of the noise levels likely to be encountered
with propulsion systems can be obtained from existing data
measured in the 7'x10' and 40'x80' tunnels. Noise levels
associated with a model scale augmentor wing have been
measured in the 7'x10' tunnel for nozzle pressures ratios 1.54
and higher. The augmentor wing was operated with and with-
out the flap. The lowest noise levels occurred at the lowest
pressure ratio of 1.54 and the spectral ranges, for several
locations at different angles to the jet axis, are shown in
Figure 53. Data are presented for the augmentor with lined
flap and shroud, and for the nozzle without flap. The
sound pressure levels were measured at a radius of 106 cm
(42 inches) in a lined test section. The spectral levels
are similar for the two cases but the augmentor has relatively
more low frequency energy than does the nozzle alone. At a
pressure ratio of 2, which is probably more typical of full
scale operational conditions, the measured noise levels were
5 to 8 dB higher than those shown in Figure 53 for a pressure
ratio of 1.54.

The lowest frequencies of interest for models in the
7'x10' tunnel will probably be associated with rotor noise
studies. This problem has been discussed by Arndt and Boxwell
[3] with regard to the #2 7'x10' tunnel. One of the important
factors in rotor noise is the tip Mach number and, as rotor
model scale is reduced to enable the rotor to operate without
being too close to the tunnel walls, rotational speed will
have to increase to maintain a constant tip Mach number. For
example, if a full scale 50-foot diameter rotor with two
blades operates at 100 rpm the blade passage frequency will
be 3.5 Hz. A model scale rotor with a diameter of 2.5 feet
will have a blade passage frequency of 67 Hz for the same
tip speed.

Frequencies as low as 67 Hz pose two problems. One is
the ambient noise level and the other is the long acoustic
wavelength of about 17 feet. In a 7'x10' test section it is
difficult to get into the far field for acoustic signals with
such a long wavelength. However, the problem can be alleviated
in an open test section by placing the microphone outside the
tunnel flow, although the ambient noise problem will still be
present.

Measurements of noise from full scale rotors have been
made in the 40'x80' wind tunnel at NASA Ames [26], where the
sound pressure levels were 90 to 110 dB. For a 1/20 scale
model rotor the acoustic power level would decrease by 26 dB.
However, because of the relationships between sound power
level and sound pressure level (Figure 9), the sound pressure
levels in the 7'x10' tunnel will be about 10 dB lower than those
in the 40'x80' tunnel. This places the rotor noise in the
same range of sound levels as the model scale jet and augmentor
wing shown in Figure 53.

In the case of airframe noise, measurements have again
been made in the 7'x10' tunnel test section with a model scale
augmentor wing. The model was mounted on large end plates and
was positioned with an angle of incidence of -30° and a flap
angle of 30°. One-third octave band spectra measured in
the test section were normalized with respect to test section
dynamic pressure and an average curve is shown in Figure 54.
Inspection of the measurements has shown that the noise levels
measured in the test section when the model was present were
only slightly higher than those measured in an empty test
section. Thus the curve in Figure 54 may be influenced by
tunnel noise, and the levels may be higher than those for
airframe noise alone.

A lower limit of model noise levels will be provided
by airframe noise from a clean wing. Noise levels for this
configuration can be estimated from Hayden [13], and typical
free field sound pressure levels at a radius of 106 cm (42
inches) are shown in Figure 54. Diffuse field sound pressure
levels calculated on the basis of power level, converted to
sound pressure level by Figure 9, would be about 9 dB higher
than the levels shown in Figure 54. It will be noted that
the spectrum has a maximum at a frequency of about 500 Hz,
for the particular conditions of q = 1197 N/m² (25 lb/ft²)
and a wing chord of 0.61 m (2 ft). Hobeche and Williams
[7], on the basis of 1/10 scale model external jet flap noise
measurements, have observed that there is a requirement for
measurements at frequencies down to 250 Hz, or lower.

6.2 Comparison of Model and Tunnel Noise Levels

Ambient noise levels in the tunnel test section are
presented in Figure 14, and smoothed curves are plotted in
Figure 55 for comparison with sound pressure levels for the
augmentor wing. The data show that the augmentor noise levels
exceed the measured ambients, although at low frequencies the
desired 10 dB signal-to-noise ratio would not be achieved in
the present tunnel configuration when the 14-foot Transonic
Tunnel is operating.

The corresponding comparison when the tunnel is operating
is shown in Figure 56, where the augmentor wing noise levels
are compared with test section sound levels measured in the
absence of the model. It is seen that, when the tunnel is
operating at the higher dynamic pressures, tunnel noise and
augmentor wing noise are similar in level. Sound pressure
levels estimated for a clean wing at a dynamic pressure of
1197 N/m² (25 lb/ft²) (Figure 54) are well below the measured
tunnel noise levels at the same dynamic pressure.

6.3 Criterion for Tunnel Noise Levels

A practical lower limit to noise levels measured in the test section in the presence of flow appears at present to be imposed by the characteristics of the microphone support structure. The levels achieved by Noiseux [22, 23] with either a B and K ½ inch microphone or a BBN porous airfoil sensor are shown in Figure 54 for a dynamic pressure of 1197 N/m² (25 lb/ft²). These levels are similar to those measured in the acoustics tunnel of the United Aircraft Research Laboratory (Figure 47), which was specially designed for acoustic investigations. Thus, from a minimum cost stand point it is not worthwhile to reduce tunnel noise levels below those generated by the microphone system.

Consequently, a criterion spectrum for test section noise has been constructed on the basis of microphone self-noise measurements of Noiseux. The criterion is shown in Figure 57, normalized with respect to a test section dynamic pressure of 1197 N/m² (25 lb/ft²), and the spectrum is essentially a smoothed, average curve for the porous airfoil and ½ inch microphone spectra in Figure 54. Figure 57 compares the criterion with the predicted fan noise spectrum and with measured data. The measurements are presented in two parts, the upper bound being associated with discrete frequency components and the lower levels being a range of values obtained by smoothing the experimental data.

Figure 55 has shown that, even when the 7'x10' tunnel is not operating, the ambient noise levels in the test section can be high. The "tunnel-on" criterion in Figure 57 can be used as a goal for "tunnel-off" case, although the situation is probably not quite as critical since the model powered lift systems generate fairly high sound levels.

6.4 Criterion for Reverberation Characteristics

The reverberant characteristics of the test section can be expressed in several ways - hall radius, absorption coefficient, (PWL-SPL) etc. However, the most appropriate parameter in the present case is probably the hall radius since this specifies the maximum distance between microphone and noise source. An approximate relationship between hall radius and absorption coefficient is given by equation (2). For a lined test section it is probable that

$$4mV \ll S\alpha$$

In addition the term $S\alpha$ should be replaced by the more accurate $S\alpha/(1-\alpha)$

$$\text{Then } r_H \simeq \left[\frac{QS\alpha}{16\pi(1-\alpha)} \right]^{\frac{1}{2}} \tag{26}$$

When a model is installed on the centerline of the test section, the minimum distance to the tunnel side wall is 1.5 m (5 ft). Taking this distance to be the hall radius for an omnidirectional source (Q=1), the corresponding value of α is 0.56. For a radius of 3m (10 ft), equation (26) gives a value of $\alpha = 0.84$. The associated differences between power level and sound pressure level are 25 and 31 dB respectively. It is probable that a hall radius of 3 m (10 ft) would satisfy most test requirements regarding sound pressure level measurements.

Criteria for correlation measurements are much more stringent if all maxima, except that for the direct path, are to be eliminated from the correlation coefficient. In this case absorption coefficients of almost unity are required and such a criterion is not pactical.

Based on the above arguments the recommended criterion
for the reverberant characteristics of the lined, closed
test section is that the hall radius should be at least 3m
(10 feet) for the frequency range of interest.

7. NOISE CONTROL METHODS

A noise control program for the 7'x10' wind tunnel with closed test section has three main parts.

(1)   Reduce noise generated in the test section by items such as the microphone support struts, pitot tube, pitot traverse system, diffuser-entry airfoils, and air leaks,

(2)   Reduce the transmission of fan noise into the test section,

(3)   Increase acoustic absorption in the test section.

Part (3) will not be required when tests are to be conducted in a hard-walled test section, but it is still part of the overall modification program.

A proposed criterion spectrum for test section noise levels has been compared in Figure 57 with noise levels measured in the test section and with predicted fan noise levels. The data were normalized with respect to a dynamic pressure of 1197 N/m² (25 lb/ft²). Using these spectra, Figure 58 estimates the noise reductions required to meet the criterion. For fan noise alone the reduction is about 15 dB throughout the frequency range. The corresponding reductions for broadband noise generated in the test section are 15 to 40 dB, and for tones 20 to 45 dB, where the higher reductions occur at the higher frequencies.

7.1 Noise Generated in Test Section

Analysis of measurements made in the test section of the #1 7'x10' wind tunnel indicated that noise is generated by at least some of the solid bodies (e.g. pitot tube) exposed to the airflow. It is reasonable to assume that the other hardware items in the test section will also generate noise. Since the noise levels generated by items such as the pitot tube are high, removal of these items should be the top priority in a noise control program.

The following modifications are recommended to reduce noise levels generated in the test section:

(i)   Remove pitot traverse system when acoustic tests are to be performed,

(ii)   Remove diffuser-entry airfoils for acoustic tests. This assumes that the resulting changes in diffuser airflow do not cause an unacceptable deterioration in aerodynamic performance and do not cause an unacceptable increase in low frequency noise due to unsteady flow in the diffuser. A check of the tunnel operation is required to determine that these conditions are satisfied,

(iii)   Improve the aerodynamic shape of the pitot strut and determine the minimum insertion length for acceptable measurements of tunnel flow. Alternatively, if other means of measuring tunnel dynamic pressure are available, remove the pitot tube for acoustic tests. The alternatives could include direct read out of fan rpm, or flow measurements in the settling chamber or diffuser.

(iv)   Redesign microphone support struts so that (a) the microphone cable is located within the strut, and (b) the microphone cathode follower and adaptor are provided with an aerodynamic housing. Designs such as those of Noiseux [23] can be used as a guide,

(v)   Remove the U-channel beams used in the present test section to support the porous lining. These will not be required in the modified tunnel if the test section is redesigned so that the walls move outward to accommodate the lining.

(vi)   Seal air leaks and other holes or cavities in the tunnel contraction and test section. This is important for two reasons. Firstly, air leaking into the tunnel can generate noise particularly when the leak is outside the test chamber where the pressure differential is largest,

as in the case of the region connecting the contraction
and the test section. Secondly, flow over a cavity will
generate broadband noise or tones even when there is no
air leakage.

7.2 Fan Noise

Since one of the constraints on the program is that no
modifications shall be made to the fan, the only means of
reducing fan noise levels in the test section is by placing
absorptive material such as Scottfelt in the settling chamber
and diffuser. Both regions have to be treated because, as
shown earlier, fan noise propagates equally in the upstream
and downstream directions.

Two alternative designs with similar acoustic performance
are proposed to allow cost comparison. Alternative A (Figures
59 and 60) places absorptive material on the walls of the
tunnel and Alternative B (Figures 61 and 62) utilizes a single
splitter in the diffuser and settling chamber. There is no
acoustical material on the tunnel floor or ceiling in either
installation.

In Alternative A the side walls of the settling chamber
and diffuser are lined with porous material which is 2 inches
thick and is held between wire mesh screens at a distance of
18 inches from the tunnel wall. Details of the installation
are shown in Figure 60. Vertical and horizontal supports will
be required to prevent excessive movement of the porous material
when the tunnel is operating. In the diffuser the spacing of
the supports should be about 24 inches but in the settling
chamber, where the flow velocity is lower, a wider spacing
is acceptable.

Alternative B replaces most of the wall treatment with a splitter along the tunnel centerline (Figure 61). One splitter is located in the cross-leg of the diffuser and another splitter is on the cross-leg of the settling chamber. Wall treatment is retained on the inner wall of the settling chamber. The splitters and wall treatment extend over the full height of the tunnel. Details of the splitter are shown in Figure 62. Solid nose cones are provided to deflect the flow and protect the porous treatment which is held between wire mesh screens with about 50% open area. The total thickness of the splitter is 24 inches and the airgap between the porous material is 20 inches. Internal bracing is present in the splitter to provide overall stability for the installation and local support for the porous material. Horizontal stiffeners will be required in addition to the vertical members.

If the present walls of the 7'x10' tunnel are not moved, the presence of the acoustic treatment will reduce the open area of the diffuser and test section. The reductions will be:

	Alternative A	Alternative B
Diffuser	15-18%	9-11%
Settling Chamber	10%	11%

The contraction ratio from settling chamber to test section will be reduced from 14 to a value of about 12.5

During some non-acoustic tests in the 7'x10' wind tunnel small quantities of mineral oil are used for flow measurement. It is possible that the oil will permeate the porous material and cause deterioration of the acoustic and physical properties. One method of overcoming the problem is to place an impervious cover on the porous material. However, the cover should be very thin to minimize the loss of high frequency absorption. Recommended covers are 1-mil thick sheets of Mylar or Tedlar.

It is estimated that the presence of the cover will reduce
the absorption coefficient at 4,000 Hz by about 30%. This
deterioration in performance is probably acceptable for most
projected tests, even though the criterion spectrum will not
be met. The deviation from the criterion at 4 kHz is predicted
to be about 8 dB.

7.3 Test Section Reverberation

The criterion selected for reverberation conditions in the
test section is a hall radius of 3m(10 ft), or a mean absorption
coefficient of 0.84. At present the test section has a removable
lining composed of 7.6 cm (3 inches) of Scottfelt 3-900 with
no covering material. Absorption coefficients for the lining
have been measured by two investigators, and the results show
a wide variation ($0.74 \leq \alpha \leq 1.0$) at frequencies above about
500 Hz. However, average values of α in this high frequency
range lie in the range 0.82 to 0.89 and essentially satisfy
the above criterion.

At frequencies below 500 Hz the measured absorption
decreases rapidly as frequency decreases, and additional
absorption is needed if the criterion is to be satisfied at
frequencies of 200-250 Hz. This additional low frequency
absorption can be achieved by increasing the thickness of the
lining, moving the lining away from the wall to create an
air gap, or a combination of both. For ease of installation
and maintenance it is recommended that the thickness of
Scottfelt be increased from 7.6 cm to 15.2 cm (3 inches to
6 inches) and that the material be placed on a rigid backing
with no air gap. If this is achieved by moving the test section
walls outwards through a distance of 6 inches there will be a
minimal loss in aerodynamic performance. The lining can be
protected, and restrained in place, by a wire mesh screen with
an open area of at least 50%.

It should be noted, as is discussed in Section 6.4, that
this criterion will not eliminate secondary peaks in cross-
correlation functions of acoustic pressure. However, test
data can be corrected to account for these secondary peaks if
necessary.

7.4 Test Chamber Reverberation

Reverberation measurements in the test chamber indicate
that the criterion of a 4.5m (15 ft) hall radius can be met
in the frequency range above 250 Hz without the need for
additional acoustic treatment. However, there is a possible
exception to this statement. If there are reflective surfaces
such as control panels, tunnel walls and diffuser collectors
in the neighborhood of the microphones the free field conditions
will deteriorate and the hall radius will decrease. Thus, all
reflecting surfaces have to be removed or treated with
absorptive material.

The treatment may require up to 15cm (6 inches) of
Scottfelt if the surfaces are large. However, since the
test section lining will not be required for an open test
section, it may be possible to utilize these panels in the
test chamber.

7.5 Tunnel Ambient Noise

The preceding noise control methods are not designed to
reduce ambient noise levels in the test section when the
tunnel is not operating. Noise from adjacent tunnels can
enter the tunnel at all points around the circuit. However,
one of the main sources appears to be the 14 foot Transonic
Tunnel which is adjacent to the north-west corner of the settl-
ing chamber. Much of the acoustic energy from the 14 foot
tunnel will enter the 7'x10' tunnel via the ventilation tower

and the north-west walls of the settling chamber. To this
extent the acoustic treatment in the settling chamber and
diffuser will reduce the sound levels propagating into the
test section. The recommended noise control methods will
not reduce noise entering the tunnel through the walls of
the south leg of the diffuser and settling chamber, includ-
ing the contraction. Attenuation of this noise can be achieved
by either increasing the transmission loss of the tunnel walls
or by having acoustic treatment throughout the south leg of
the tunnel. Neither method appears to be worth the cost at
the present time.

8.   CONCLUSIONS AND RECOMMENDATIONS

8.1   Acoustic Characteristics of Tunnel

As a result of the measurement program in the #1 7'x10' wind tunnel, several conclusions can be drawn regarding the noise characteristics of the test section, diffuser and settling chamber. In some cases the conclusions are tentative, and additional testing is recommended with regard to noise radiation from the microphone support systems.

Tunnel ambient noise levels, without flow, vary considerably depending on activities at the NASA Ames Research Center and Moffett Field. Variations of 40 dB (34 to 74 dB) were measured at 1000 Hz in the test section. Higher ambient levels may be encountered when other tunnels are operating.

Discrete frequency and broadband noise components are present in the test section. The discrete frequency tones are generated by items such as the pitot support strut and other airfoils in the test section. Also, at lower frequencies, tones are generated by the fan blades and neighboring struts.

In the case of broadband noise, the following observations can be made.

(a)   One-third octave band spectrum levels vary as U^6 or q^3,

(b)   When adjusted for cross-sectional area, low frequency sound levels are lower in the test section than in the settling chamber, probably due to poor transmission from the settling chamber,

(c)   High frequency levels in the test section are higher than elsewhere in the tunnel,

(d)   There is no significant variation of sound levels with position in the test section,

(e) Spectrum levels are similar to those measured in other
    tunnels, when normalized with respect to dynamic pressure,

(f) Sound radiated by the turbulent boundary does not appear
    to be significant at present, but may become so when noise
    control methods are implemented,

(g) There is an indication that high frequency sound levels
    are reduced when the test section walls are lined with
    Scottfelt absorptive material,

(h) Measured sound levels are higher than those measured using
    microphones with carefully designed aerodynamic shapes,

(i) The data can be interpreted in terms of low frequency
    noise being generated by the drive fan and transmitted
    to the test section. Mid- and high-frequency noise appears
    to be generated in the test section by pitot tube, air-
    foils and, probably, microphone support struts.

In the diffuser and settling chamber, broadband noise is
found to have the following characteristics:

(a) Spectrum levels at a given location vary as U^6 or q^3,

(b) At a given tunnel speed, spectrum levels at different
    locations scale as tunnel cross-sectional area,

(c) Sound power levels are similar to those predicted for
    the drive fan,

(d) Sound levels do not appear to be generated by flow over
    the microphone and supports.

Discrete frequency sound in the diffuser and settling
chamber originates in the test section at high frequencies
(eg f> 400 Hz when q_t = 1915 N/m² or 40 lb/ft²) and in the
neighborhood of the fan at low frequencies.

8.2 Acoustic Characteristics of Test Chamber

Reverberation measurements in the test chamber indicate that the average absorption coefficient in the frequency range 250 to 8000 Hz is about 0.57. The corresponding hall radius is approximately 5m (17 feet). This should be adequate for testing with an open test section provided that there are no local reflections from tunnel control panels, instrumentation and other nearby items.

8.3 Recommended Future Testing

It is recommended that further noise measurements be made in the wind tunnel test section to identify acoustic generation from microphone support struts and other items in the test section. Noiseux [23] has obtained relatively low flow noise levels with a porous strip microphone and a B and K ½ inch microphone, when specially designed airfoil stands and fairings were used. These designs could be used in the recommended test program. Two important factors of the designs are the improved aerodynamic characteristics around the B and K microphone and cathode follower, and the placement of the microphone cable within the support strut.

Flow obstructions in the test section should be removed progressively so that their contributions to tunnel noise levels can be identified. The main obstructions are the pitot traverse system, the diffuser-entry airfoils, and the pitot tube used to determine tunnel operating speed. In addition all air leaks in the contraction should be sealed to prevent air from being drawn into the test section from regions outside of the test chamber.

8.4 Criteria

A criterion for test section noise levels has been
selected based on current technology regarding the design
of microphone systems for low aerodynamic noise. The
criterion requires a reduction of about 15 dB for fan noise
and 20 to 45 dB for noise generated in the test section.
The higher reductions occur at the higher frequencies. The
criterion spectrum should be adequate for most model tests
envisaged for the future.

For test section reverberation, a hall radius of 3m
(10 ft) has been selected as a criterion adequate for most
test conditions. This criterion will be achieved with a
mean absorption coefficient of about 0.84.

When the test section is open, microphones can be placed
further from the model, out of the tunnel flow. Thus a
greater hall radius is required; a radius of about 4.5m
(15 ft) has been selected as a criterion. The corresponding
mean absorption coefficient is approximately 0.51.

8.5 Noise Control Methods

Noise control methods are recommended to reduce the noise
levels in the tunnel test section when the fan is operating.
The methods include the removal of all unnecessary flow obstruc-
tions on the test section, improved design of the microphone
support struts, sealing of cavities and air leaks and installa-
tion of acoustic treatment in the settling chamber and diffuser.
The treatment can consist of absorptive material on the vertical
walls or the installation of a vertical splitter on the tunnel
centerline.

To meet the hall radius criterion for the test section
at frequencies down to 250 Hz it is recommended that the acoustic
treatment be increased in thickness from 7.6 cm to 15.2 cm
(3 inches to 6 inches).

No changes are recommended for the test chamber, but
care should be taken to prevent local acoustic reflections
from the tunnel control panels, external wall surfaces etc.

8.6 Recommendations for Instrumentation

During the past few years the Large Scale Aerodynamics
Branch at NASA Ames Research Center has been building up an
inventory of acoustic instrumentation for use in the 40'x80'
wind tunnel and other test facilities. When the #1 7'x10'
tunnel becomes a primary acoustics research facility it will
be appropriate to have acoustic instrumentation dedicated
the tunnel so that a permanent system can be maintained for
improved data acquisition and reduced set-up time.

In many cases instrumentation of the type required for
the 7'x10' wind tunnel facility is already available at NASA
Ames. However, a list is presented here for completeness.

Transducers:

(a) Microphones for measurement of sound levels in the test
     section. These should be mounted on low-noise supports
     and fitted with nose cones. B and K microphones can be
     used with axis parallel to the flow. Other designs such
     as the BBN porous strip sensor can be used over a limited
     range of angles to flow direction. Microphones should
     be no larger than $\frac{1}{4}$ inch in diameter because of high
     frequency sensitivity requirements.

     The number of microphones in the test section should be
     as small as possible to minimize acoustic and flow dis-
     turbances. The possibility of mounting a microphone on
     a rotating boom suspended from the test section roof could
     be explored as an alternative installation.

(b) Pressure transducers for measurement of aerodynamic
    pressure fluctuations on surfaces such as wings, flaps,
    rotors etc. These should be flush mounted to minimize
    flow disturbances. Experience has shown that there are
    vibration problems with piezo-electric type of transducers.
    These should be vibration compensated and development of
    mounting techniques is required.

(c) Pressure transducers for insertion into jet flows. These
    should be small relative to the dimensions of the jet.

(d) Light-weight accelerometers with high frequency response
    to measure vibration of models. The measurements are
    required to relate structural response to excitation,
    or to determine the vibration environment for surface
    pressure transducers.

(e) Hot wire anemometer to measure turbulence of flows in
    the tunnel. The tubulence could be either the basic
    tunnel flow, disturbances introduced into the flow, or
    turbulent flows from model propulsion units.

(f) Directional microphones for use out of the tunnel flow
    with an open test section. Highly directional microphones
    such as shot-gun microphones can be used to identify
    noise source location.

Calibrators:

    Single-frequency calibrators for microphones, pressure
transducers and accelerometers are readily available. These
can be used for day-to-day calibrations. Multi-frequency
calibrators are required to determine the end-to-end frequency
sensitivity of installed systems. Also calibration systems
which can be mounted over flush-mounted transducers would be
advantageous so that the transducers need not be removed for
calibration.

Test Section Environment:

In many of the model scale tests, data are obtained at high frequencies up to 80 kHz. Atmospheric absorption can become important. Thus temperature and humidity sensors are required for the test section (and for the test chamber for open test section configurations).

On-line Data Reduction:

    One-third octave band analyzer
    Narrowband analyzer
    Correlator
    Fourier Transform Analyzer
    X-Y plotters (minimum of 2)
    Pair of matched filters (octave band and one-third
        octave band)
    Level recorder with capability for polar plots
    Oscillator and Random Noise Generator
    True RMS Voltmeter

Tape recorder with high frequency capability and good phase matching between tracks.

It is obvious that the complete list of equipment will not be required on any one test. However various combinations will be reuqired from test to test.

REFERENCES

1. Bies, D. A., "Investigation of the Feasibility of Making Model Acoustic Measurements in the NASA Ames 40x80 ft. Wind Tunnel," BBN Report 1870, (Contract NAS2-5742), (April 1970).

2. Bies, D. A., "Investigation of the Feasibility of Making Model Acoustic Measurements in the NASA Ames 40- by 80 Foot Wind Tunnel," BBN Report 2088, (Contract NAS2-6206), (1971).

3. Arndt, R. E. A., Boxwell, D. A., "A Preliminary Analysis of the Feasibility of Rotor Noise Measurements in the AMRDL-Ames 7x10 Foot Wind Tunnel," NASA Working Paper (October 1971).

4. Arndt, R. E. A., Boxwell, D. A., "A State-of-the-Art Report on Aeroacoustical Testing in Conventional Wind Tunnels," Paper at 84th Meeting Acous. Soc. Amer., Miami Beach, Florida, (November 1971).

5. Vér, I. L., Malme, C. I., Meyer, E. B., "Acoustical Evaluation of the NASA Langley Full-Scale Wind Tunnel," BBN Report 2100, (NAS1-9559), (January 1971).

6. Vér, I. L., "Acoustical Evaluation of the NASA Langley V/STOL Wind Tunnel," BBN Report 2288 (Contract NAS1-9559), (December 1971).

7. Holbeche, T. A., Williams, J., "Acoustic Considerations for Noise Experiments at Model Scale in Subsonic Wind Tunnels," Royal Aircraft Establishment Tech. Rep. 72155, (September 1972).

8. Oetting, R. B., "Preliminary Noise Measurements in the Open-Jet of the VKI Low Speed Wind Tunnel, L-1," Von Karman Institute for Fluid Dynamics Tech., Note 89, (May 1973).

REFERENCES (Con't)

9. Piersol, A. G., Rentz, P. E., "Utilization and Enhancement of the NASA Lewis 9x15 Foot V/STOL Wind Tunnel for Inlet Noise Research," BBN Report 2743, (Contract NAS3-18019), (May 1974).

10. Claes, H. P., Informal Report by General Electric to NASA Ames, (October 1973).

11. Soderman, P. T., Private communication, (December 1974).

12. Bauer, A. B., "Vortex Shedding from Thin Flat Plates Parallel to the Free Stream," J. Aerospace Sciences, 28, 4. 340-341, (April 1961).

13. Hayden, R. E., "Noise from Interaction of Flow with Rigid Surfaces: A Review of Current Status of Prediction Techniques," NASA CR 2126, (BBN Report 2276), (April 1973).

14. Hersh, A. S., Soderman, P. T., Hayden, R. E., "Investigation of Acoustic Effects of Leading Edge Serrations on Airfoils," J. Aircraft, 11, 4, 197-202, (April 1974).

15. Hanson, C. E., "An Investigation of the Near Wake Properties Associated with Periodic Vortex Shedding from Airfoils," M.I.T. Acoustics and Vibration Laboratory Report 76234-5, (September 1970).

16. Hodder, B. K., "The Effects of Forward Speed on Fan Inlet Turbulence and its Relation to Tone Noise Generation," NASA TM X-62381, (August 1974).

17. Nakamura, A., Matsumoto, R., Sugiyama, A., Tanaka, T., "Some Investigations on Output Level of Microphones in Air Streams," J. Acous. Soc. Amer., 46, 6 (Part 1), 1391-1396, (December 1969).

REFERENCES (Con't)

18. Nakamura, A., Sugiyama, A., Tanaka, T., Matsumoto, R.,
     "Experimental Investigation for Detection of Sound-
     Pressure Level by a Microphone in an Airstream,"
     J. Acoust. Soc. Amer., 50, 1 (Part 1), 40-46,
     (July 1971).

19. Fuchs, H. V., "Note on Aero-Acoustic Measurements in
     Open-Jet Wind Tunnels," Institut Fuer Turbulenzforschung,
     Berlin, Report IB357-74/4, (1974).

20. Rasmussen, G., "Windscreening of Microphones," Bruel and
     Kjaer, Report

21. Bruel and Kjaer Production Data Brochure 13-003, "Condenser
     Microphone Cartridges."

22. Noiseux, D. U., "Study of Porous Surface Microphones for
     Acoustic Measurements in Wind Tunnels," BBN Report 2539,
     (April 1973).

23. Noiseux, D. U., "Flow Noise Tests of the Airfoil Porous
     Surface Sensor Model 342 and of the B and K ½ inch Con-
     denser Microphone with Nose Cone," Memo #10 to J. Scheiman,
     NASA Langley Research Center, (Contract NAS1-12672),
     (September 1974).

24. Scharton, T. D., Private communication.

25. Scharton, T. D., Sawley, R. J., Wilby, E. G., "An Acoustic
     Study for the Modified 40x80 Foot Wind Tunnel," BBN Report
     2765, (Contract NAS2-8330), (February 1975).

26. Hickey, D. H., Soderman, P. T., Kelly, M. W., "Noise
     Measurements in Wind Tunnels," pp 399-408, *Basic Aero-
     dynamic Noise Research*, NASA SP-207, July 1969.

27. Bull, M. K., "Wall-pressure Fluctuations Associated with
     Turbulent Boundary Layer Flow," J. Fluid Mech. 28, Part 4,
     719-754, June 1967.
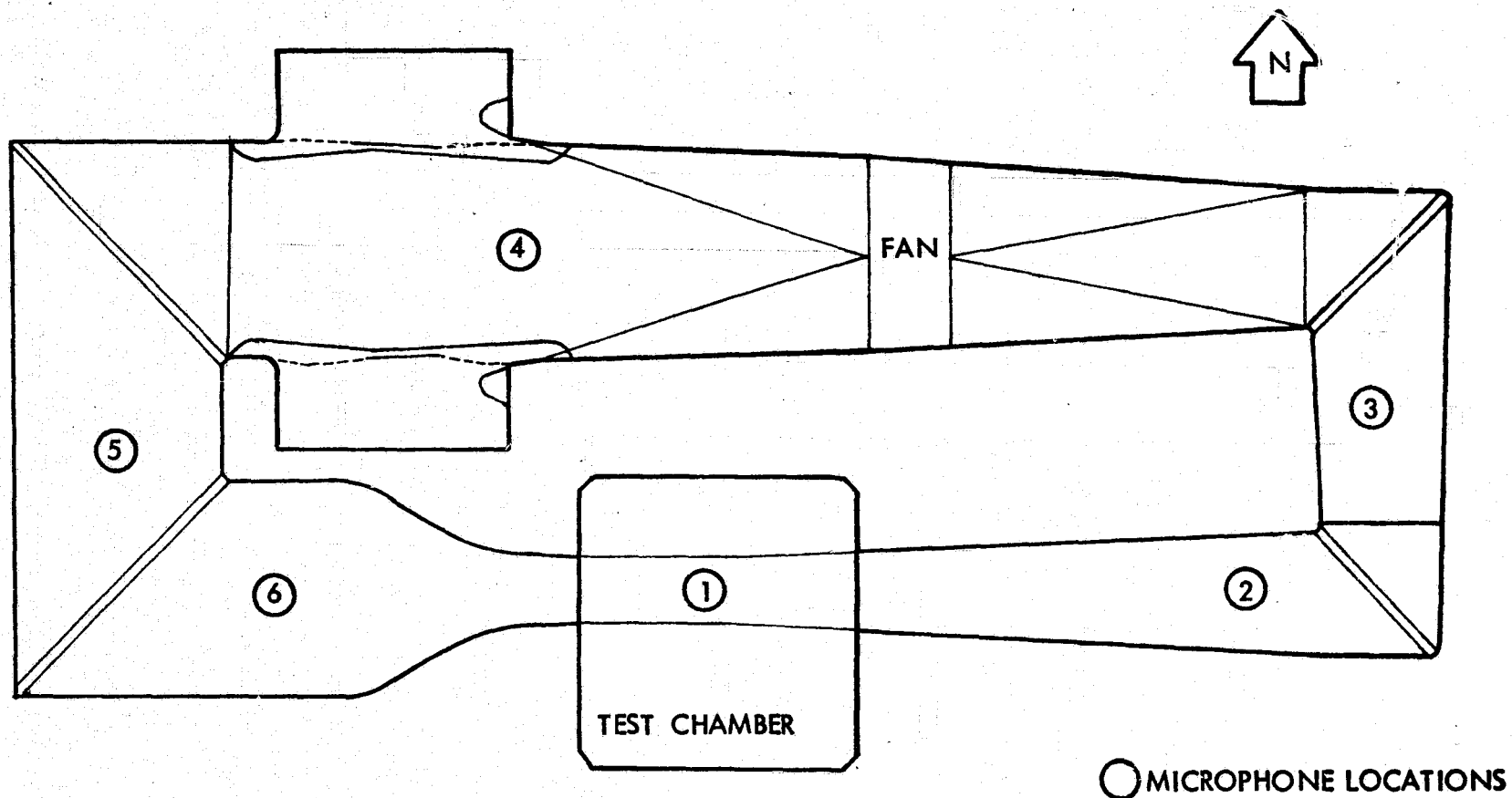
FIGURE 1.   DIAGRAM OF 7' x 10' WIND TUNNEL
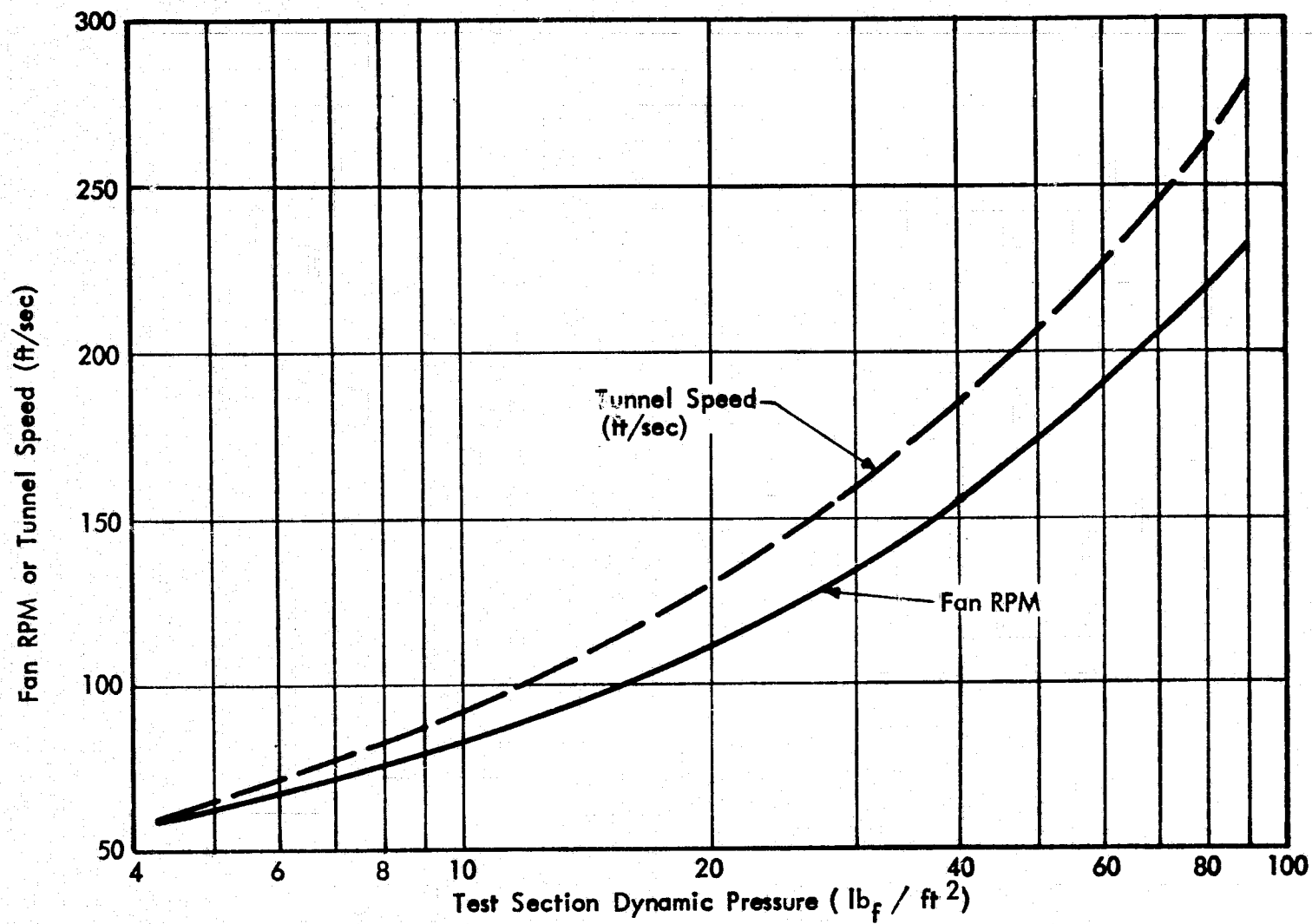
FIGURE 2. TUNNEL OPERATING CONDITIONS

SETTLING CHAMBER (#5)

10 dB

$T_R = 6.8$ sec.

DIFFUSER (# 3)

$T_R = 5.6$ sec.

1 sec.
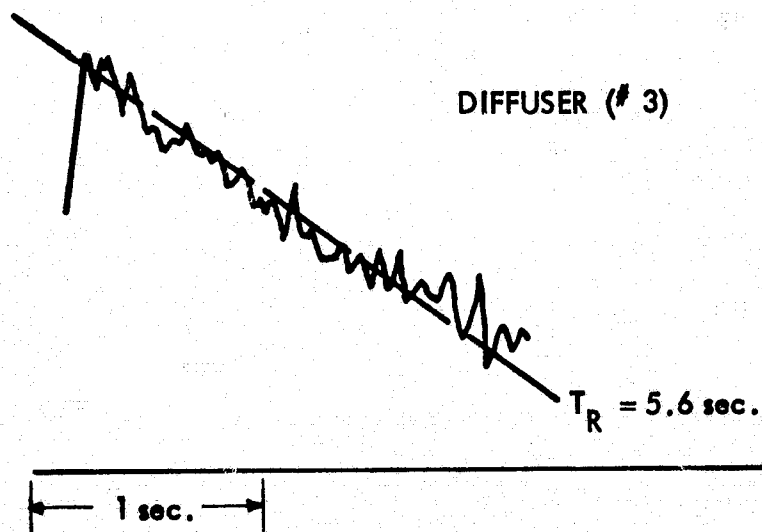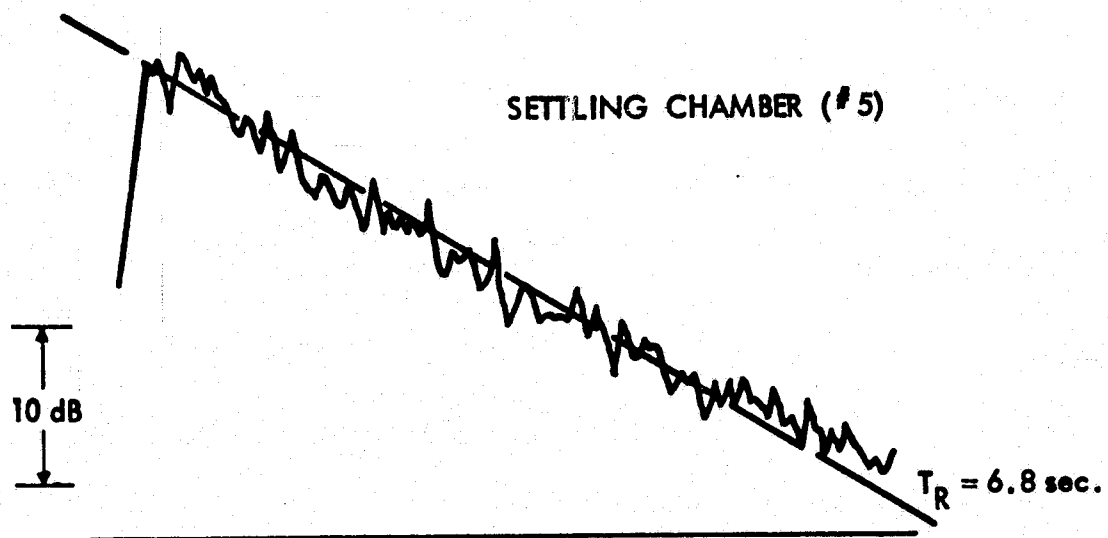
FIGURE 3. TYPICAL REVERBERATION DECAY SIGNATURES
MEASURED IN DIFFUSER AND SETTLING
CHAMBER (f = 1000 Hz)
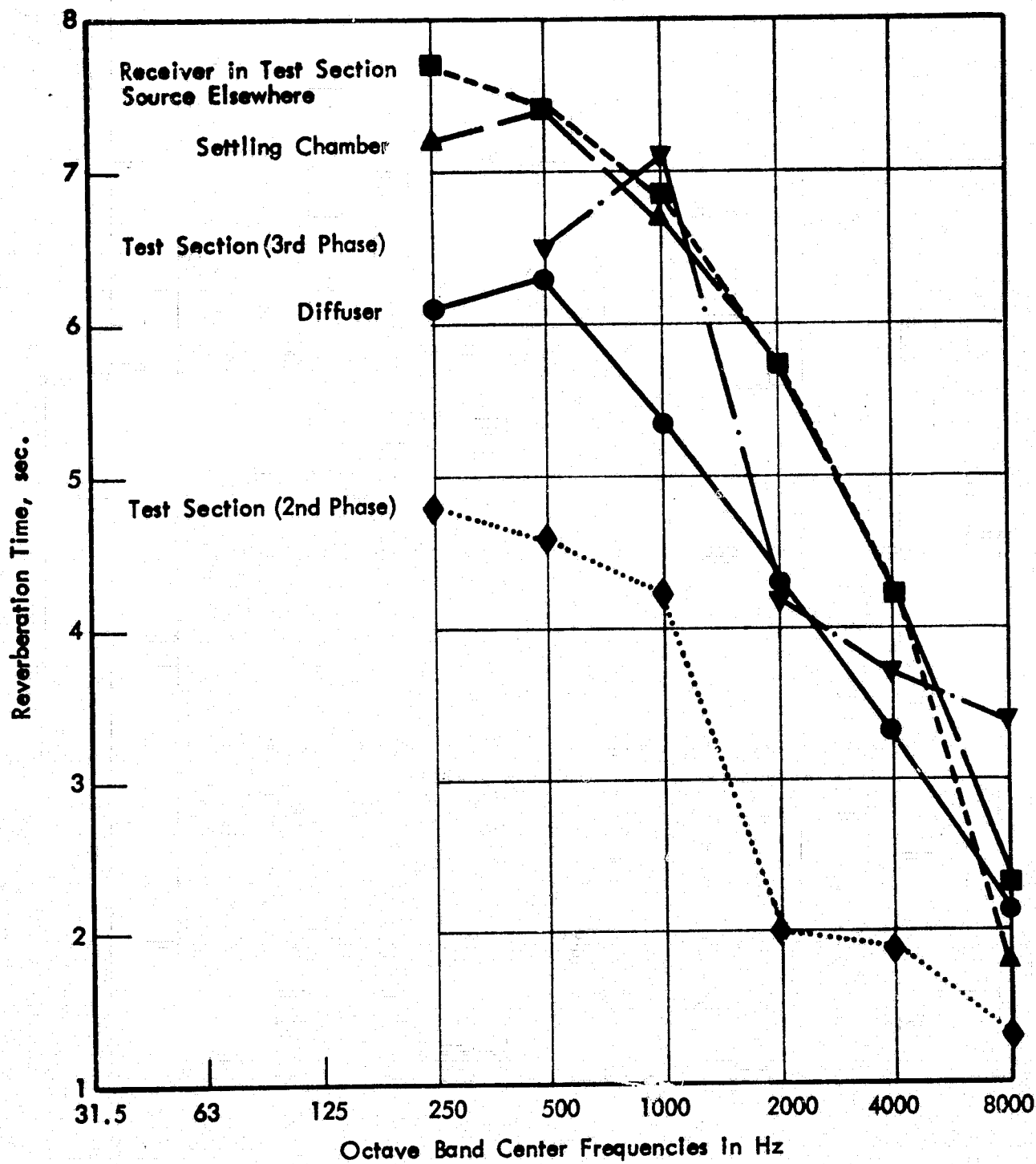
FIGURE 4. REVERBERATION TIMES MEASURED IN 7' x 10' TUNNEL
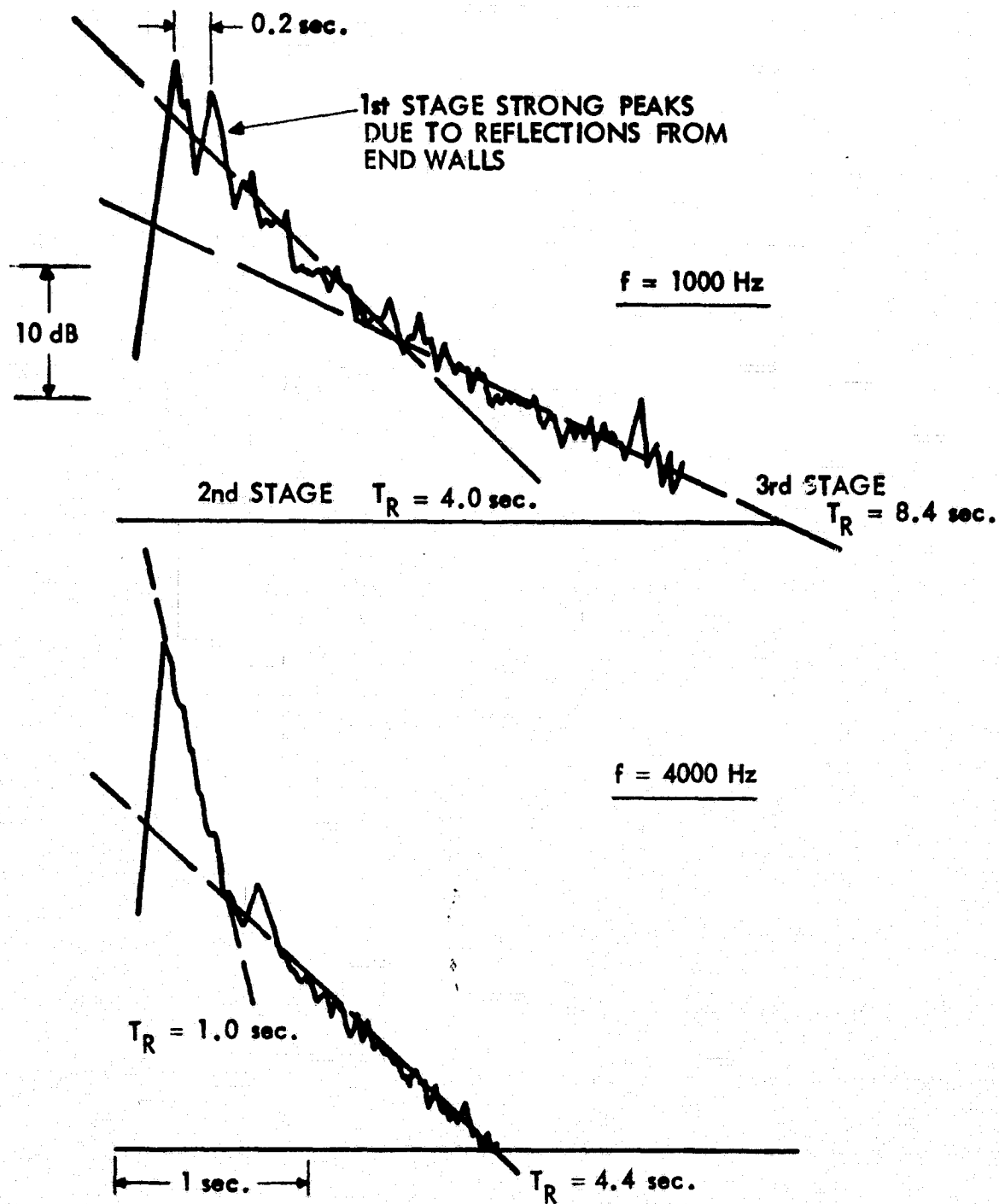
FIGURE 5.   TYPICAL REVERBERATION DECAY SIGNATURES
MEASURED IN TEST SECTION
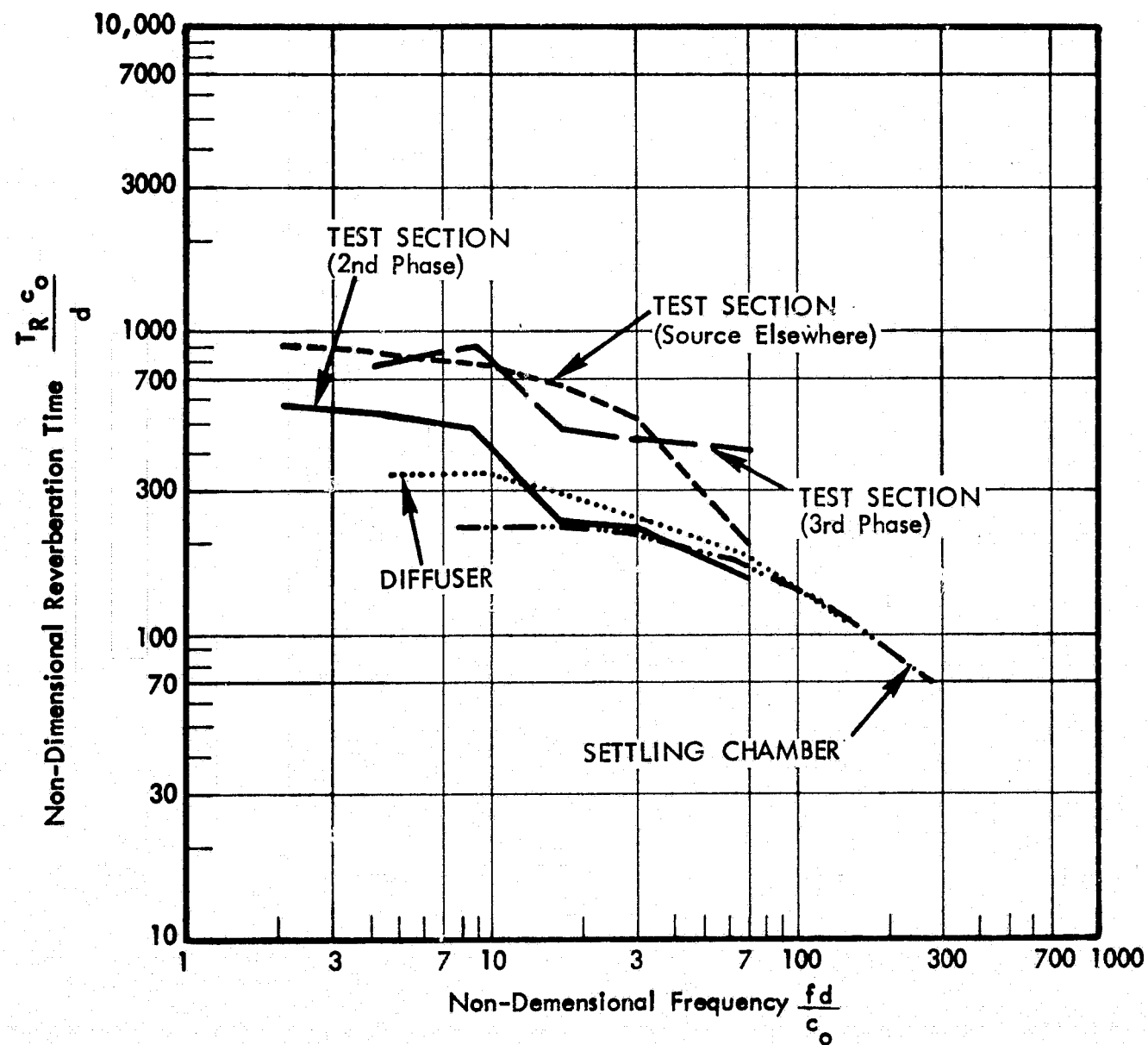
FIGURE 6. NON-DIMENSIONAL REVERBERATION TIME FOR 7' x 10' TUNNEL
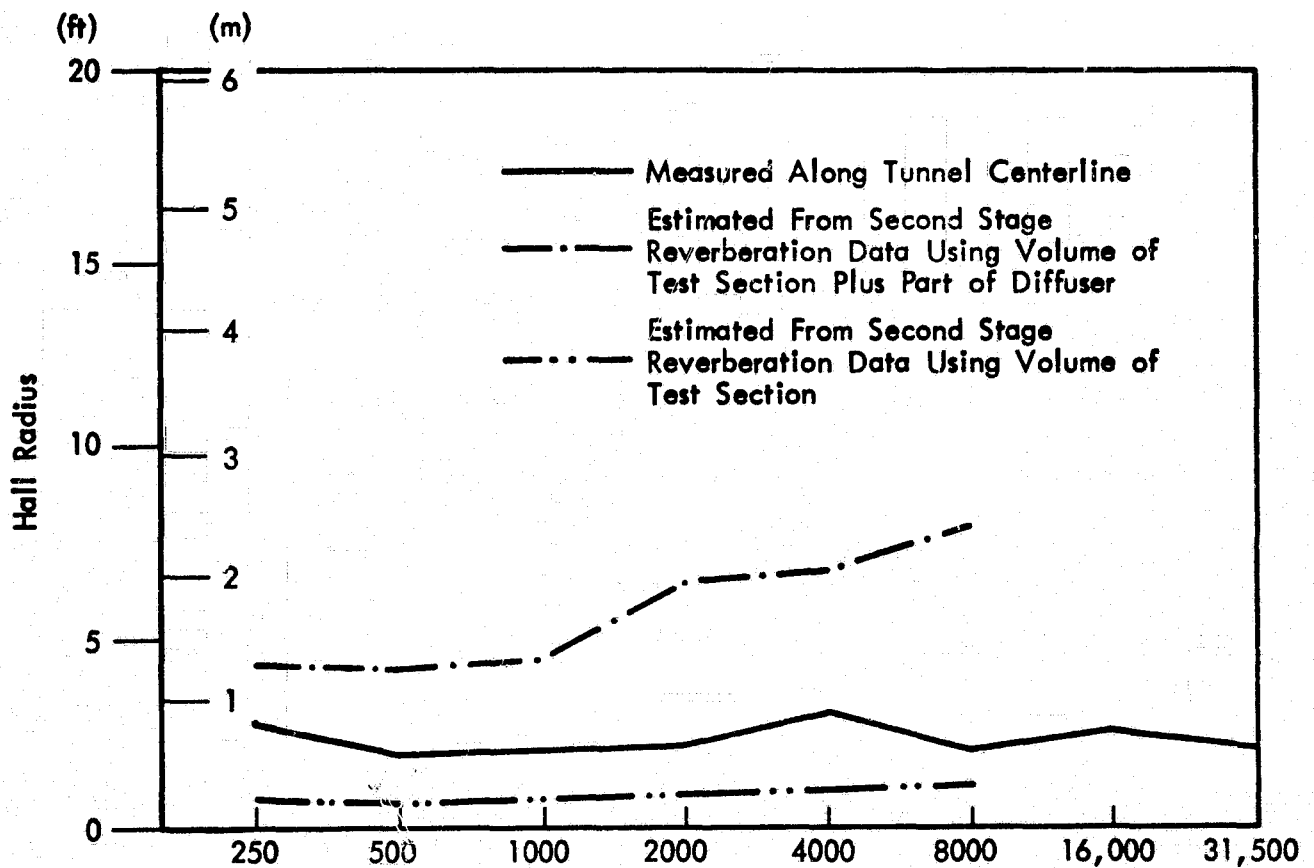
FIGURE 7a. MEASURED AND ESTIMATED VALUES FOR HALL RADIUS IN UNLINED TEST SECTION OF 7' x 10' TUNNEL
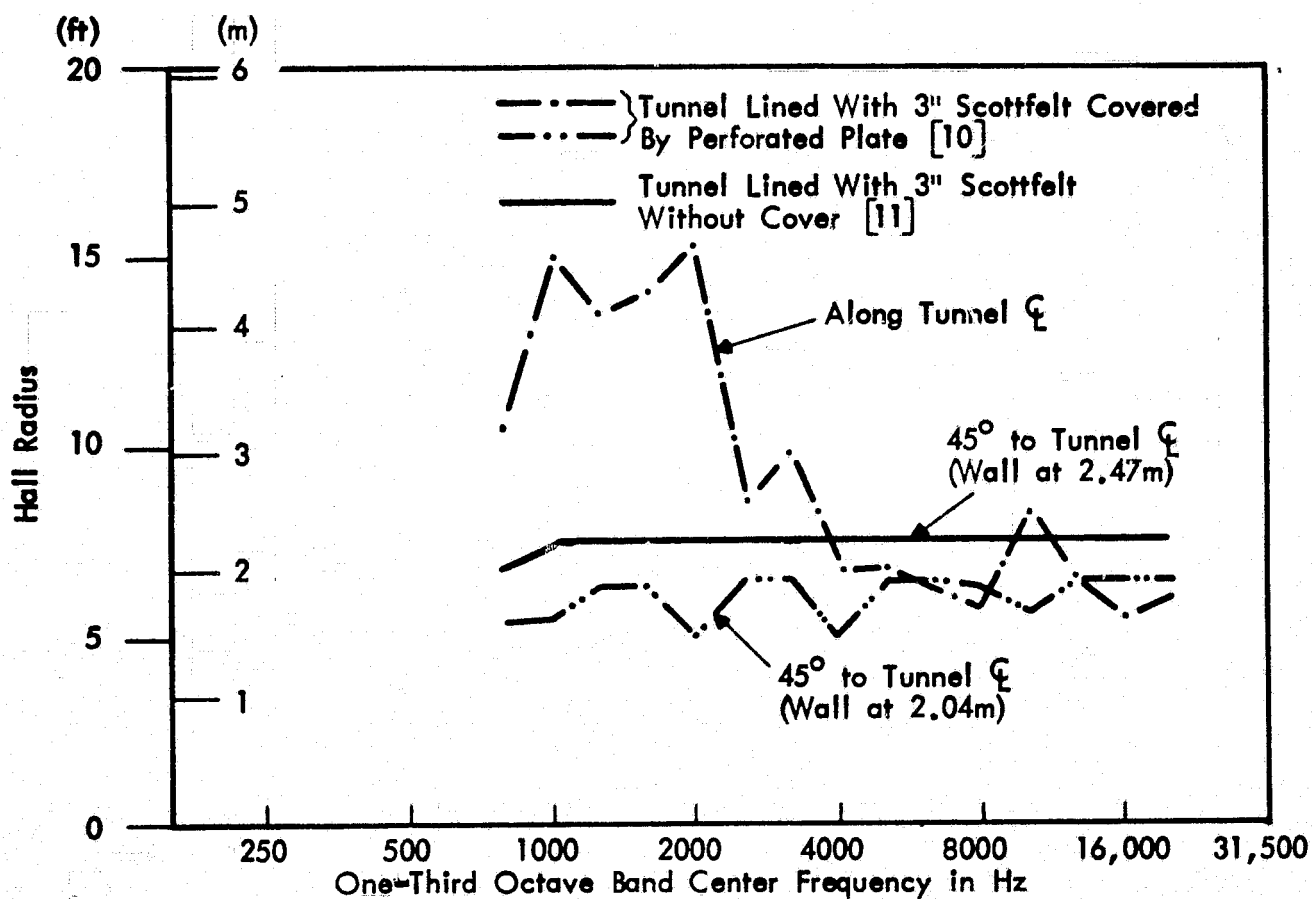
FIGURE 7b. MEASURED VALUES OF HALL RADIUS IN LINED TEST SECTION OF 7' x 10' TUNNEL

FAN SECTION
30' x 30'

30' x 30'

25' x 25'

85'

30' x 30'

20' x 20'

72'

30' x 30'

TEST SECTION 10' x 10'

15' x 15'

30'   50'   100'   50'
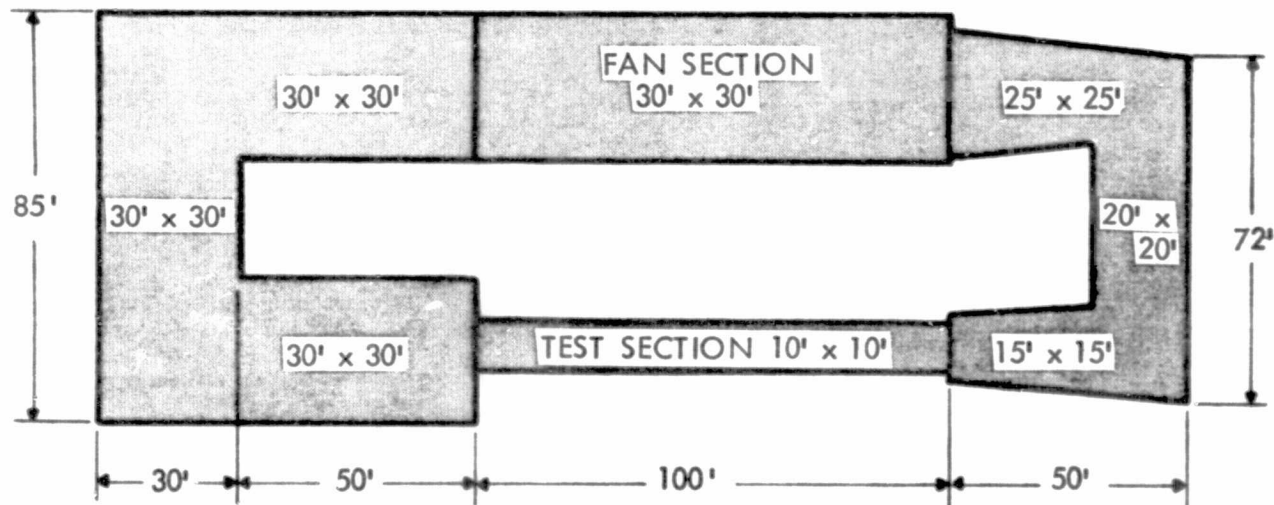
FIGURE 8.   A SIMPLIFIED ACOUSTIC MODEL OF 7' x 10' WIND TUNNEL
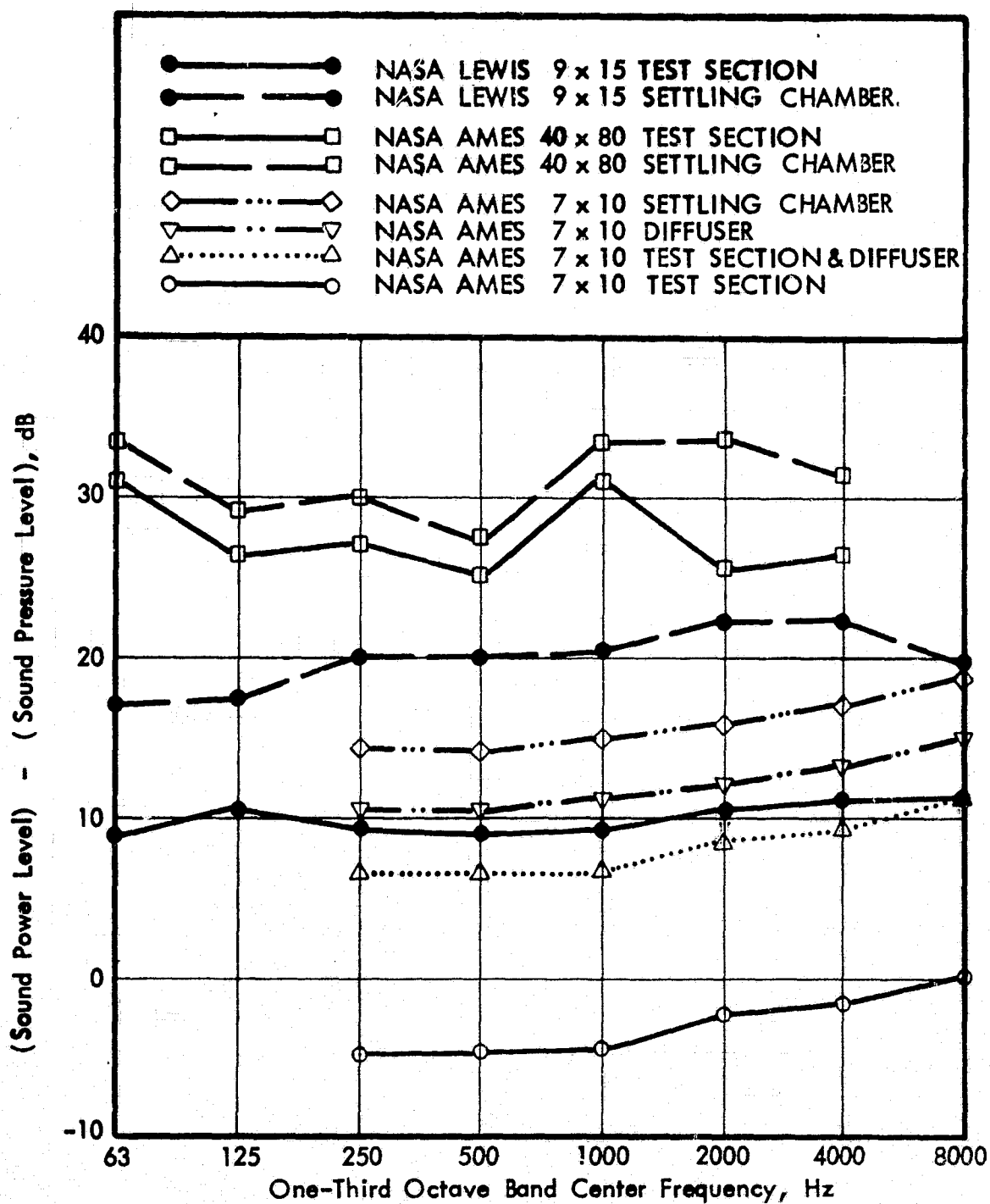
FIGURE 9. RELATIONSHIP BETWEEN SOUND POWER LEVEL AND SOUND PRESSURE LEVEL IN WIND TUNNEL
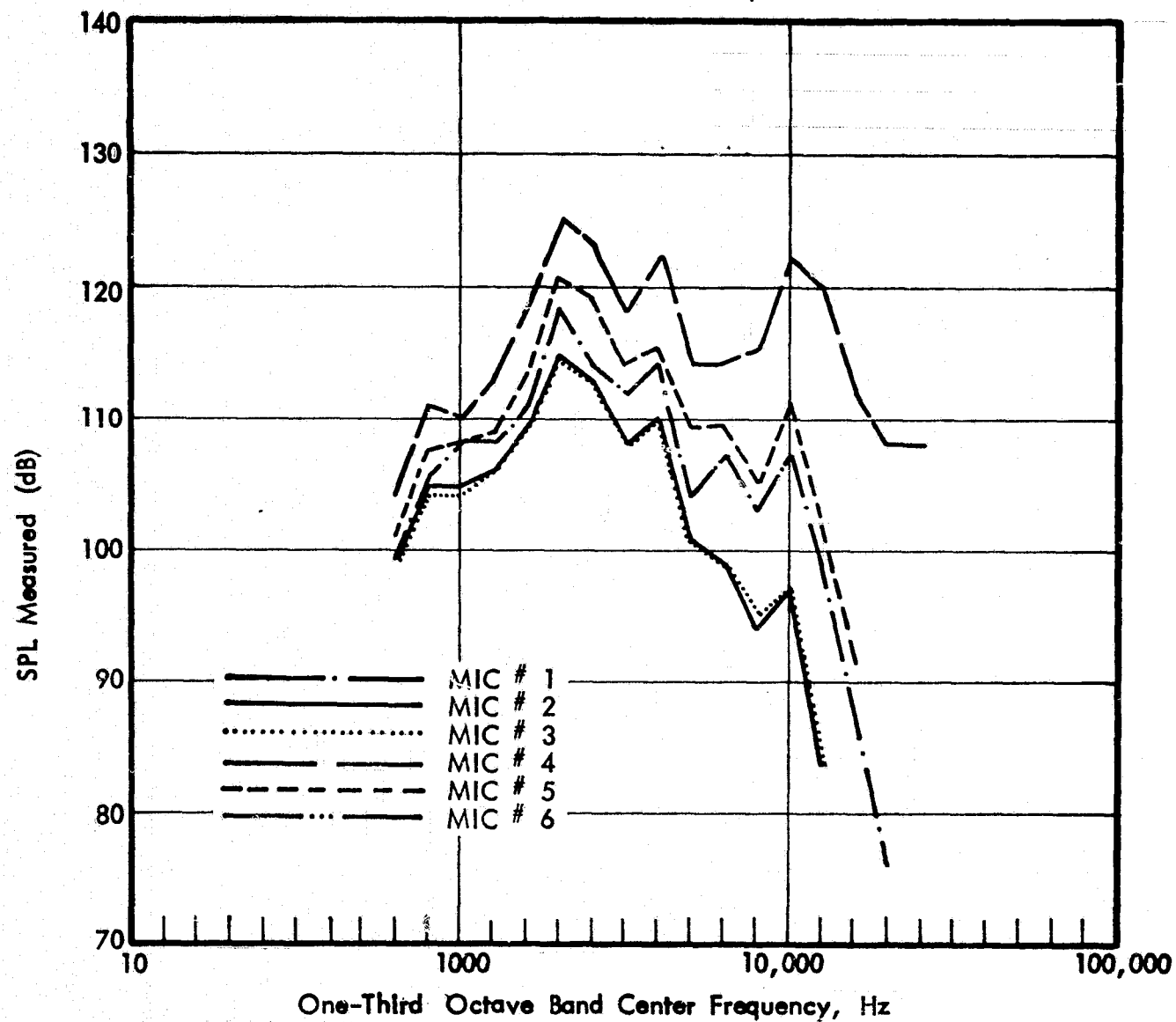
FIGURE 10. SOUND LEVELS IN TUNNEL WITH SOURCE NEAR FAN
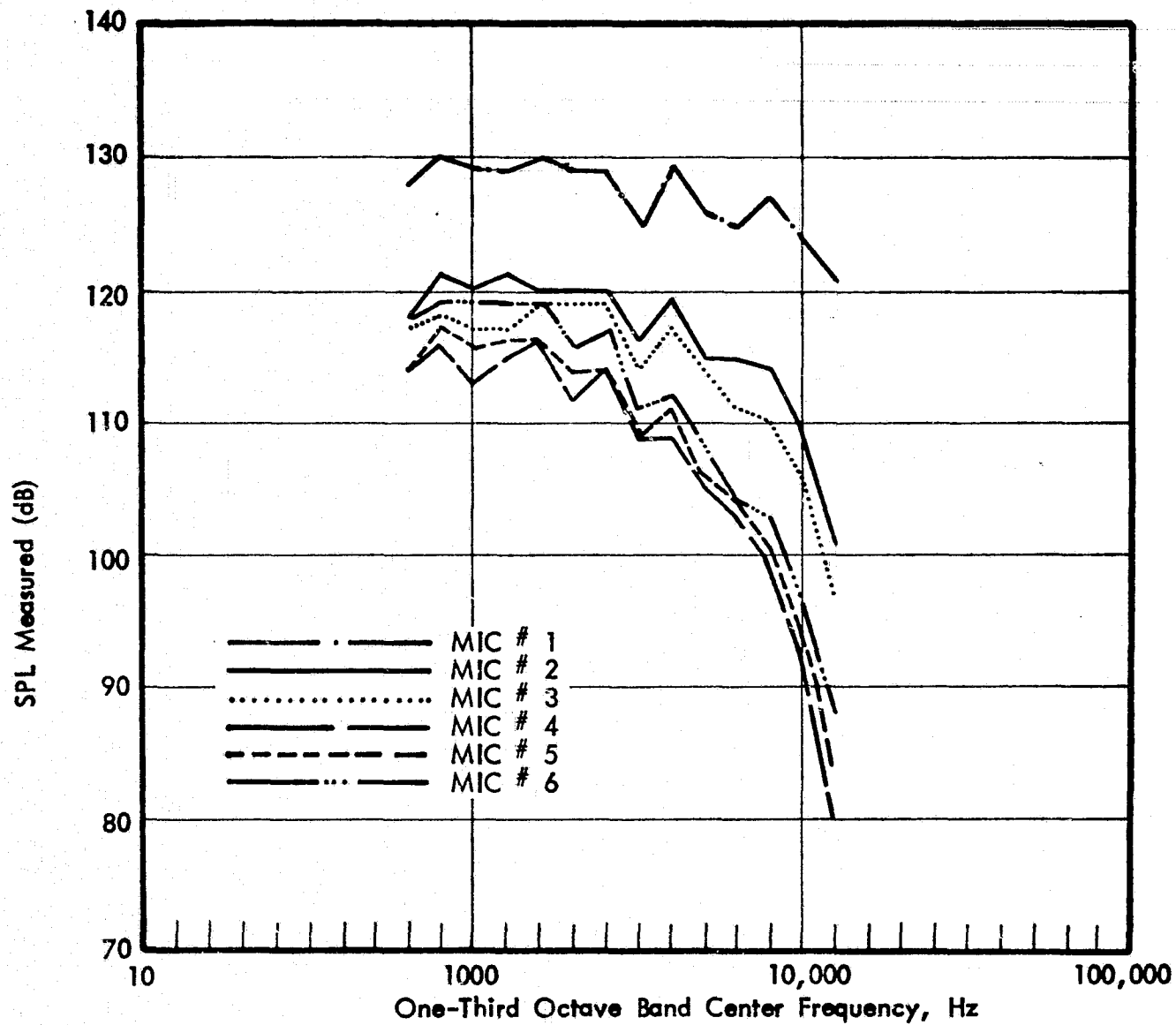
FIGURE 11. SOUND LEVELS IN TUNNEL WITH SOURCE IN TEST SECTION
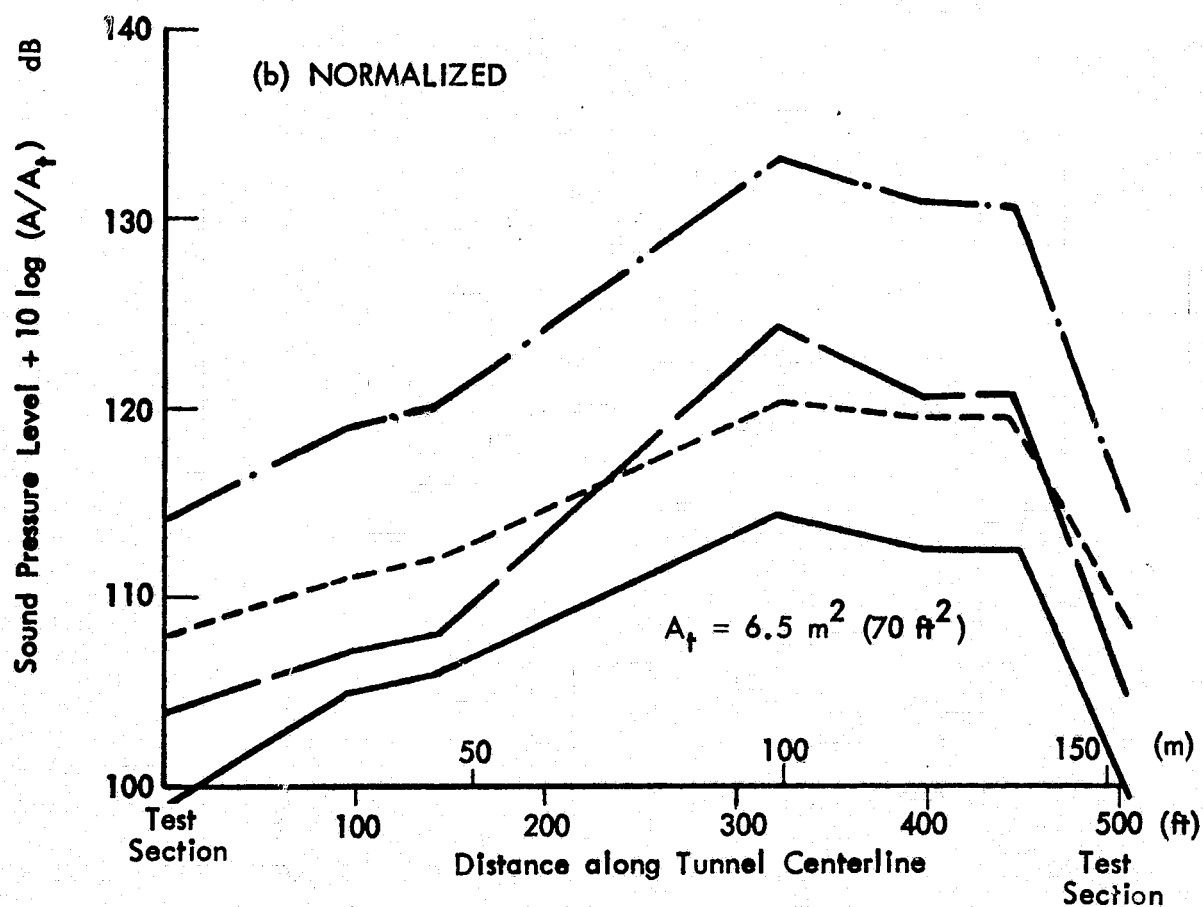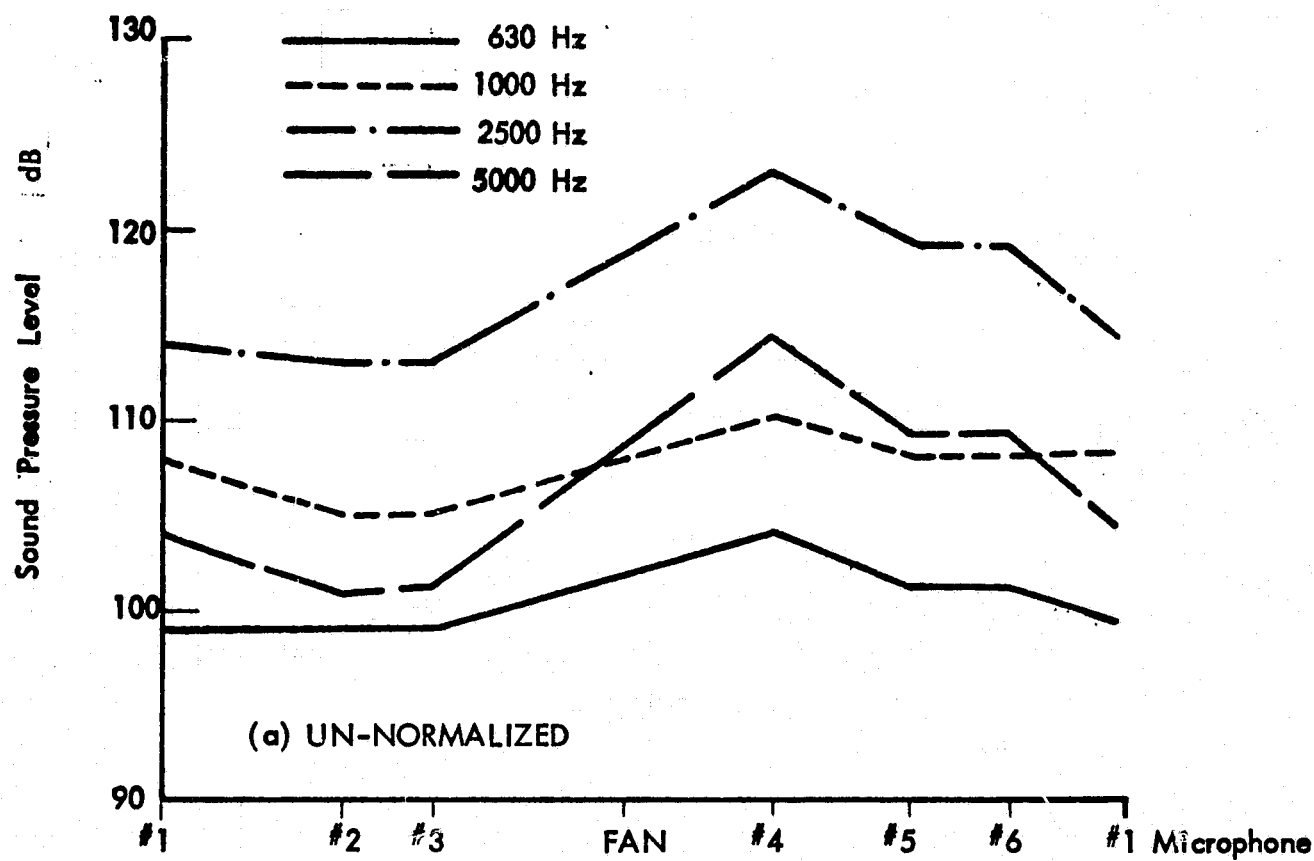
FIGURE 12.   SPATIAL DISTRIBUTION OF SOUND LEVELS WITH
SOURCE NEAR FAN
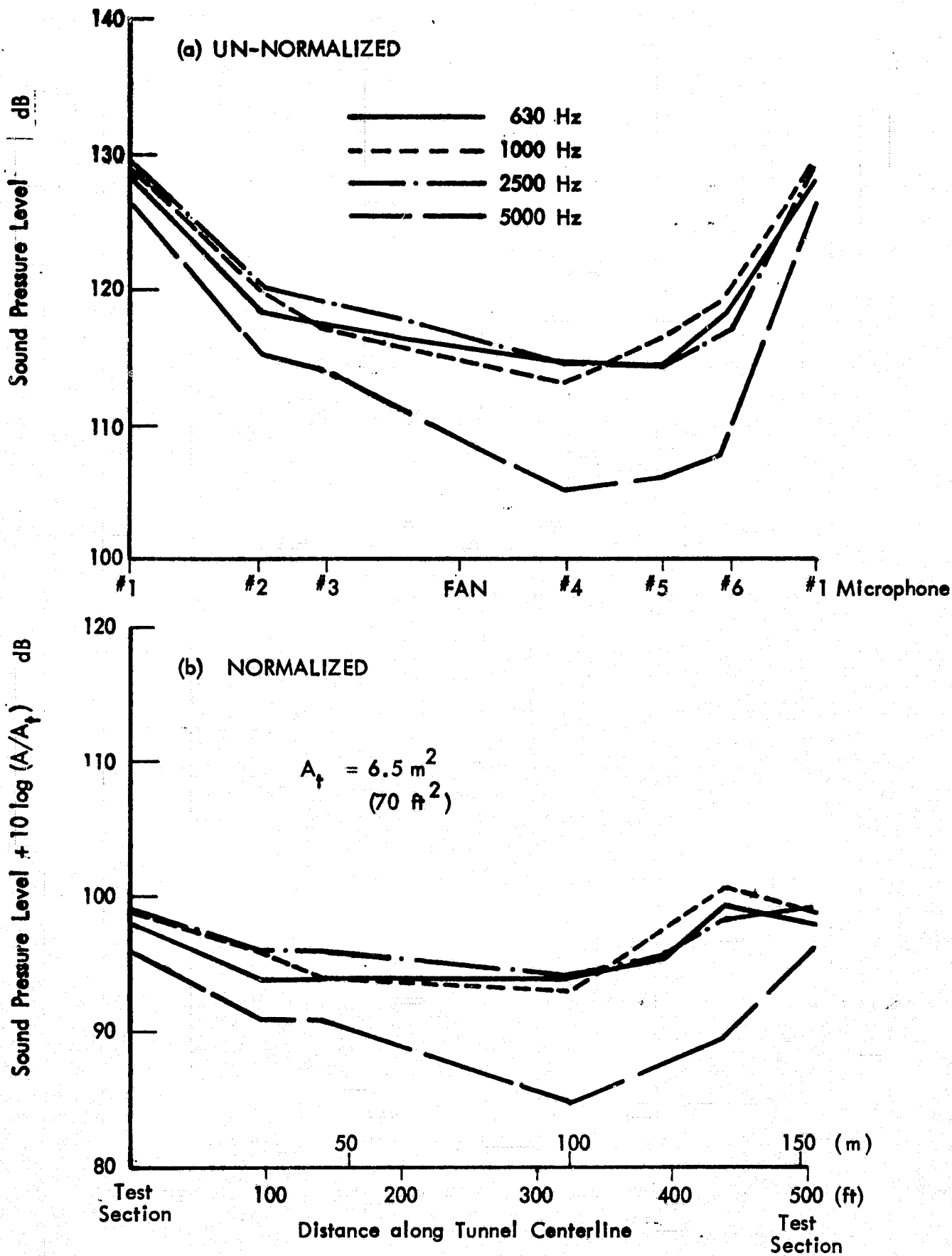
FIGURE 13. SPATICAL DISTRIBUTION OF SOUND LEVELS WITH SOURCE IN TEST SECTION
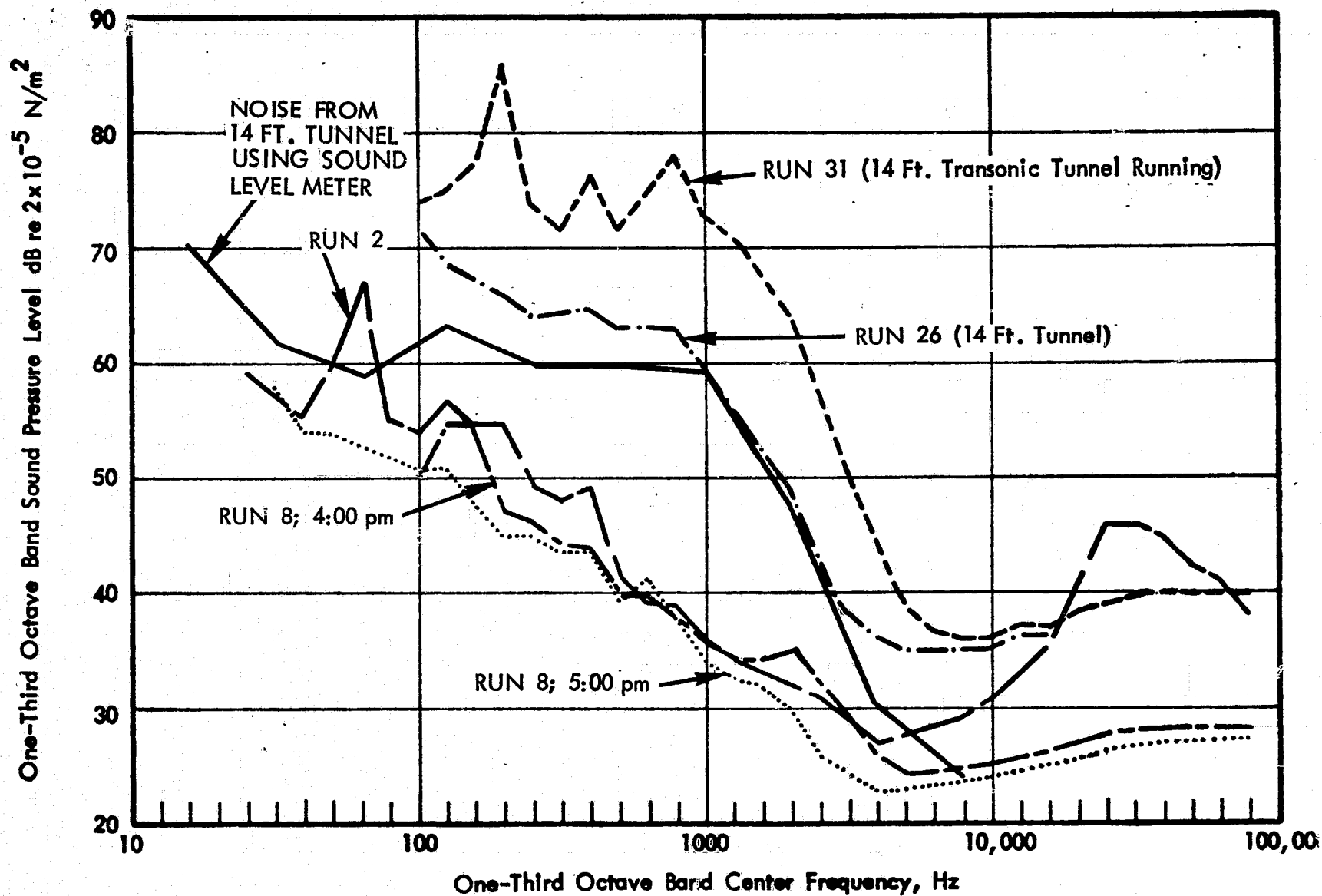
FIGURE 14.   AMBIENT NOISE LEVELS IN TEST SECTION   (NO FLOW)
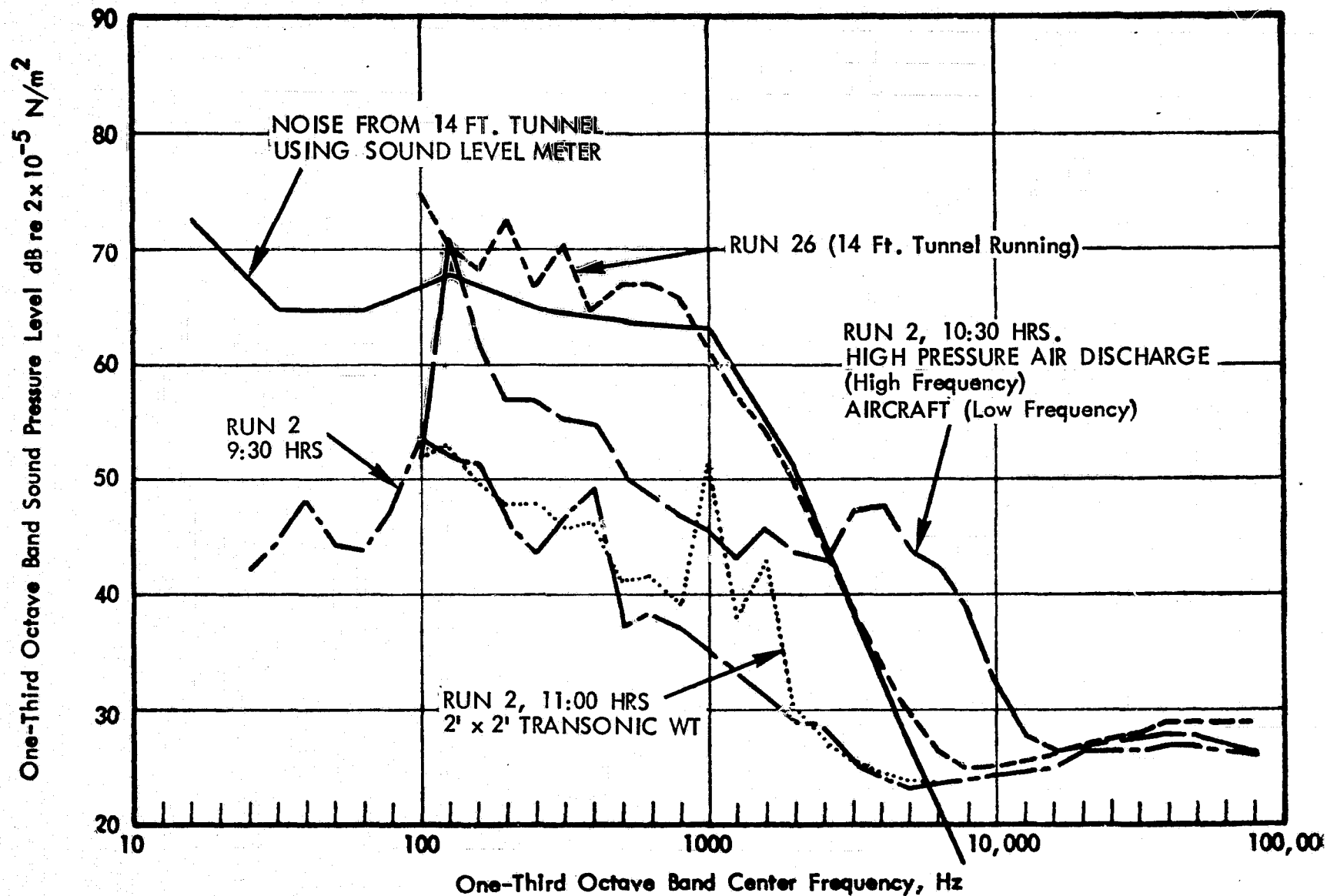
FIGURE 15. AMBIENT NOISE LEVELS IN SETTLING CHAMBER (NO FLOW)
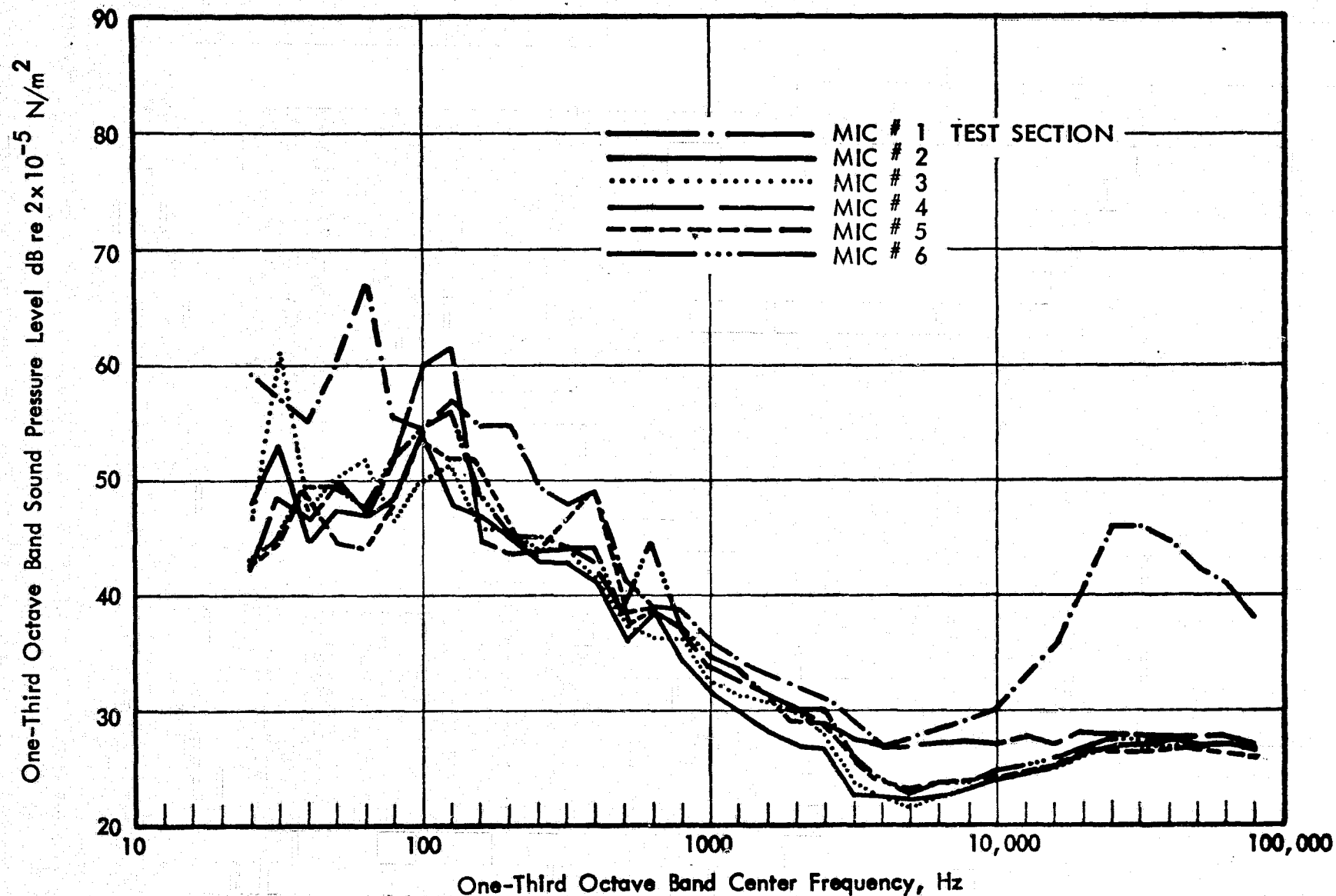
FIGURE 16. AMBIENT NOISE LEVELS IN TUNNEL DURING "QUIET" PERIOD (NO FLOW)
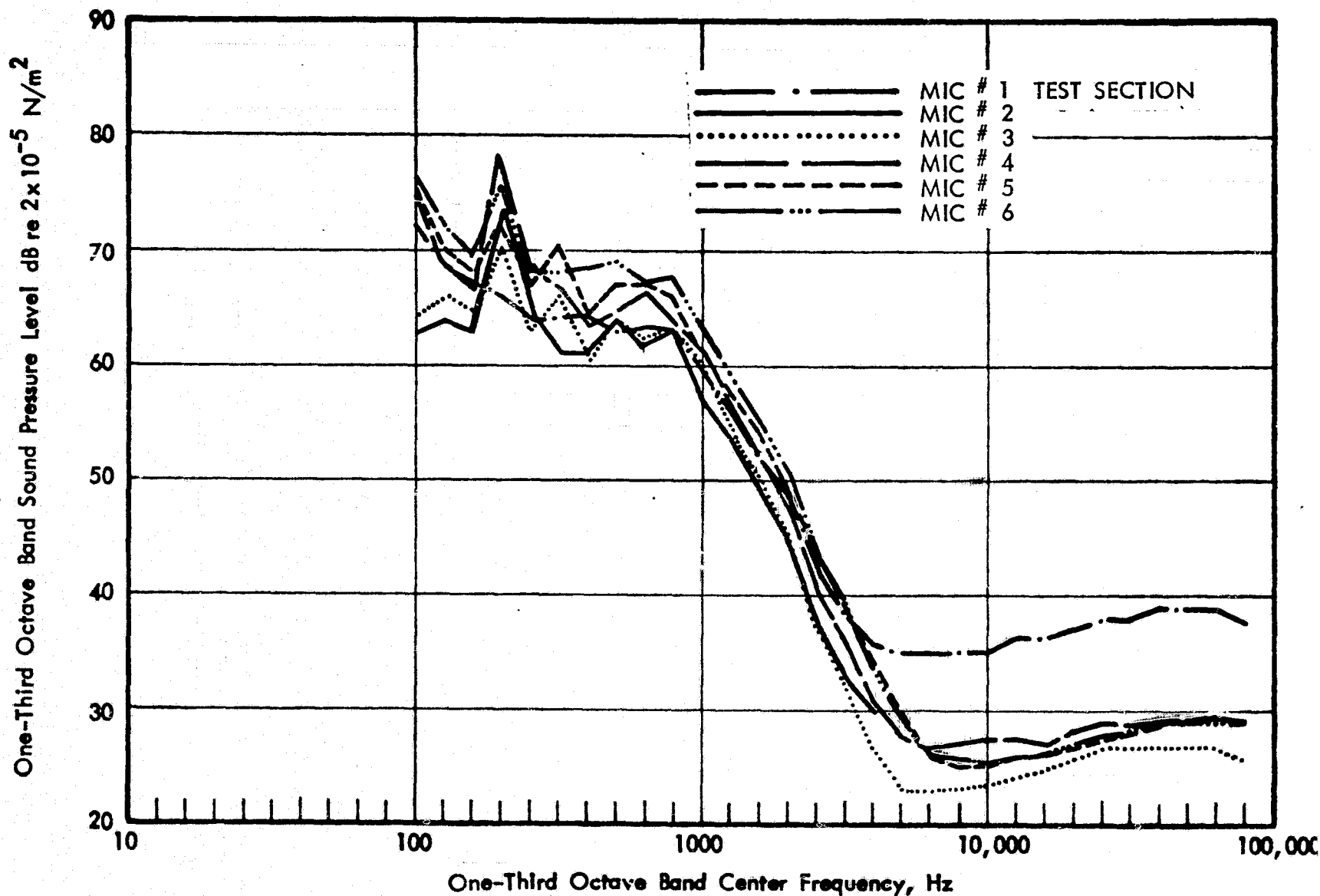
FIGURE 17. AMBIENT NOISE LEVELS IN TUNNEL WHEN 14 FOOT TRANSONIC TUNNEL OPERATING
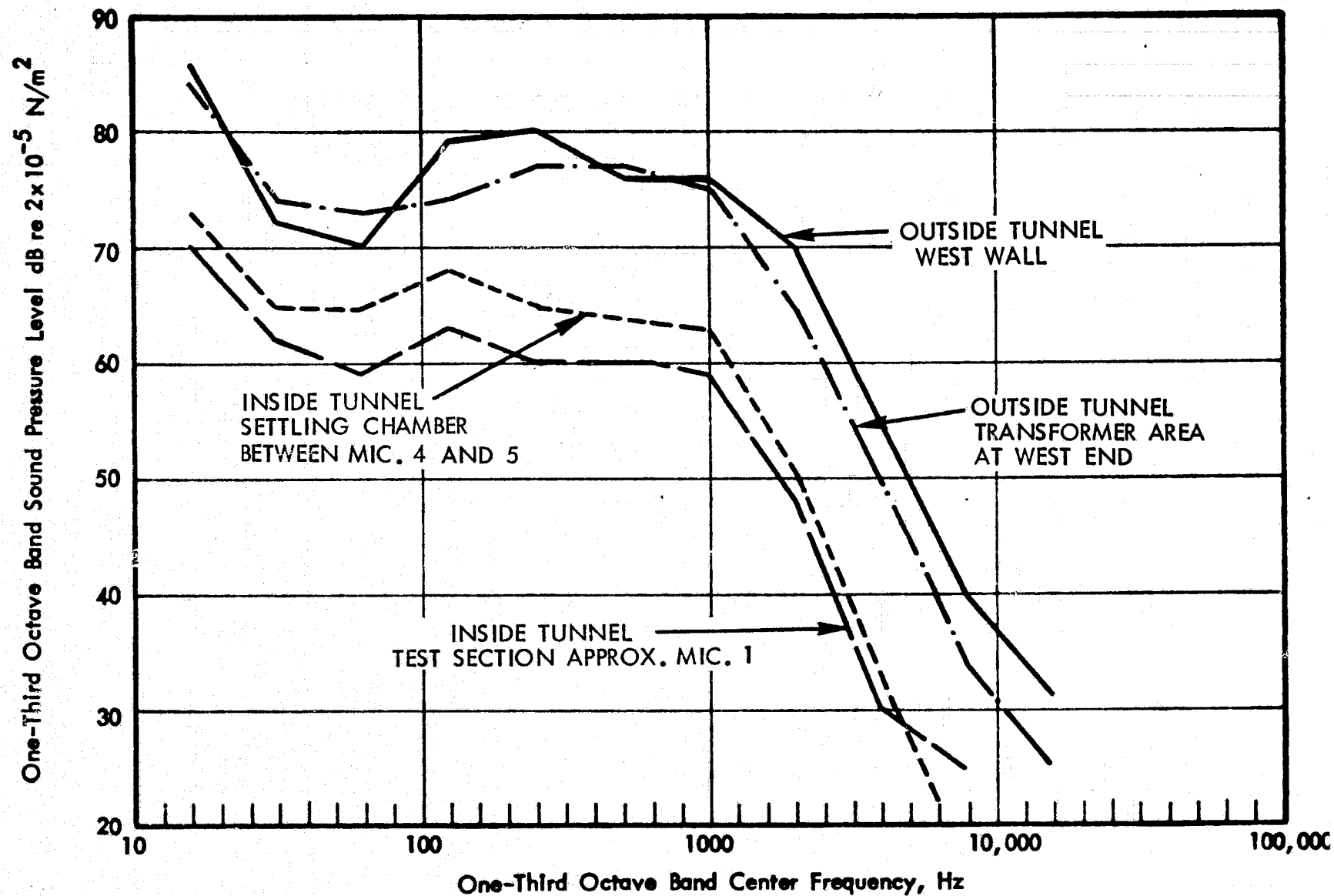
FIGURE 18.   INTERNAL AND EXTERNAL NOISE LEVELS FOR 7' x 10' TUNNEL WHEN 14-FOOT TRANSONIC TUNNEL OPERATING
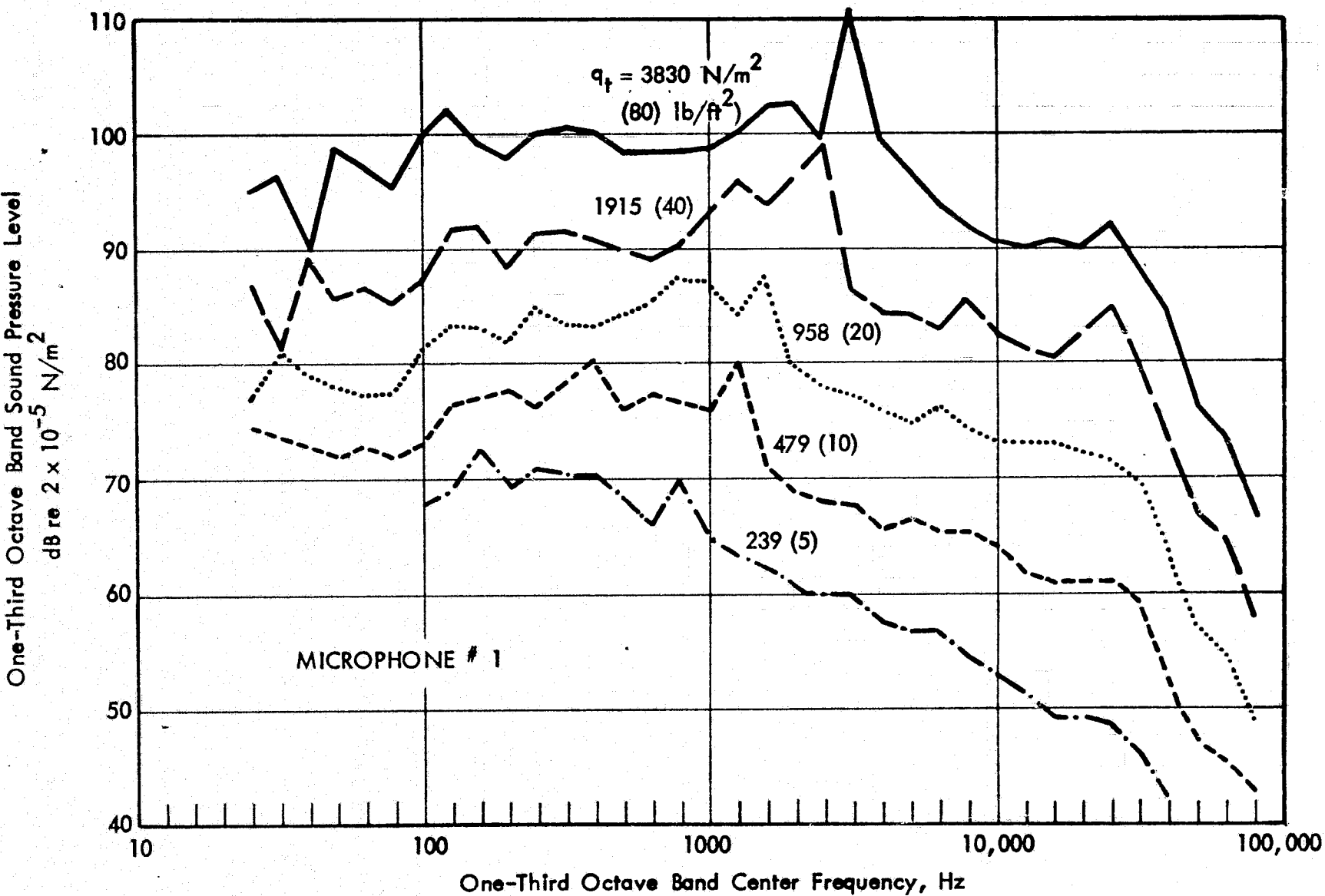
FIGURE 19.   NOISE LEVELS IN TEST SECTION WITH FLOW
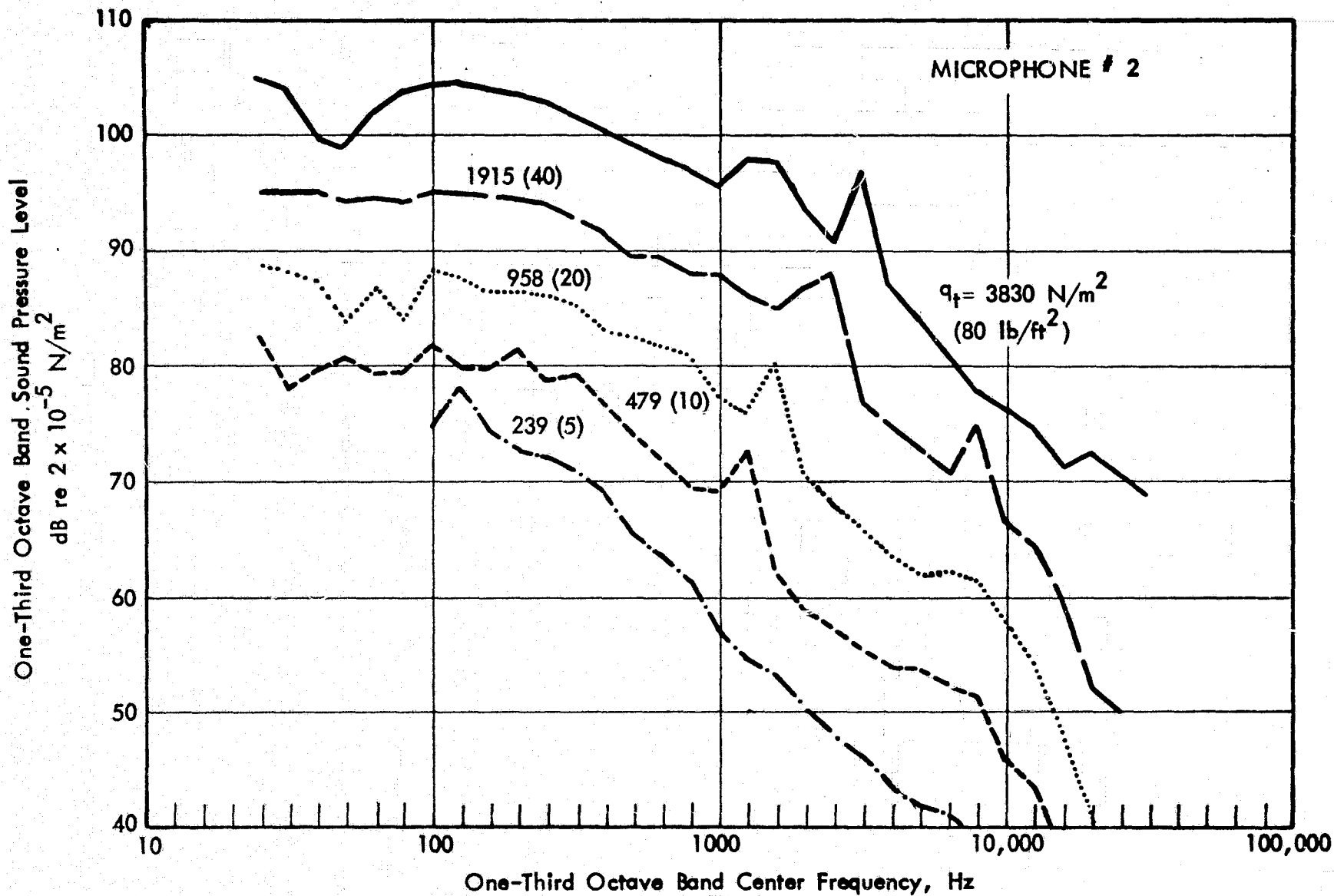
FIGURE 20.   NOISE LEVELS IN DIFFUSER (#2) WITH FLOW
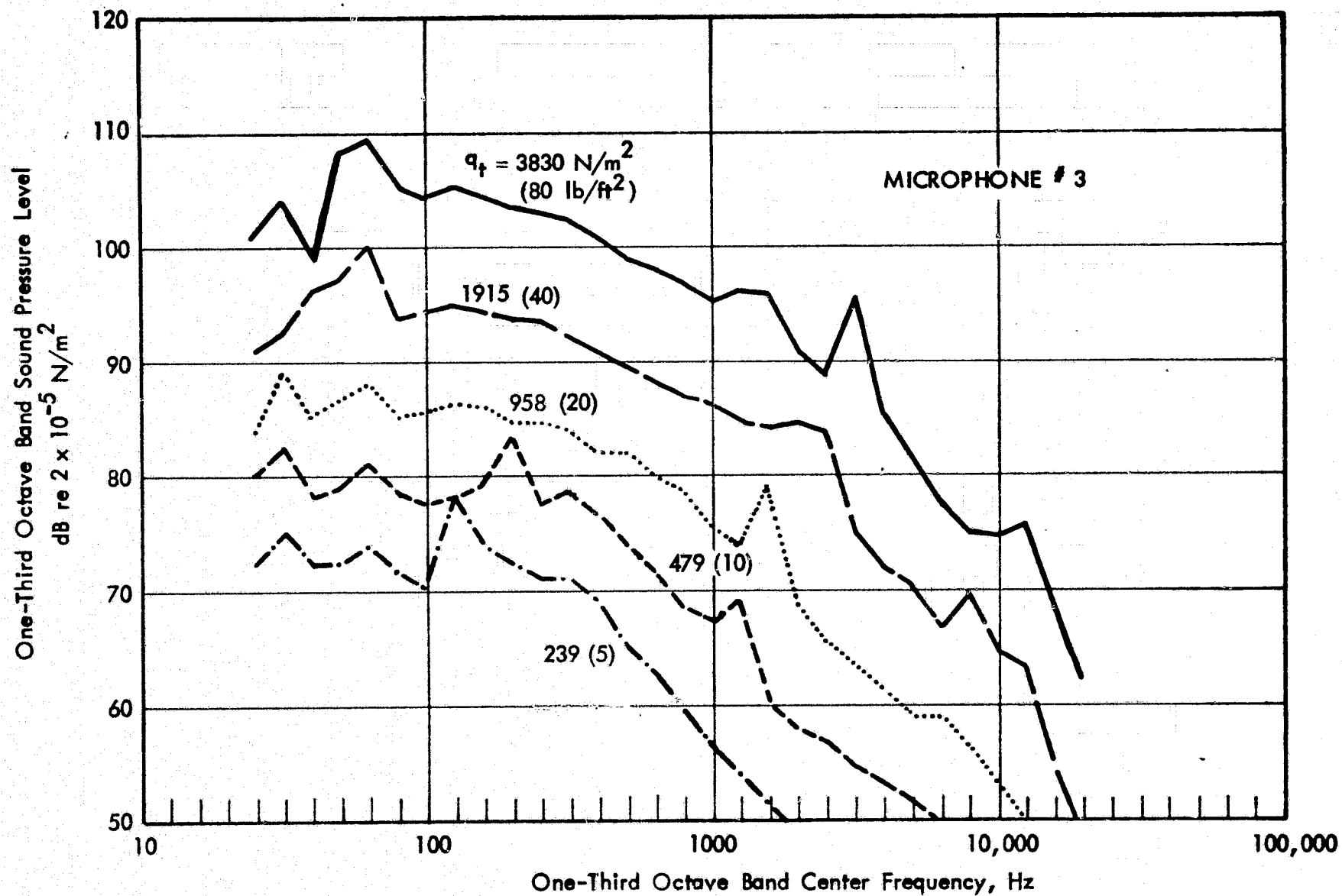
FIGURE 21.   NOISE LEVELS IN DIFFUSER (#3) WITH FLOW
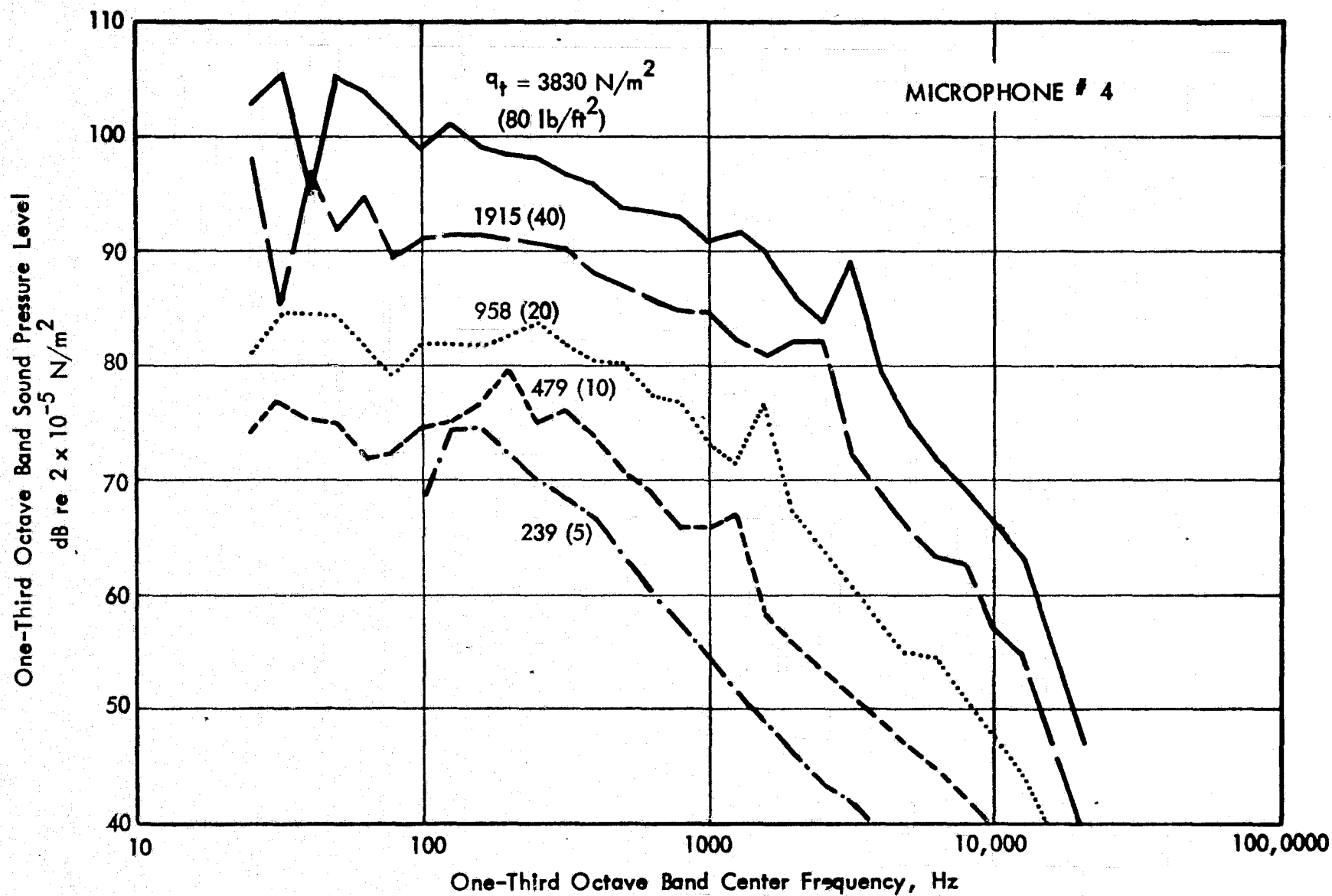
FIGURE 22. NOISE LEVELS IN SETTLING CHAMBER (#4) WITH FLOW
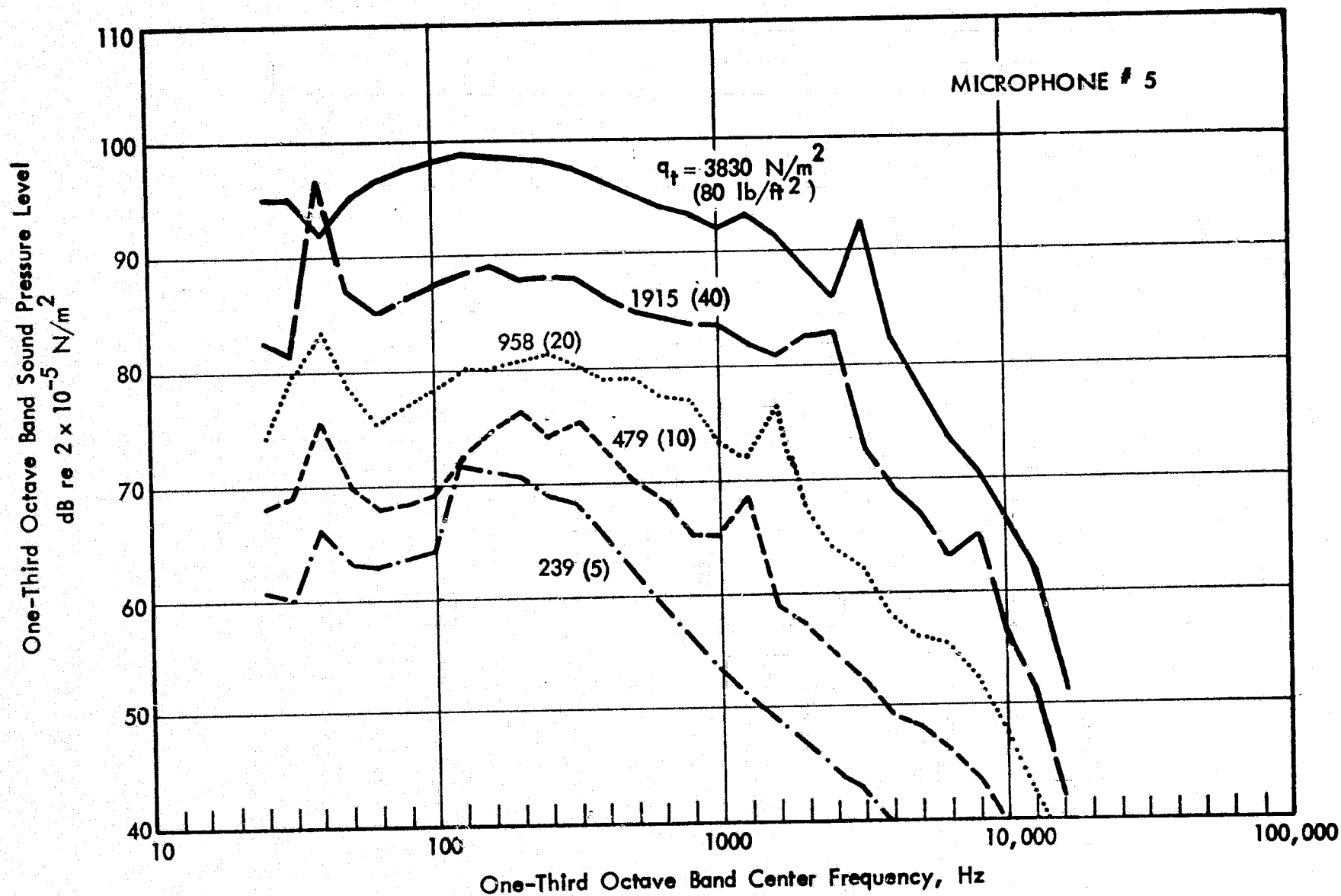
FIGURE 23.   NOISE LEVELS IN SETTLING CHAMBER (#5) WITH FLOW
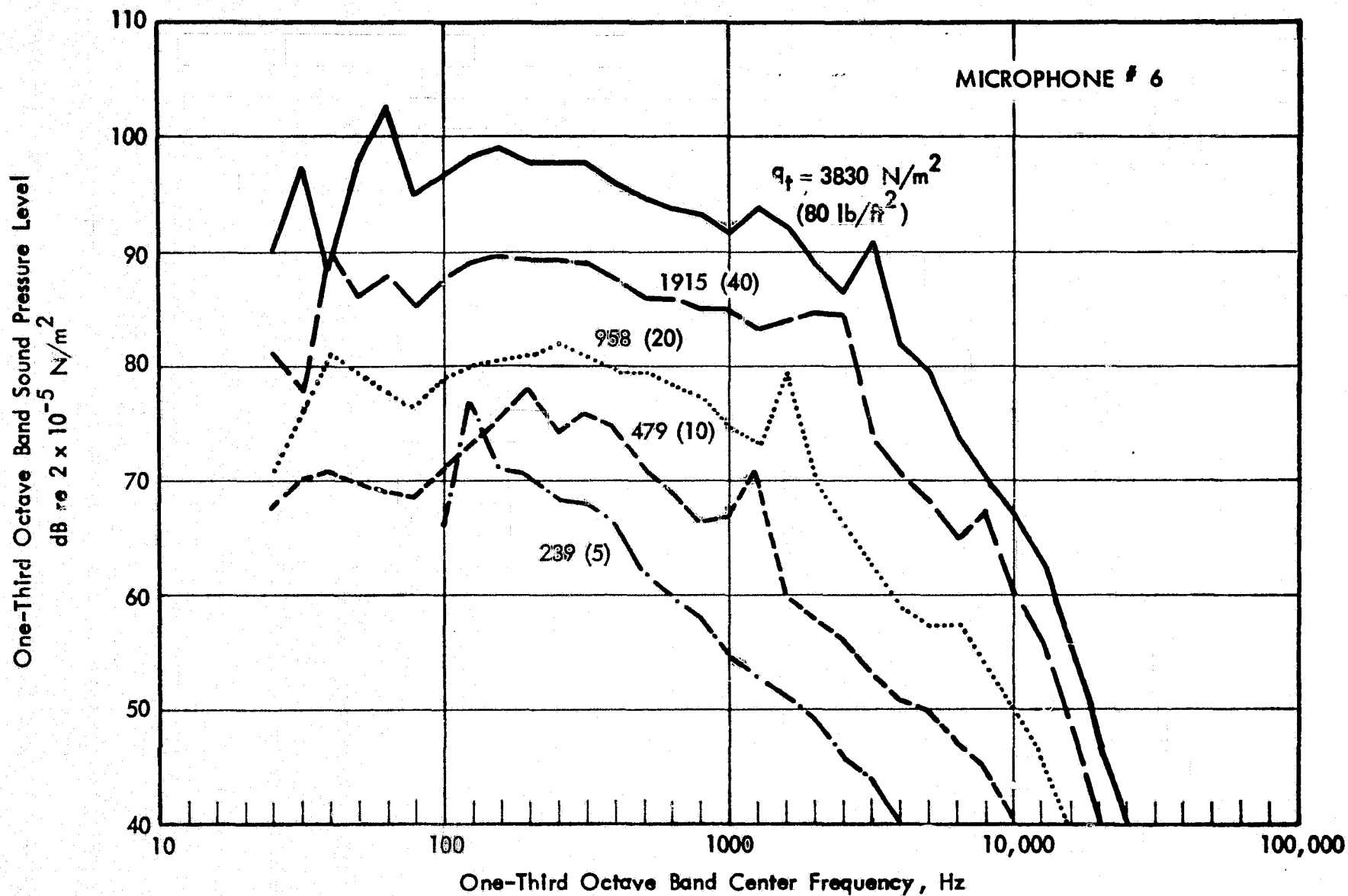
FIGURE 24.   NOISE LEVELS IN SETTLING CHAMBER (#6) WITH FLOW
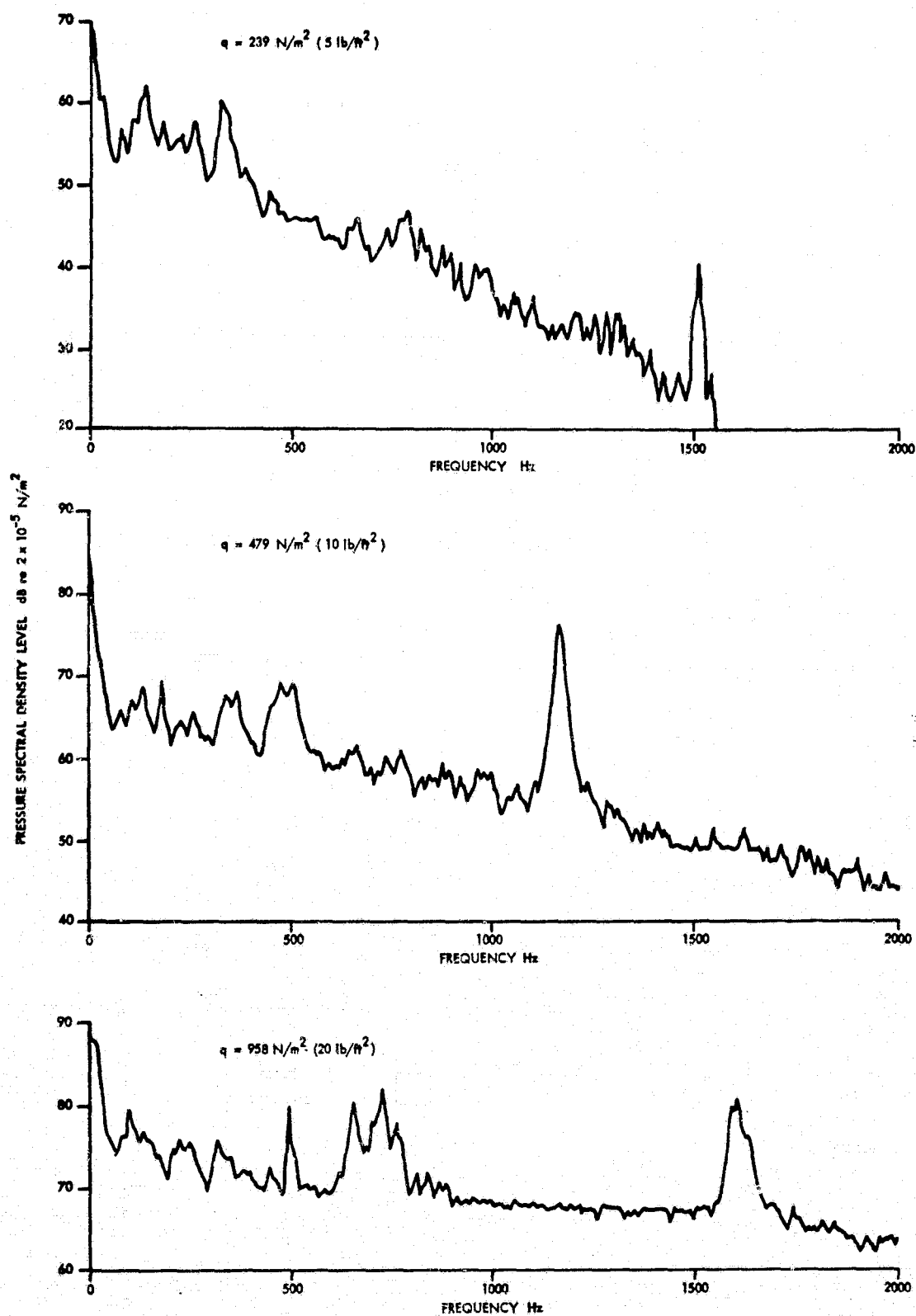
FIGURE 25.   NARROWBAND SPECTRA OF TEST SECTION NOISE
LEVELS (FILTER BANDWIDTH 5Hz)
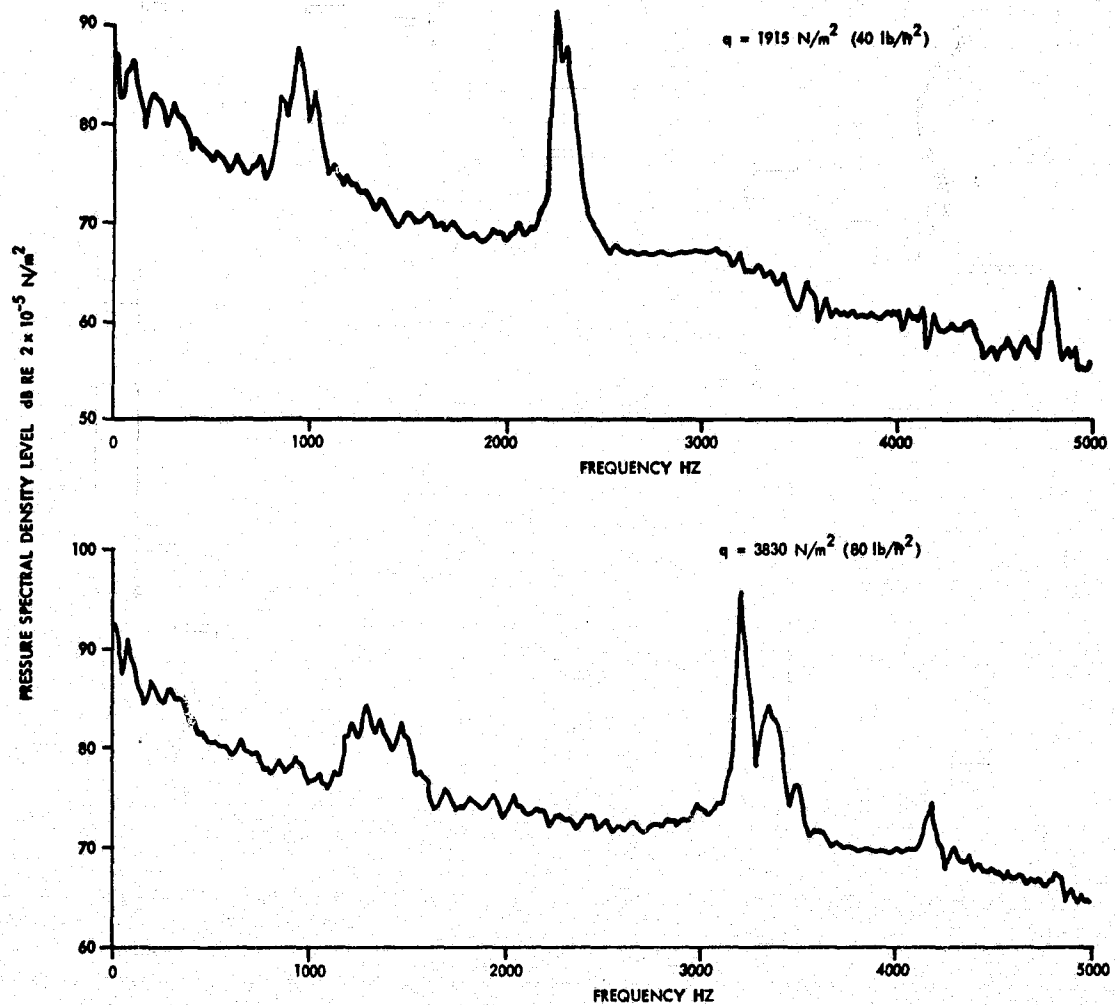
FIGURE 25 (CONT.)   NARROWBAND SPECTRA OF TEST
SECTION NOISE LEVELS
(FILTER BANDWIDTH 12.5 Hz)

C-2
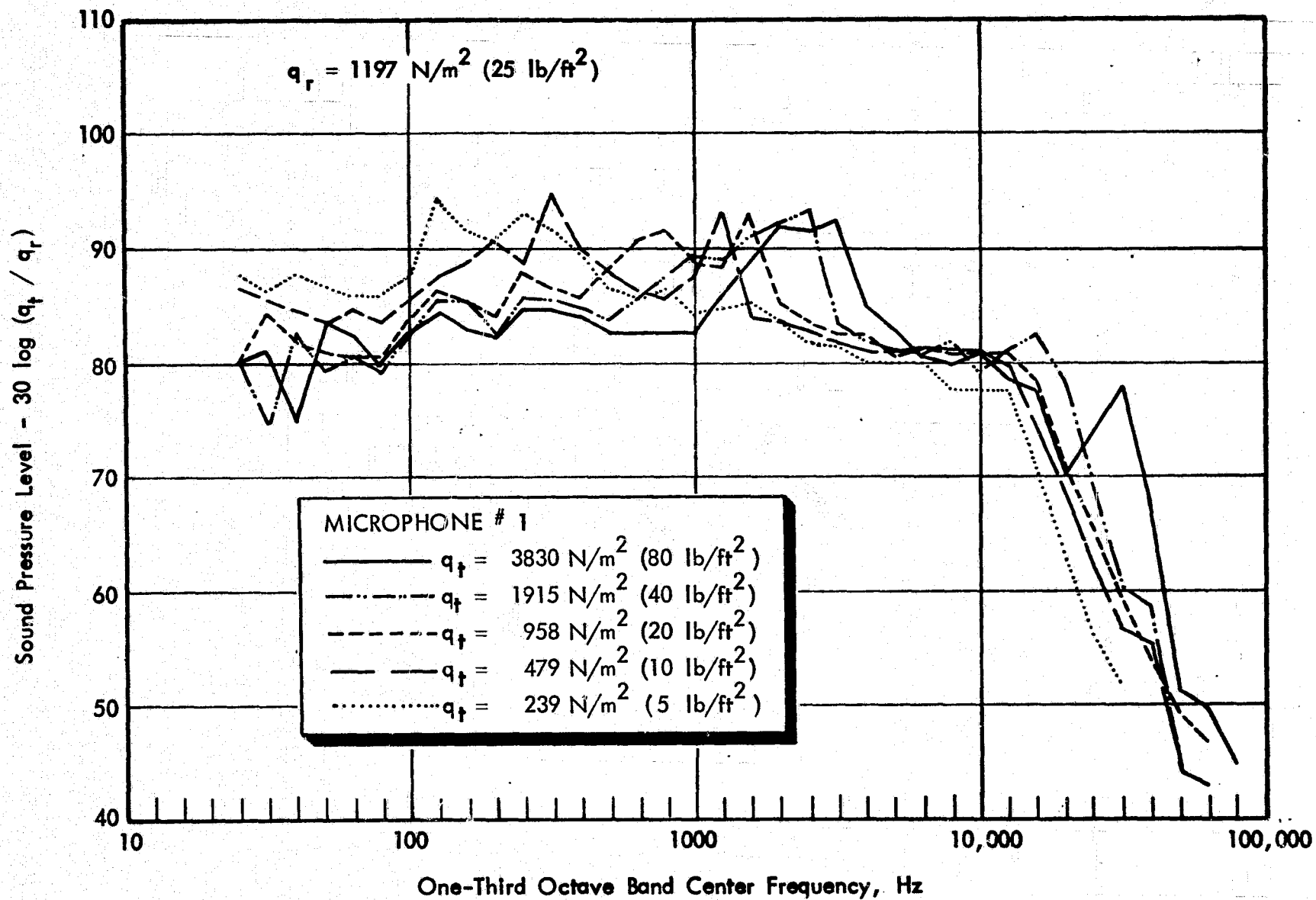
FIGURE 26. TEST SECTION SOUND LEVELS NORMALIZED WITH RESPECT TO TEST SECTION DYNAMIC PRESSURE
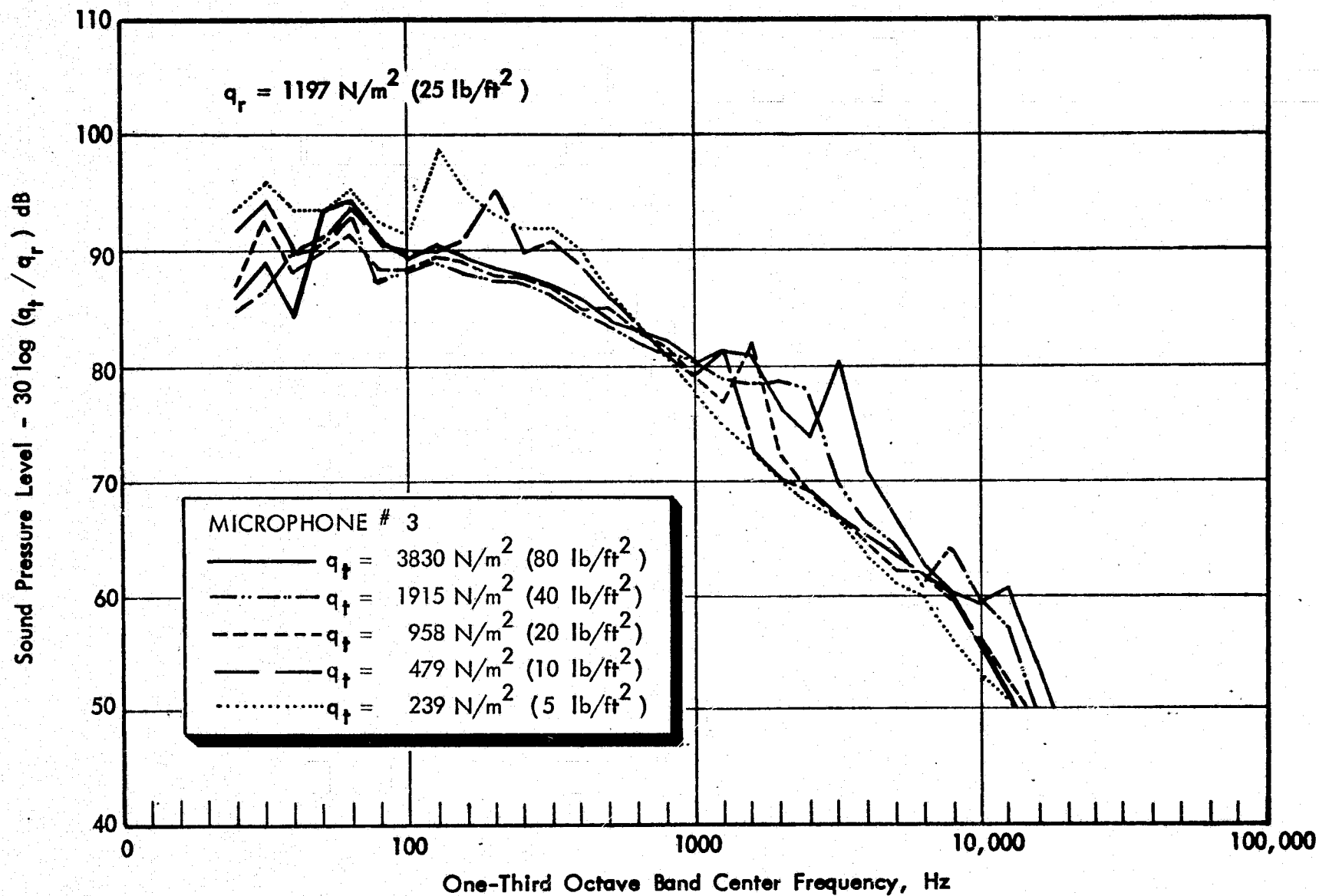
FIGURE 27. DIFFUSER SOUND LEVELS NORMALIZED WITH RESPECT TO TEST SECTION DYNAMIC PRESSURE
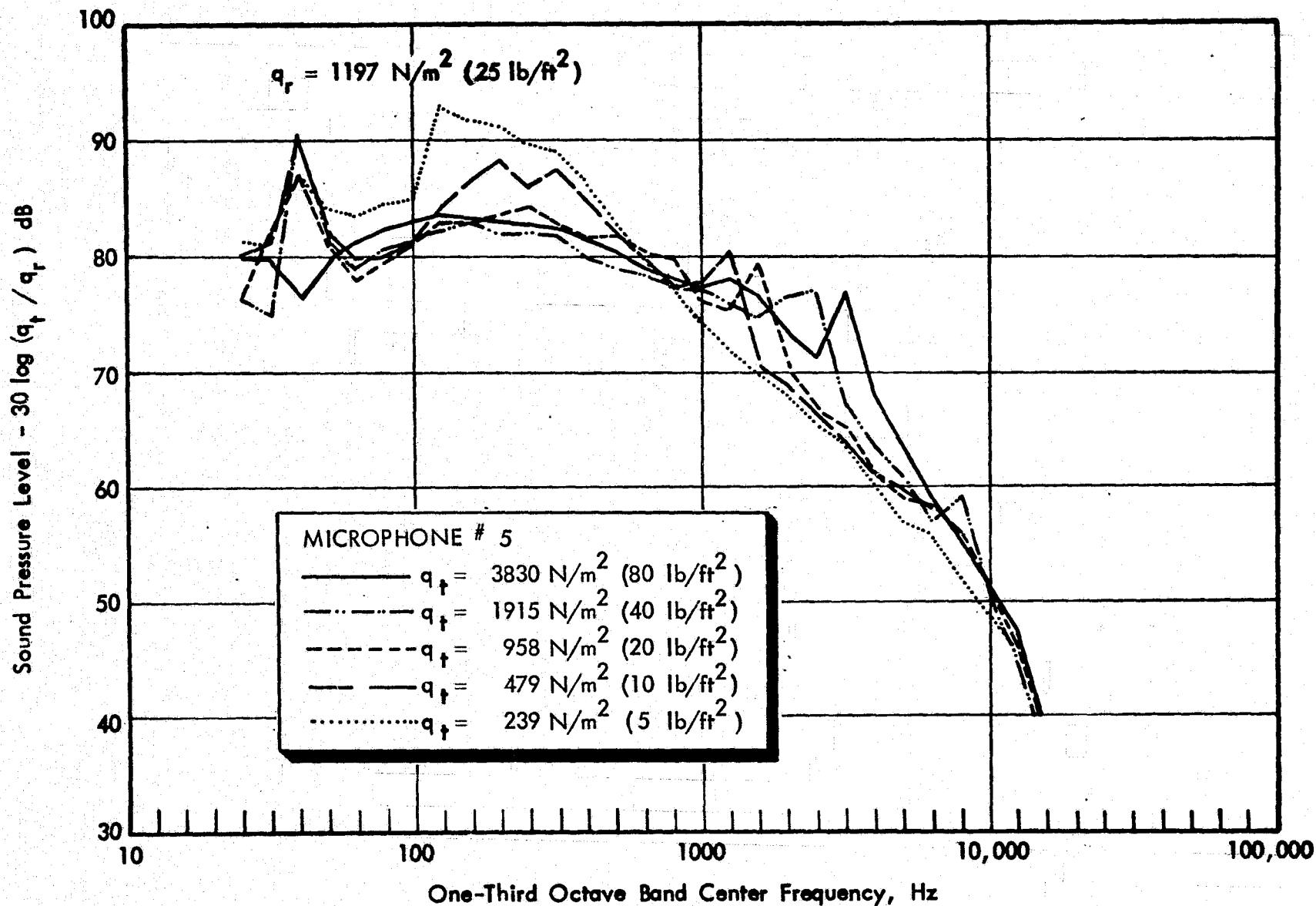
FIGURE 28. SETTLING CHAMBER SOUND LEVELS NORMALIZED WITH RESPECT TO TEST SECTION DYNAMIC PRESSURE
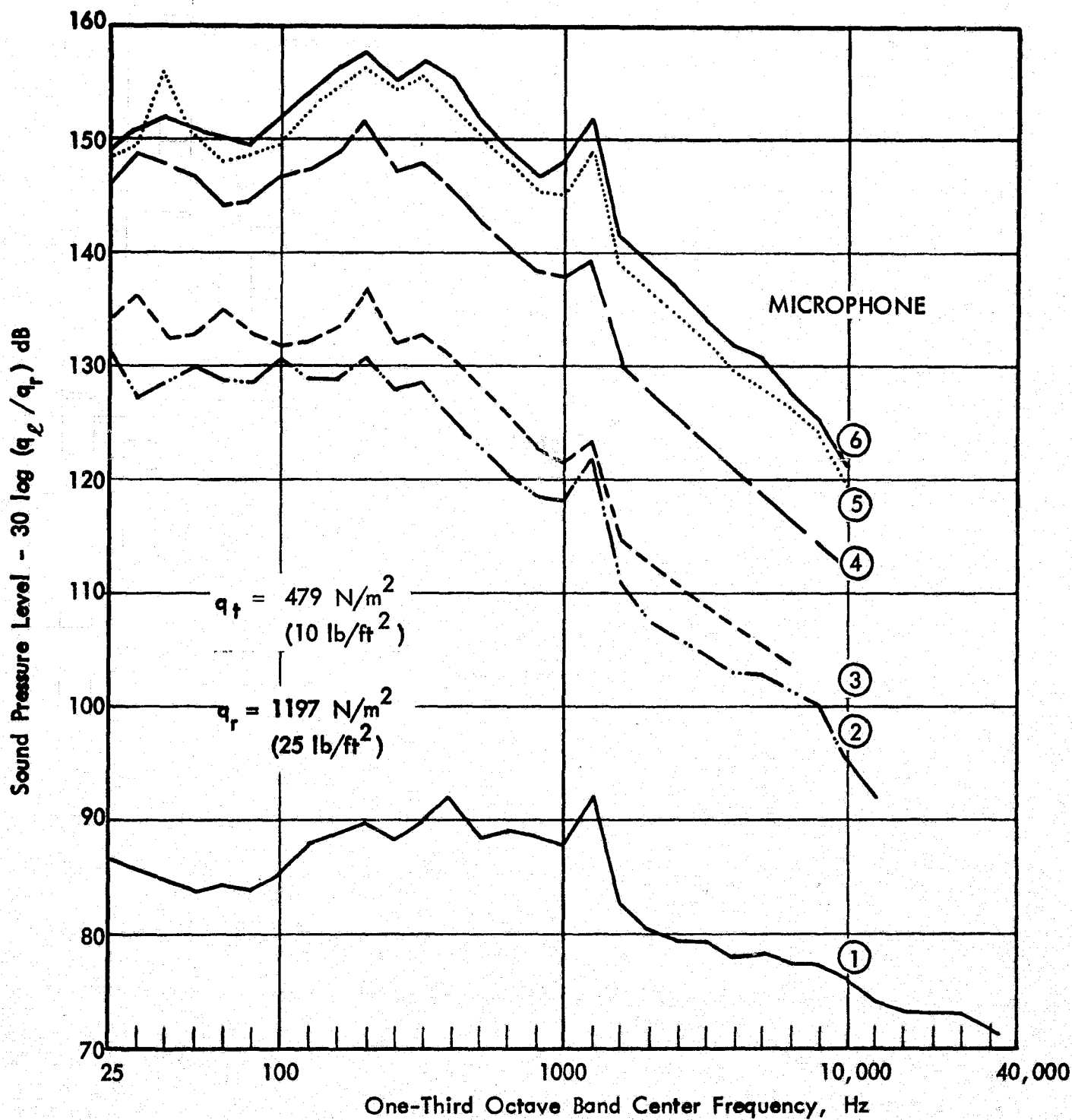
FIGURE 29. TUNNEL NOISE SPECTRA NORMALIZED WITH
RESPECT TO LOCAL DYNAMIC PRESSURE

$(q_t = 479 \ N/m^2)$
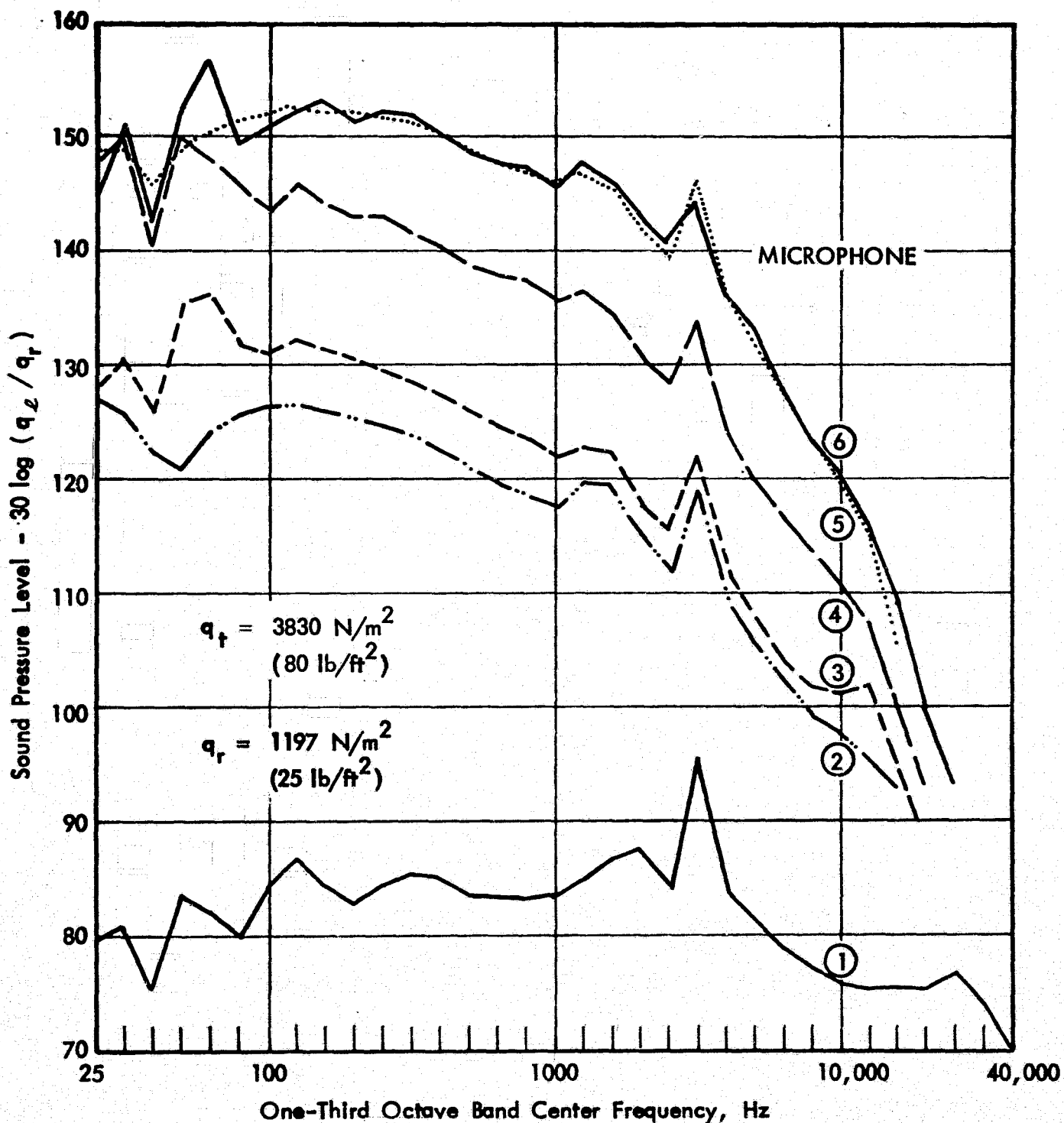
FIGURE 30.   TUNNEL NOISE SPECTRA NORMALIZED WITH RESPECT TO LOCAL DYNAMIC PRESSURE (q_t = 3830 N/m^2)
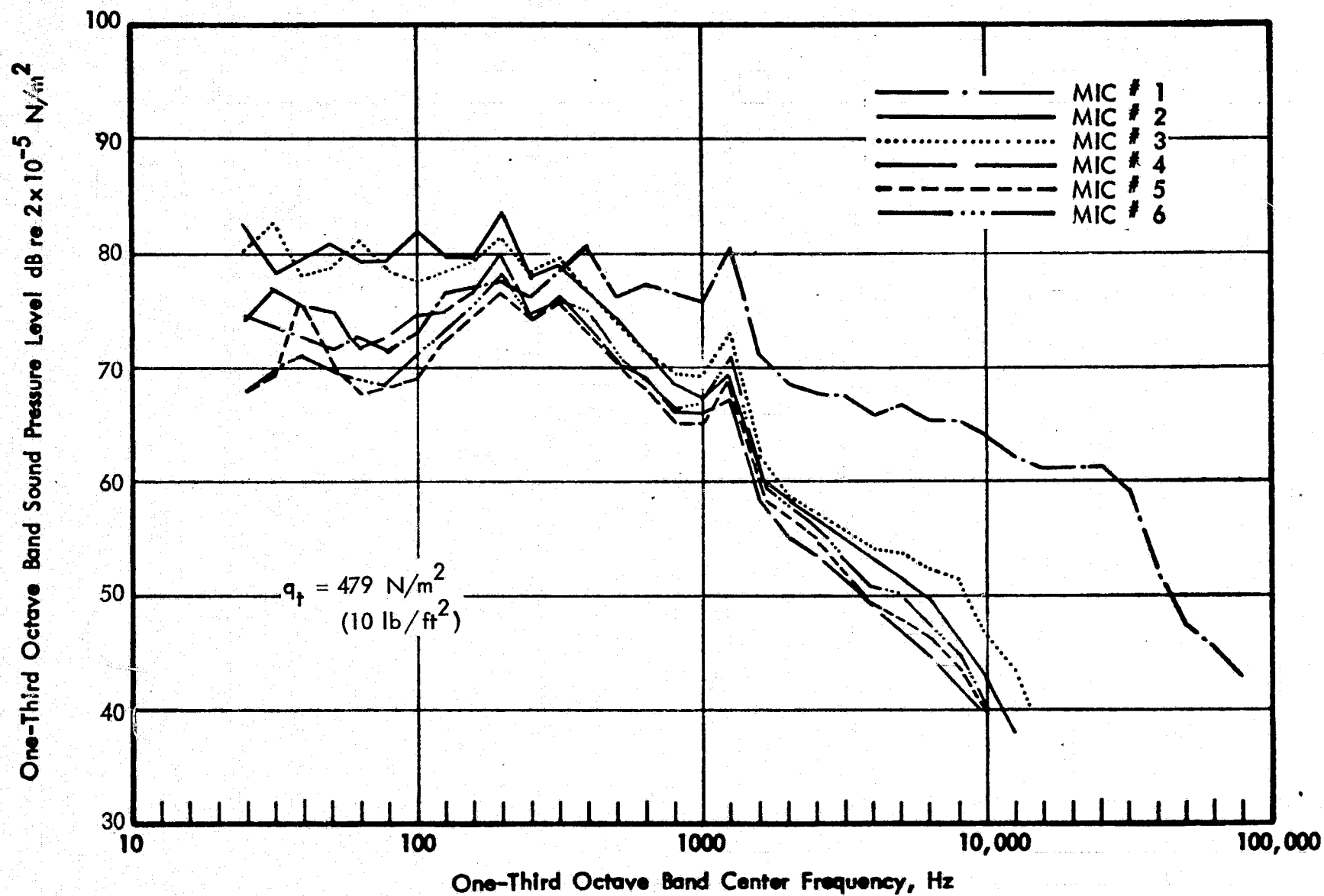
FIGURE 31.   COMPARISON OF SOUND LEVELS AT DIFFERENT LOCATIONS IN
TUNNEL (q_t = 479 N/m^2)
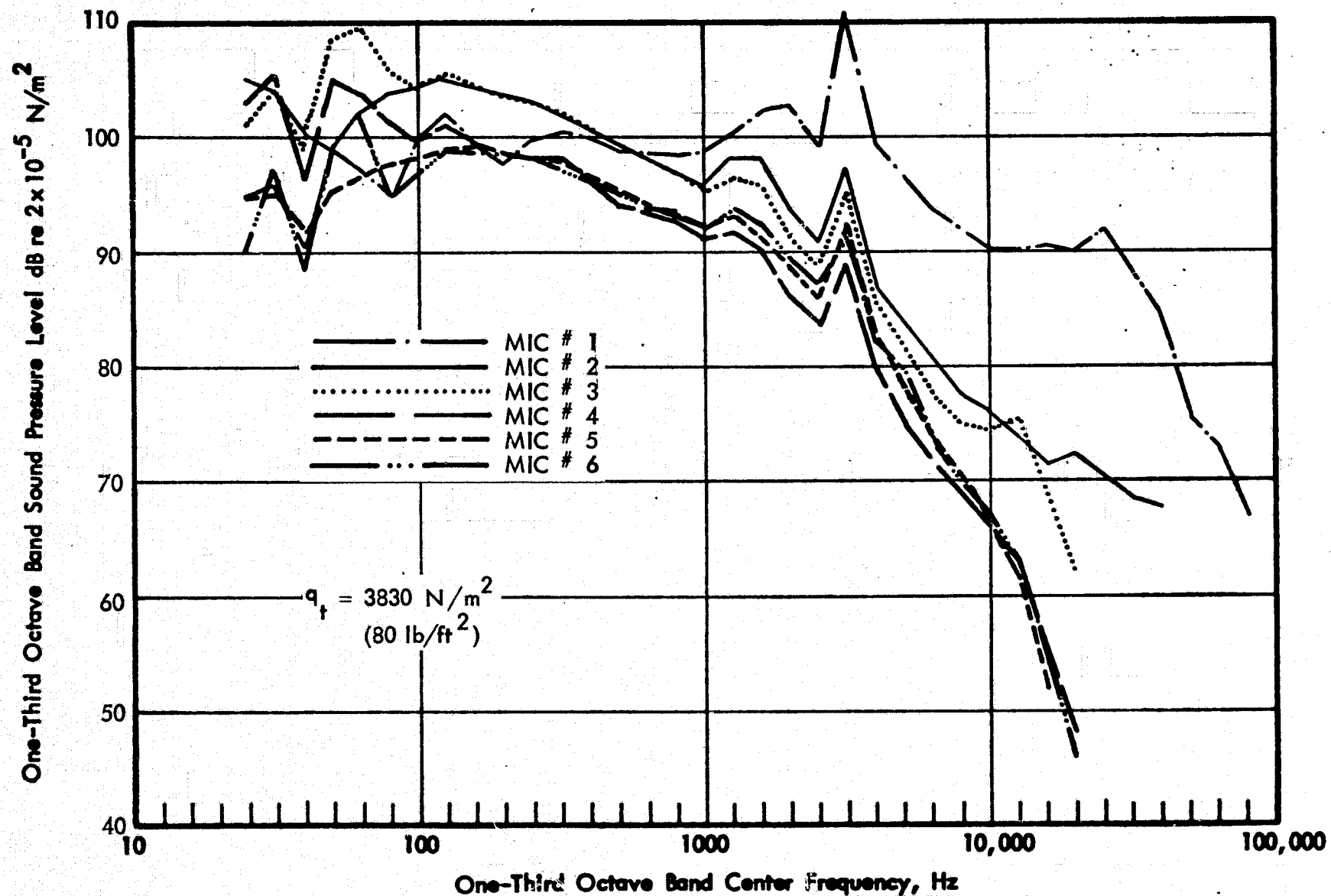
FIGURE 32. COMPARISON OF SOUND LEVELS AT DIFFERENT LOCATIONS IN TUNNEL
$(q_t = 3830 \text{ N/m}^2)$
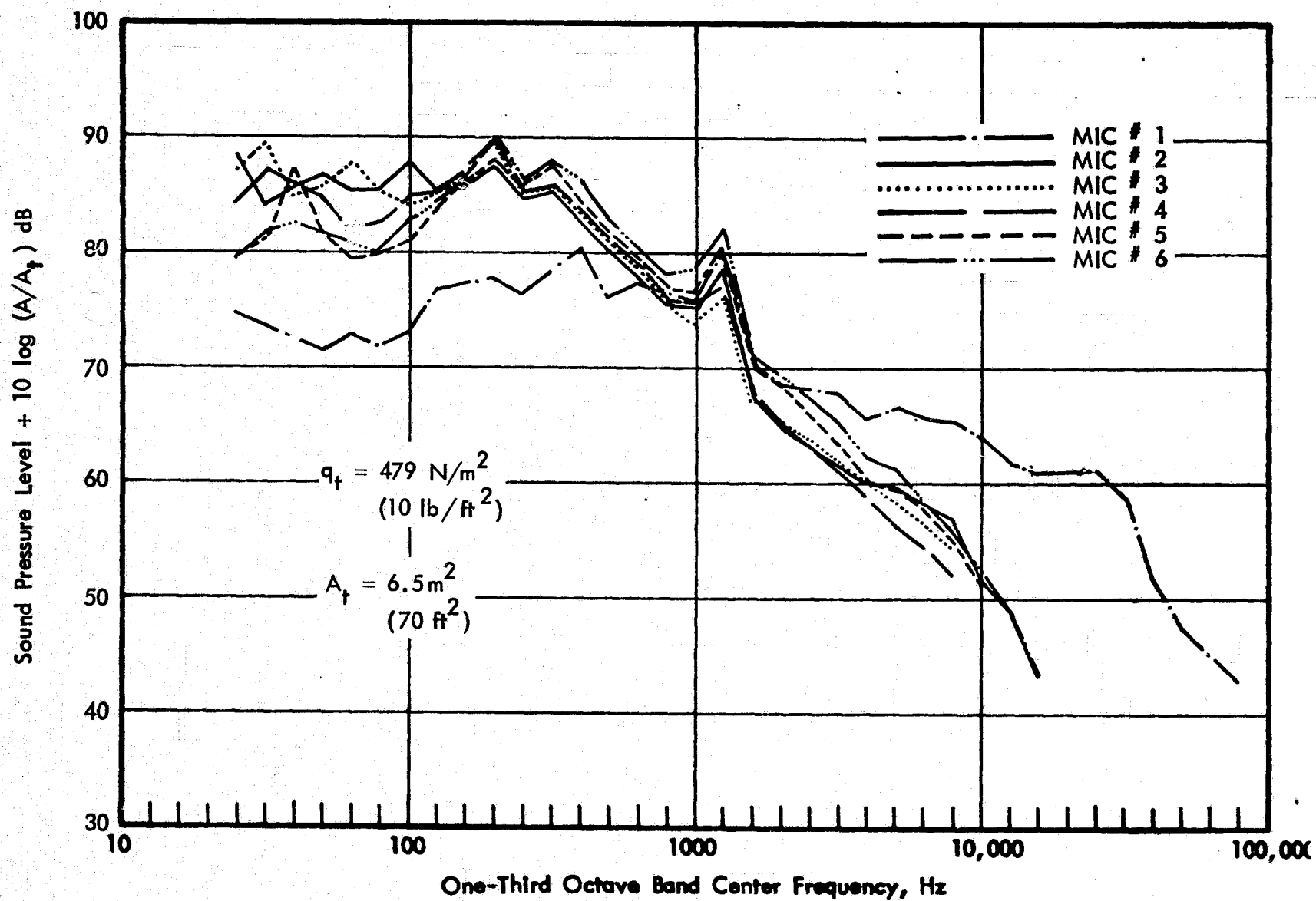
FIGURE 33.   SOUND LEVELS NORMALIZED WITH RESPECT TO TUNNEL AREA
$(q_t = 479 \text{ N/m}^2)$
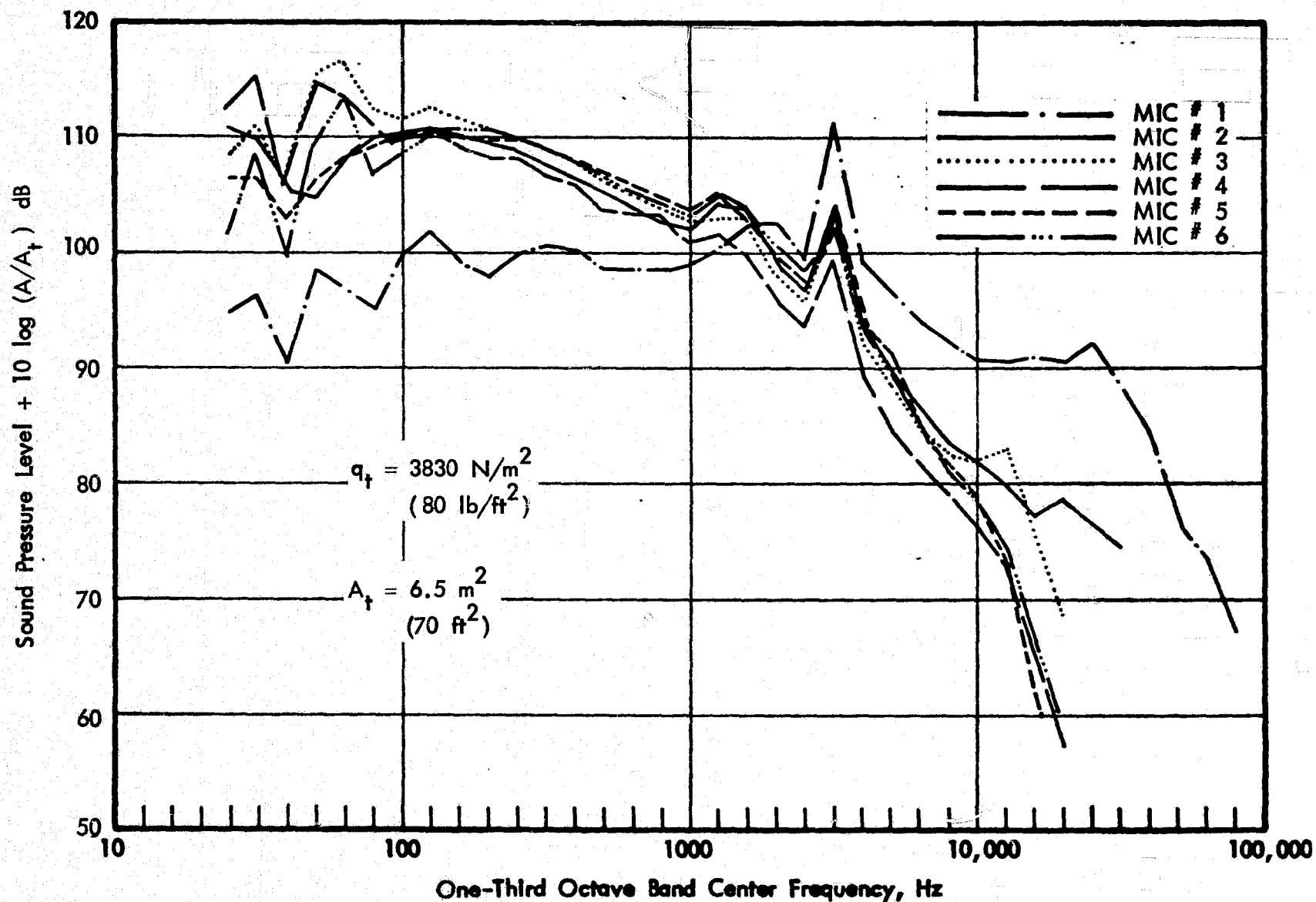
FIGURE 34. SOUND LEVELS NORMALIZED WITH RESPECT TO TUNNEL AREA
$(q_t = 3830 \ N/m^2)$

TUNNEL ROOF

PITOT TUBE AND STRUT
EXTENDED POSITION

2"

10"

Max. 13/16"

10"

1/4"

11/16"

RETRACTED POSITION

TUNNEL ROOF

7"

3/8" O.D.

3/16"

8"

2"

PITOT TRAVERSE
AIRFOILS

24"

3 1/2"

DIFFUSER ENTRY AIRFOILS
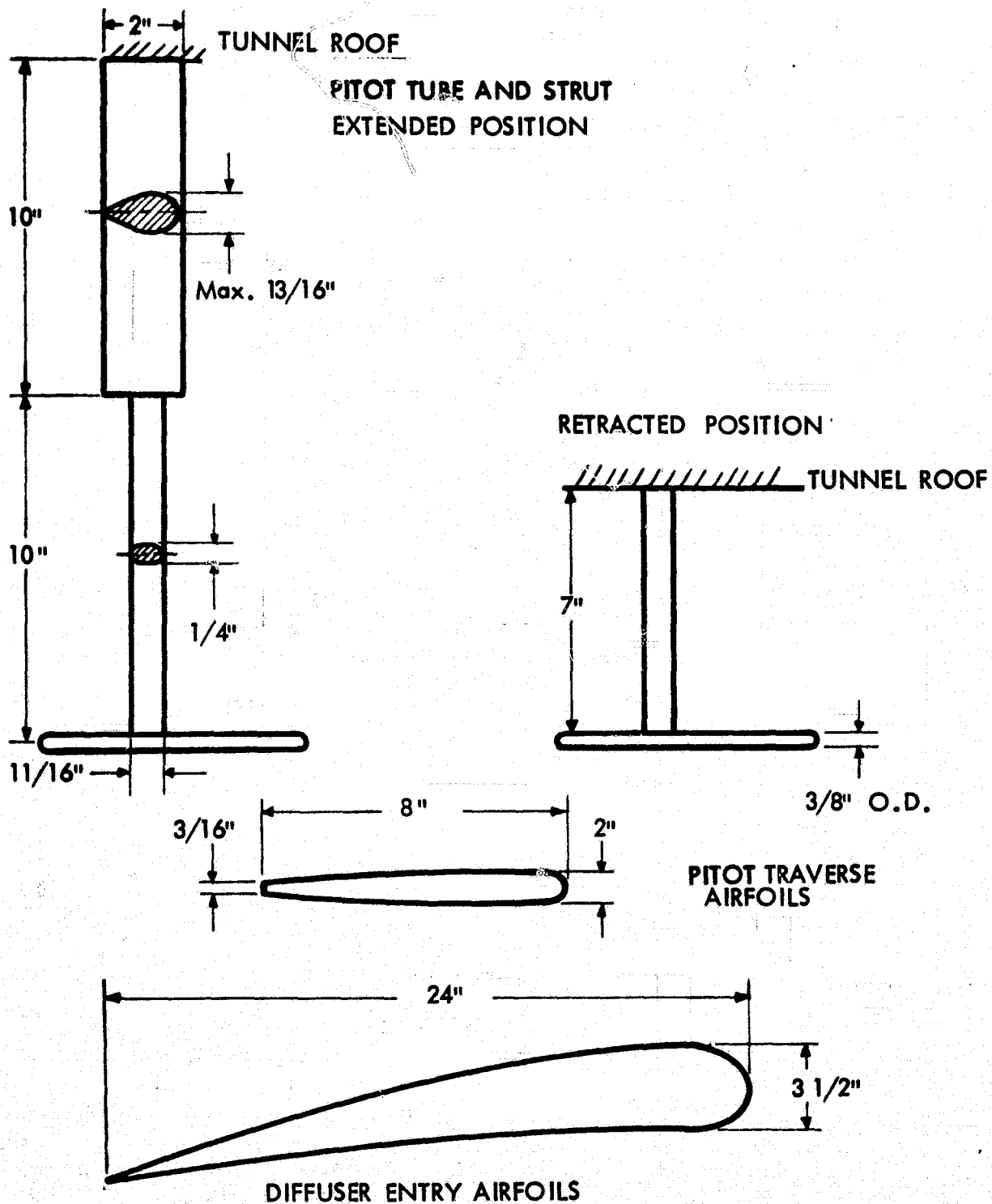
FIGURE 35. APPROXIMATE DIMENSIONS OF AIRFOIL
BODIES IN TEST SECTION
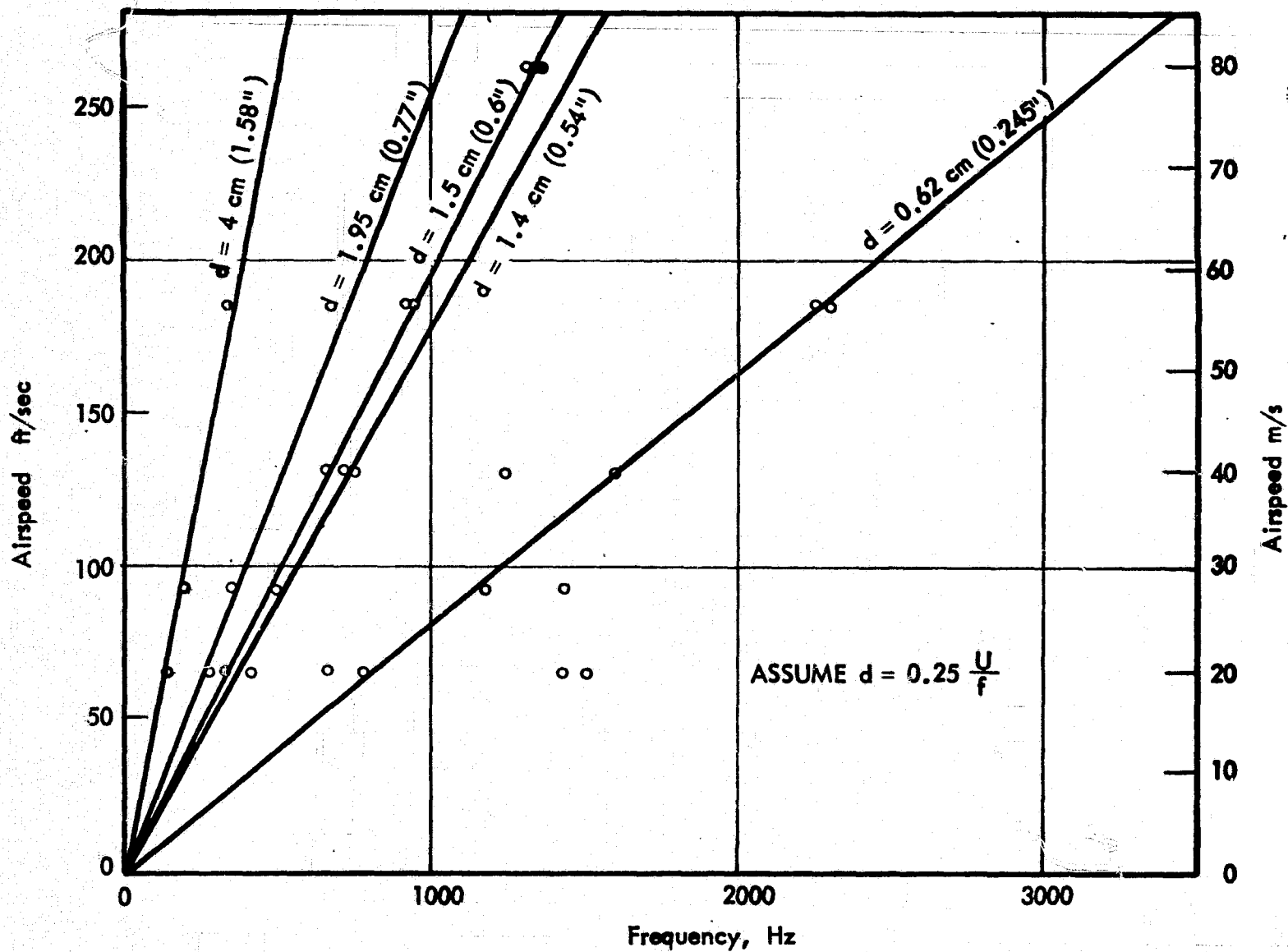
FIGURE 36.   DISTRIBUTION OF TONE FREQUENCIES WITH FLOW SPEED IN
TEST SECTION
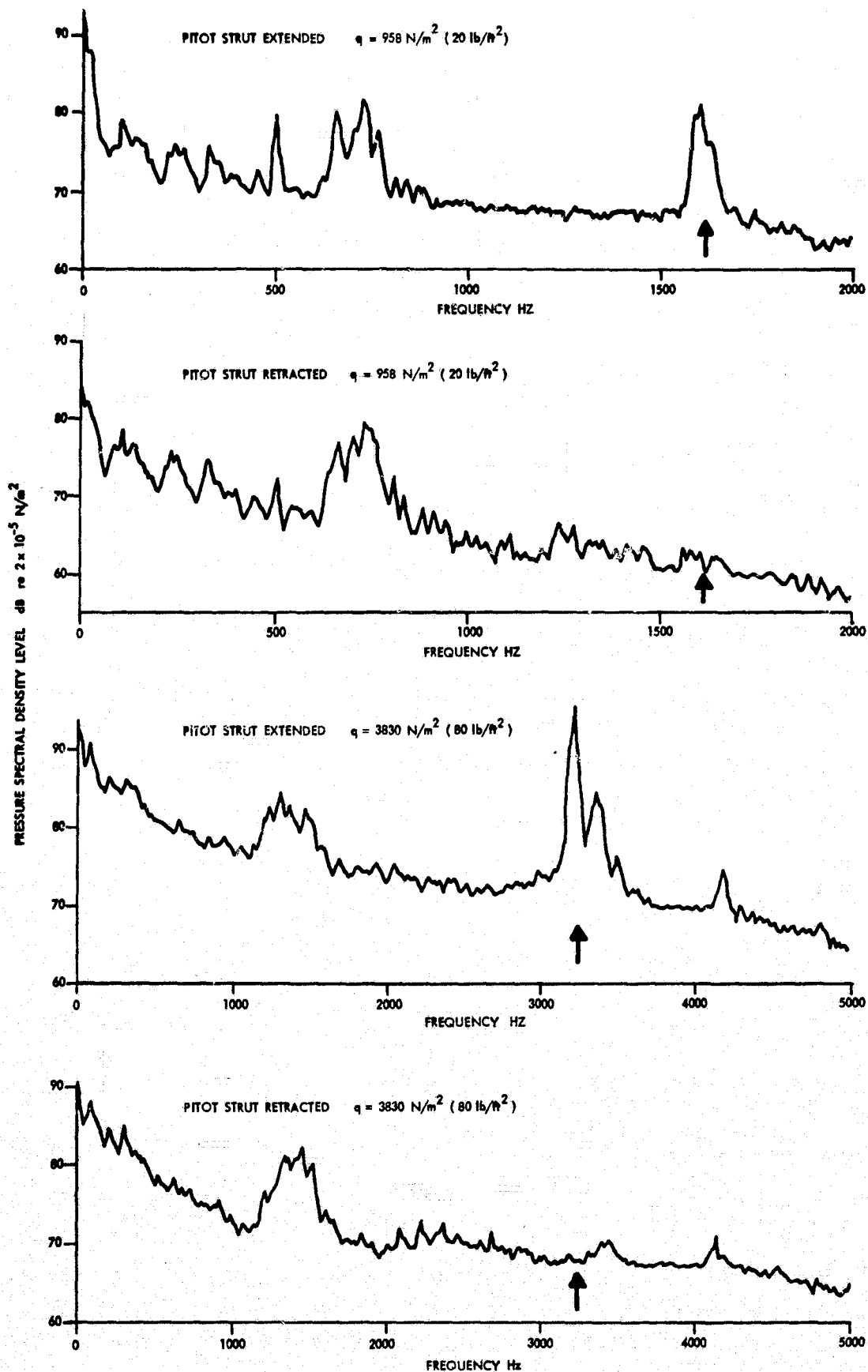
FIGURE 37. NARROWBAND SPECTRA OF NOISE LEVELS IN TEST SECTION SHOWING EFFECT OF RETRACTING PITOT STRUT (FILTER BANDWIDTH 5 Hz(UPPER CURVES), 12.5 Hz(LOWER CURVES))
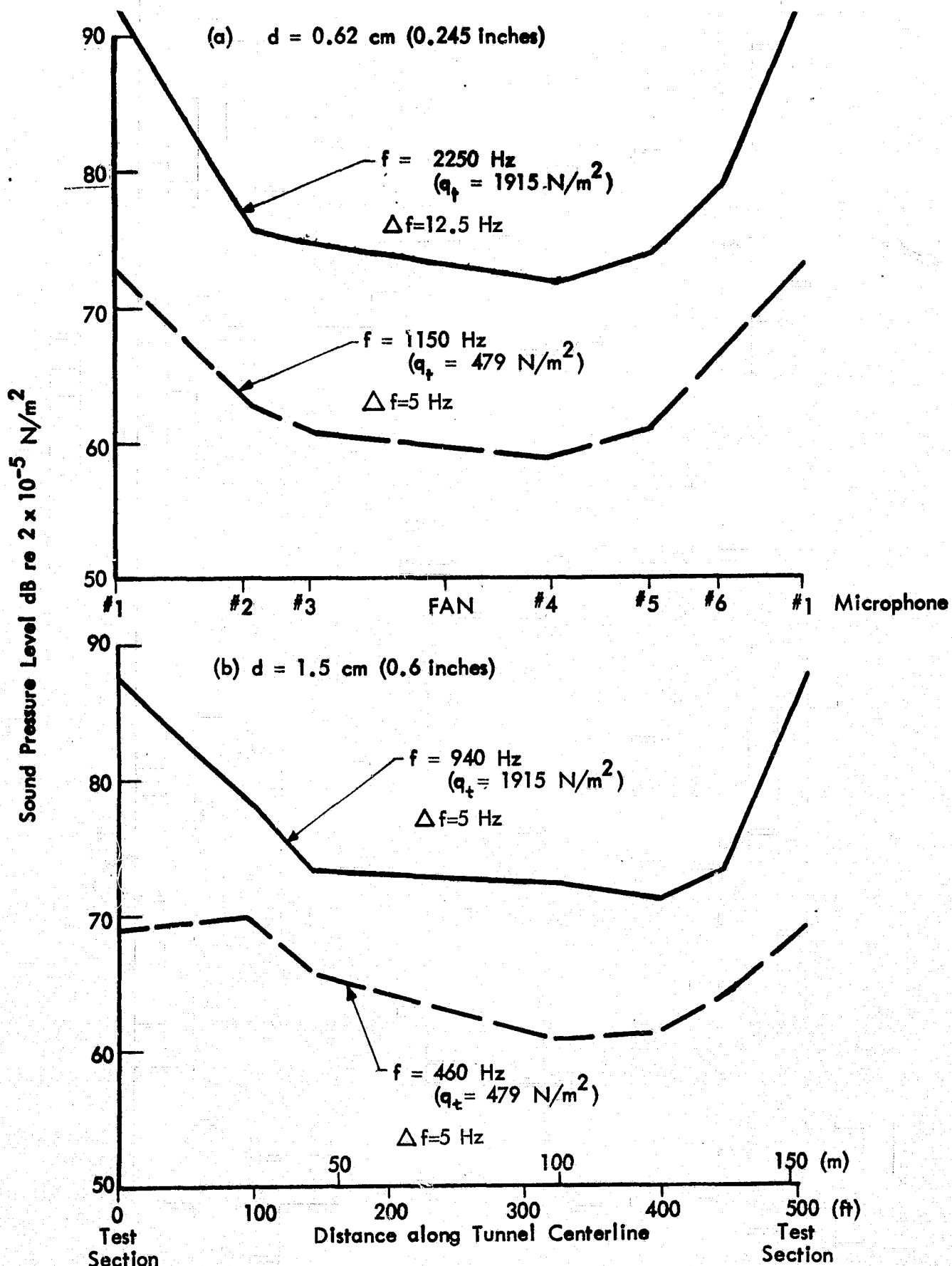
FIGURE 38.   SPATIAL DISTRIBUTION OF HIGH FREQUENCY
TONE SOUND PRESSURE LEVELS
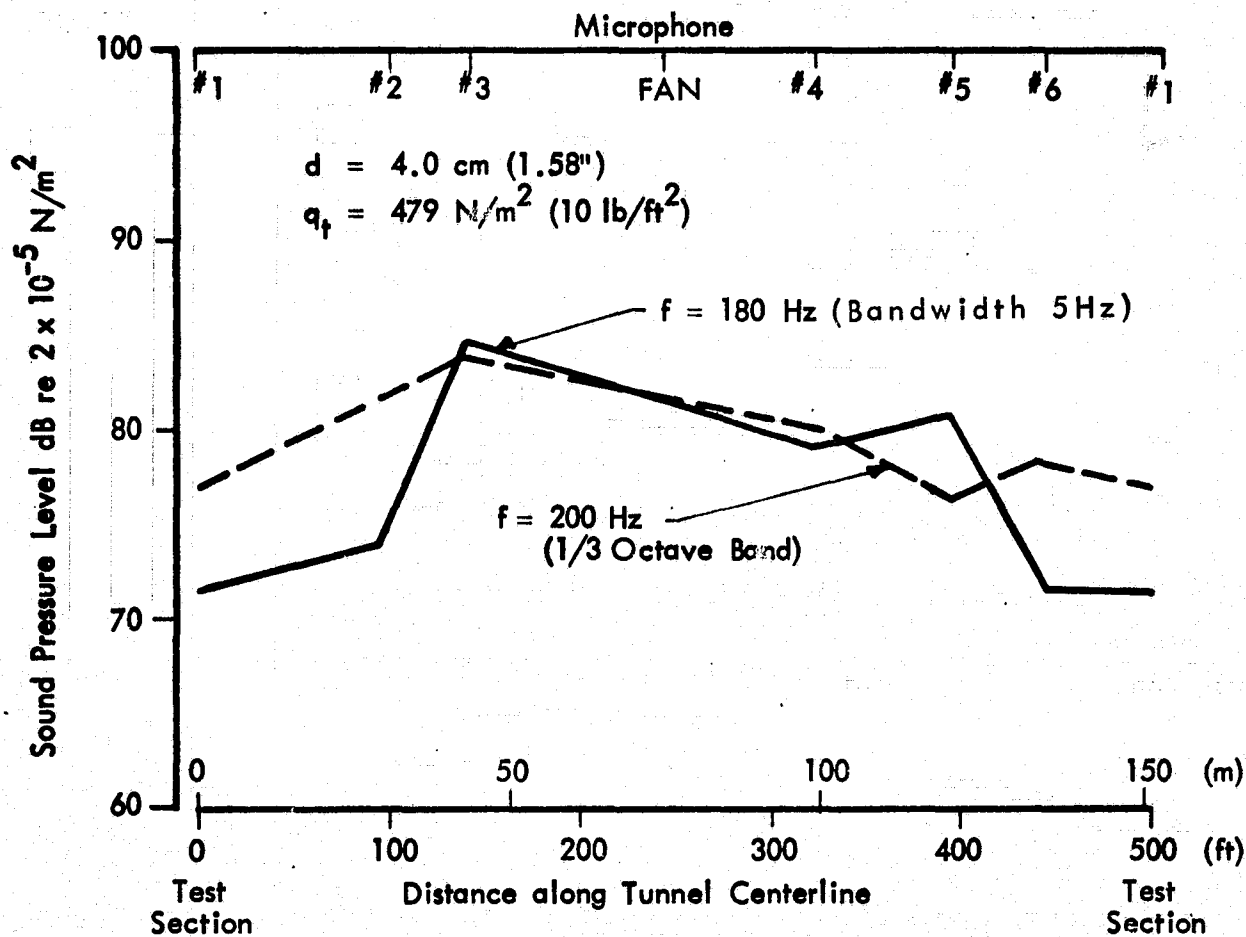
FIGURE 39.   SPATIAL DISTRIBUTION OF LOW FREQUENCY
TONE SOUND PRESSURE LEVELS
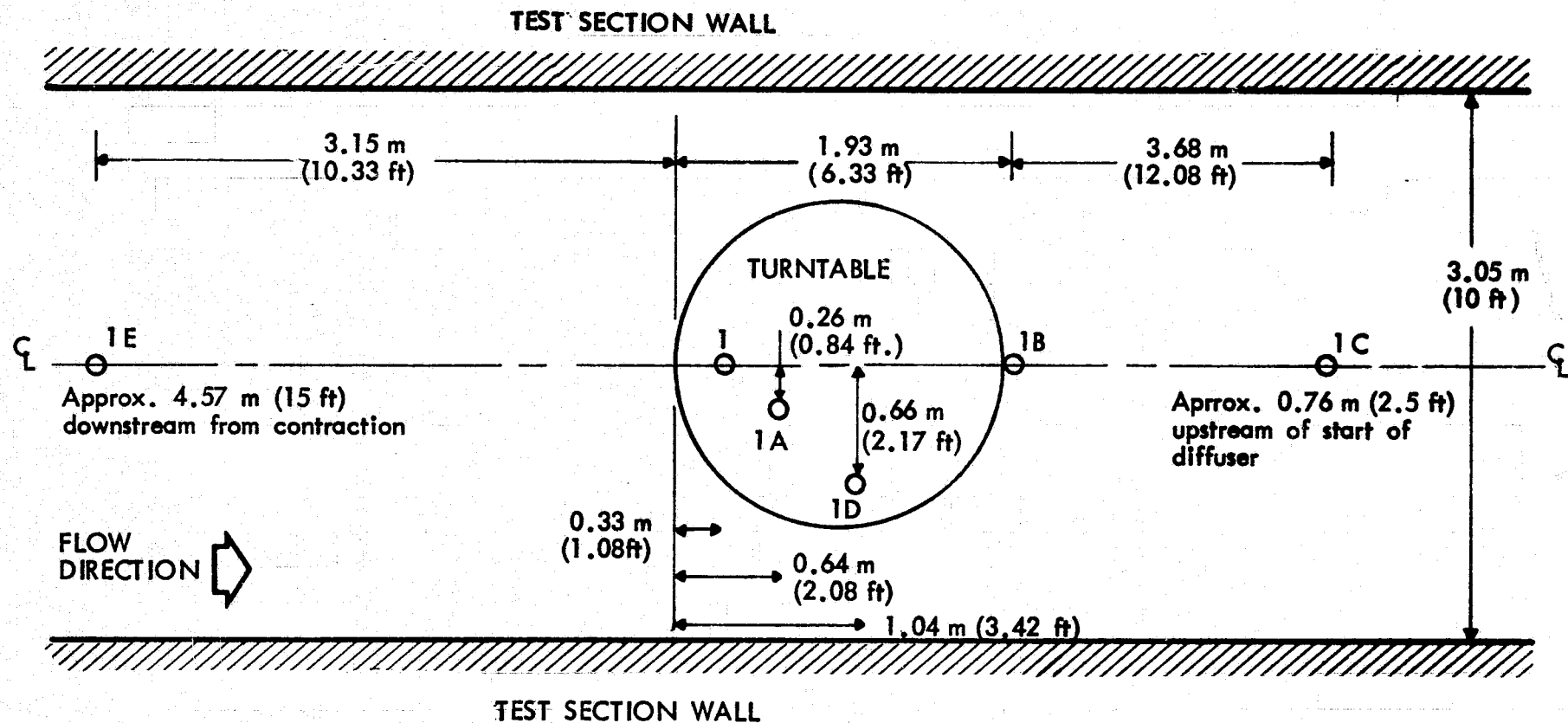
FIGURE 40. MICROPHONE LOCATIONS IN TEST SECTION
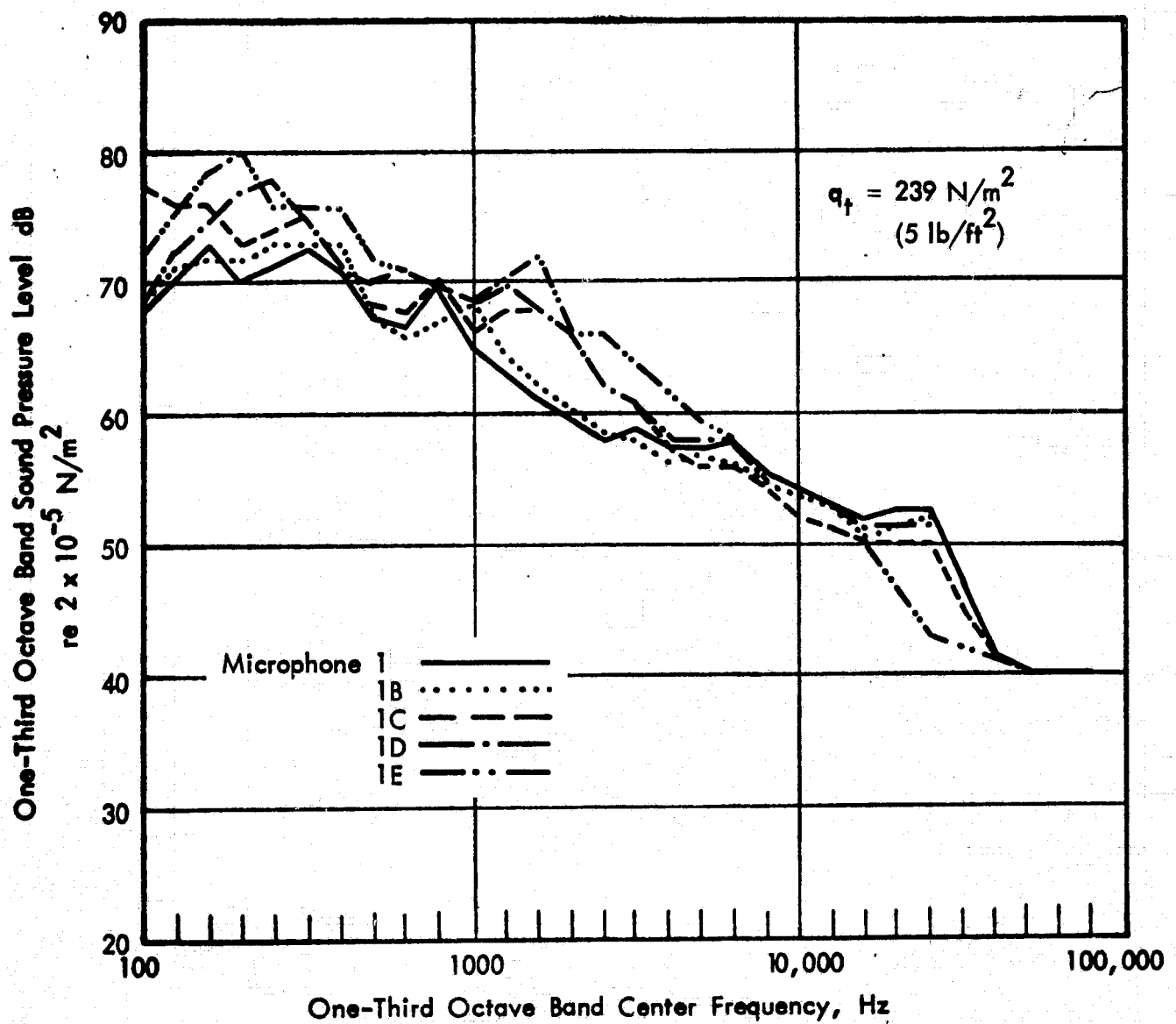
FIGURE 41A. VARIATION OF SOUND LEVELS IN TEST SECTION
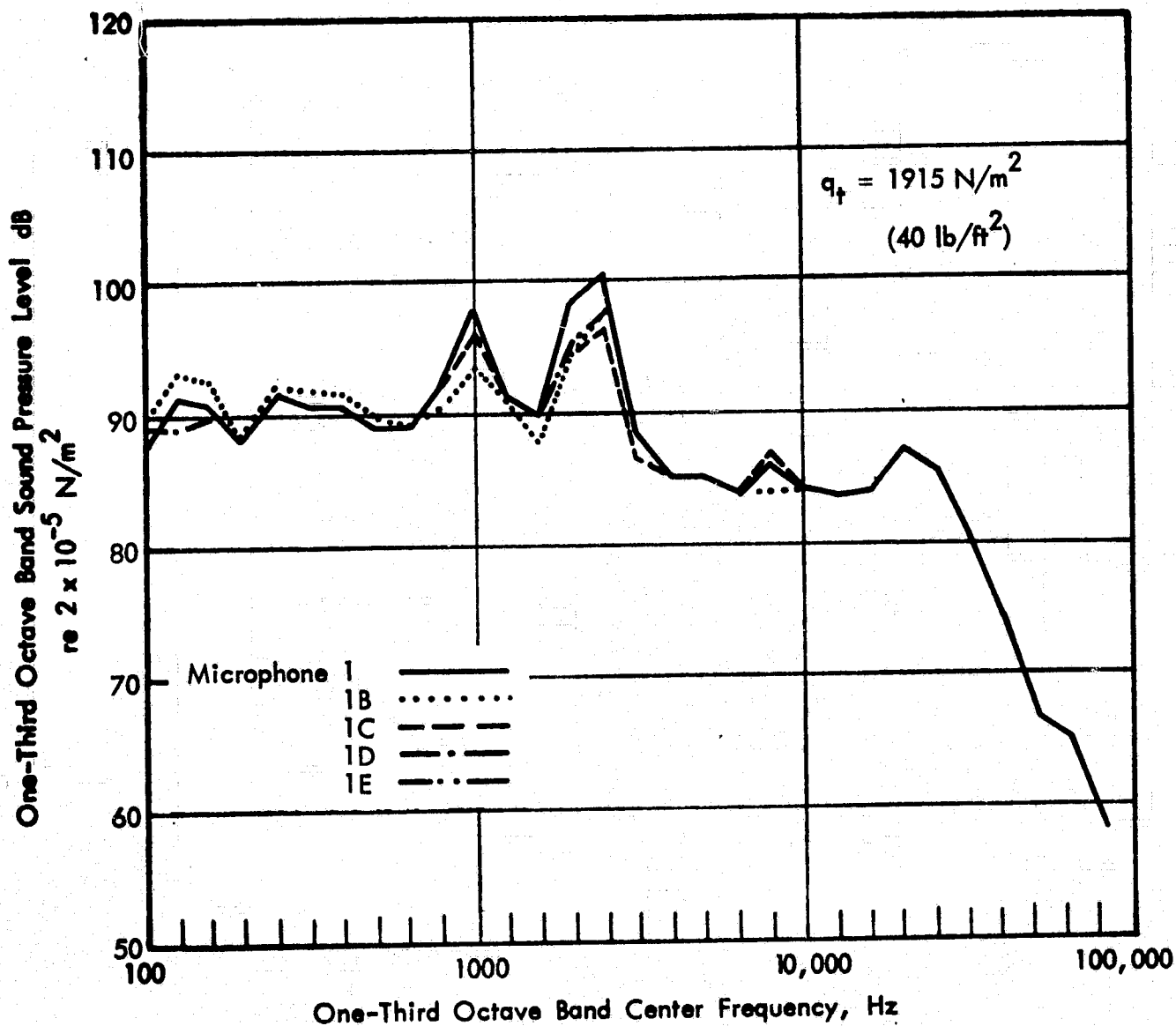
FIGURE 41B.   VARIATION OF SOUND LEVELS IN TEST SECTION
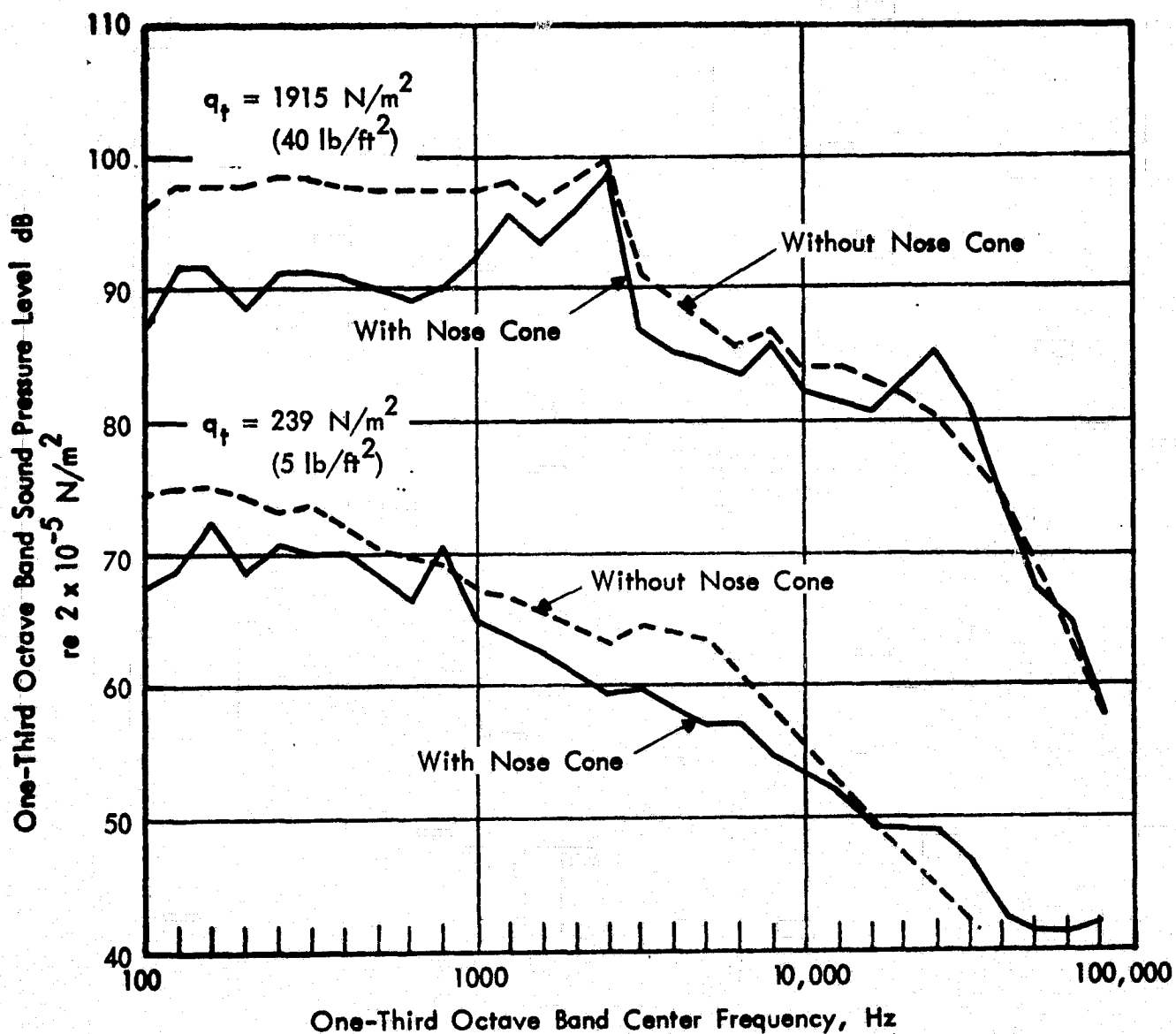
FIGURE 42. NOISE LEVELS MEASURED BY 0.25 INCH MICROPHONE WITH AND WITHOUT NOSE CONE
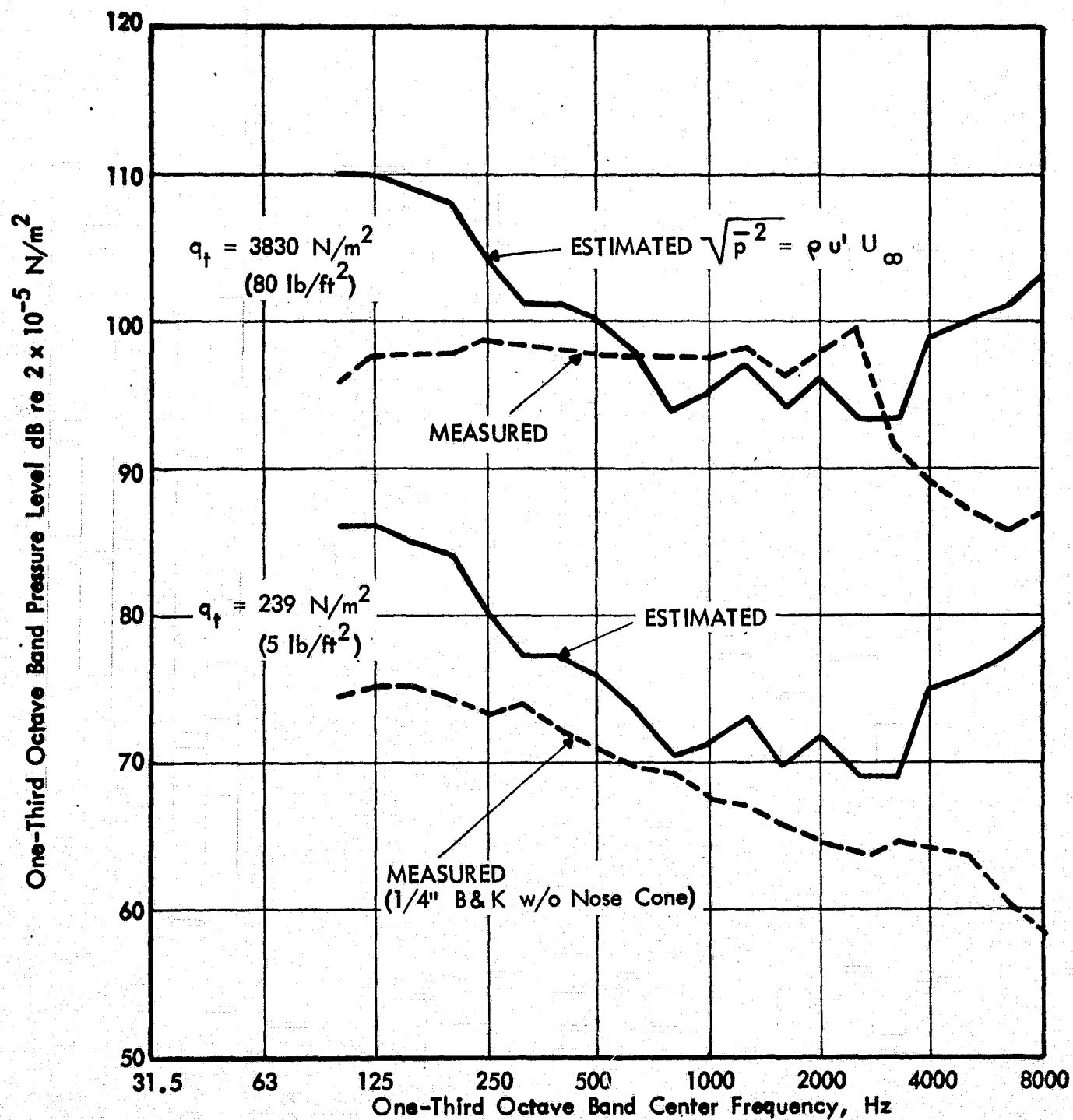
FIGURE 43. FLUCTUATING TOTAL PRESSURES IN TEST SECTION
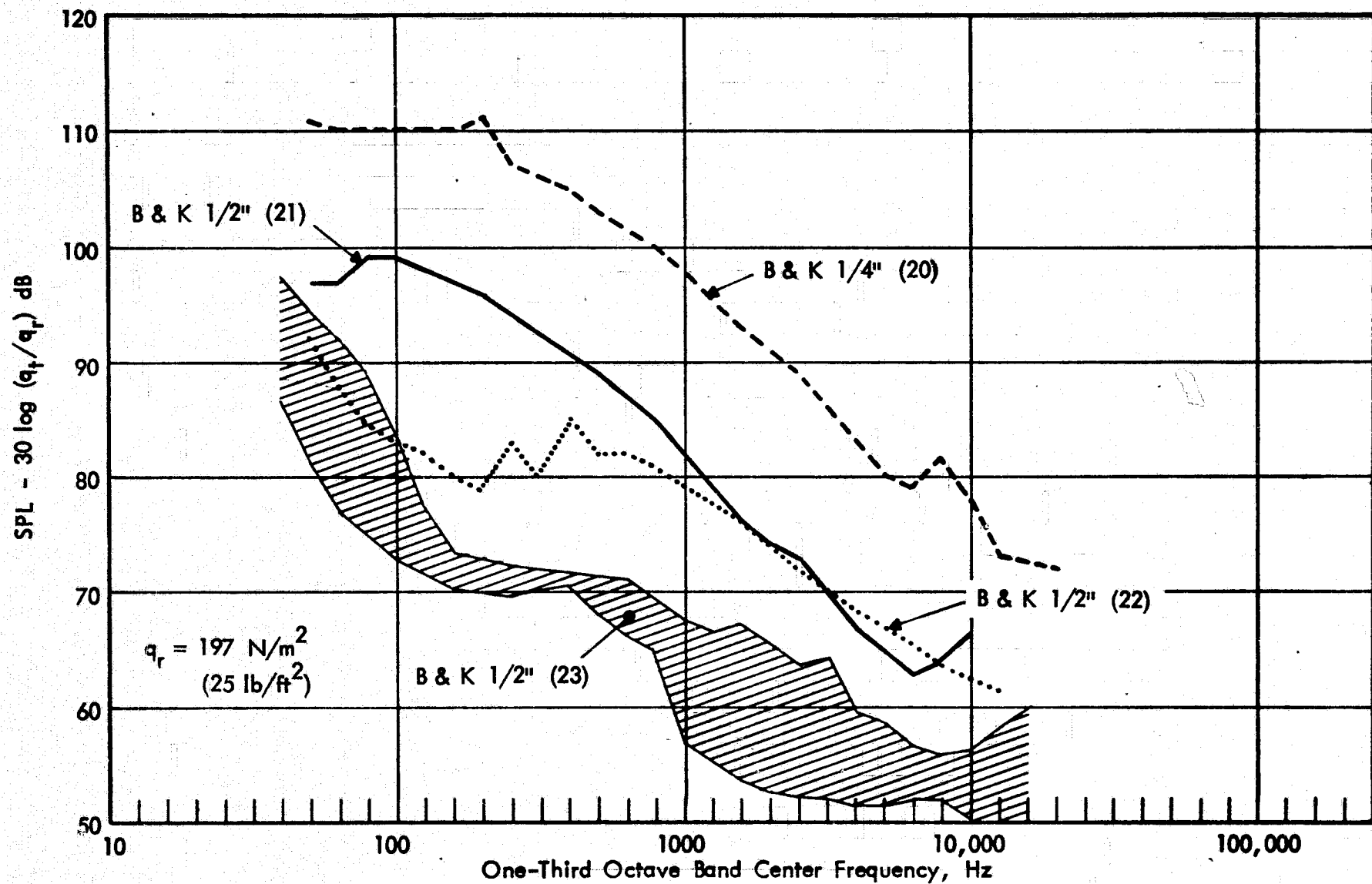
FIGURE 44. MEASUREMENTS OF AERODYNAMIC SELF-NOISE FOR MICROPHONES
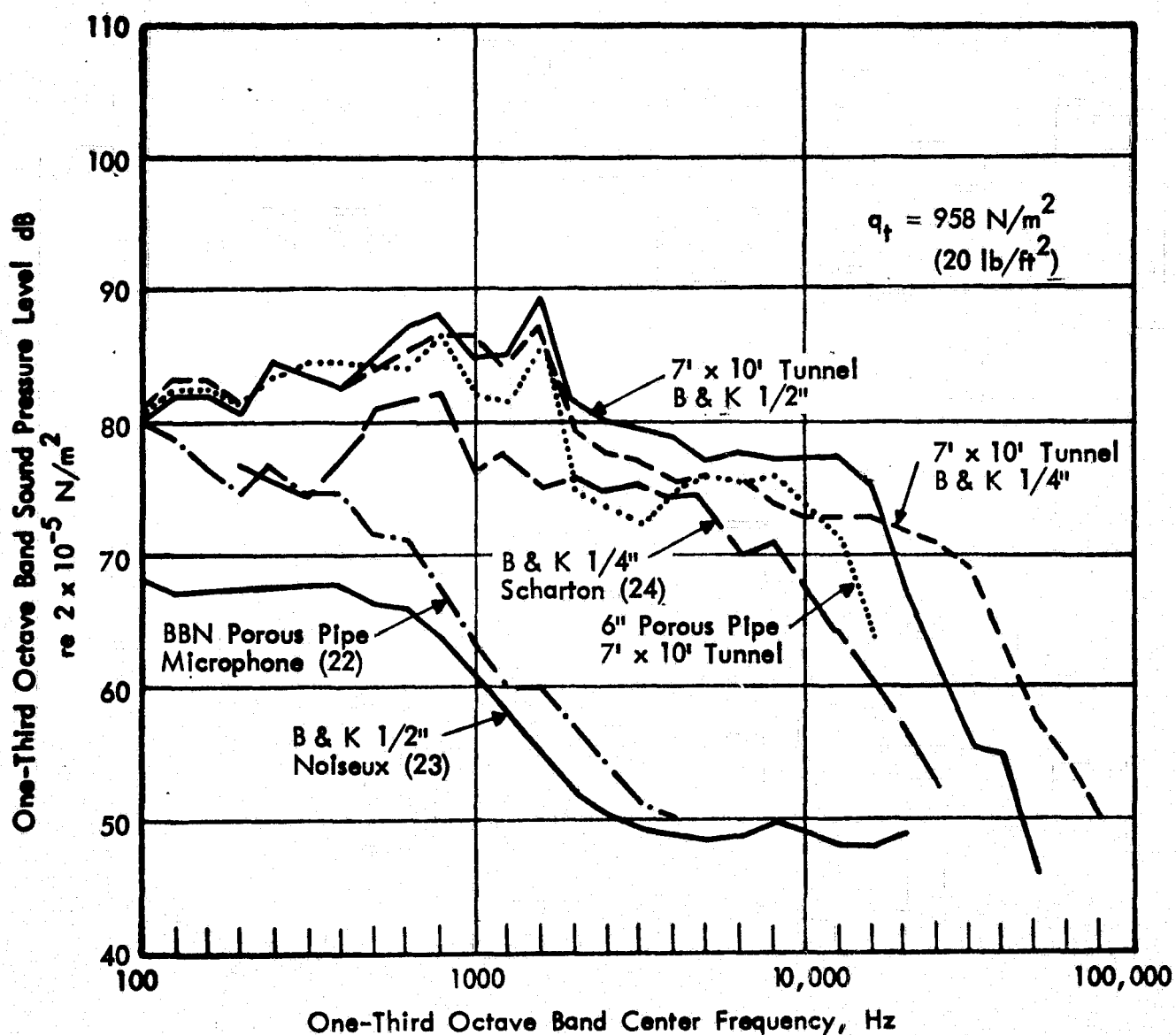
FIGURE 45. NOISE LEVELS MEASURED WITH DIFFERENT MICROPHONES
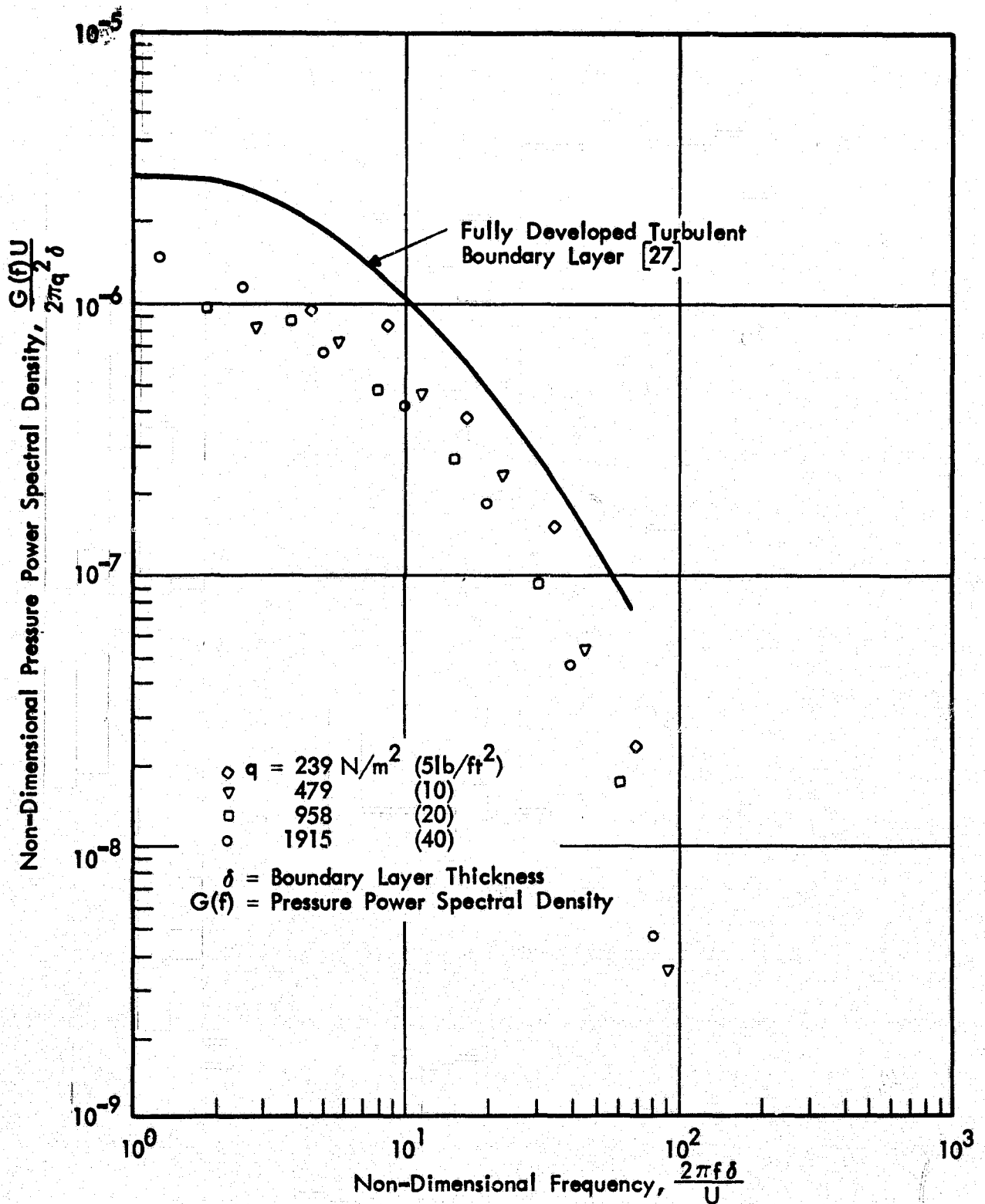
FIGURE 46. BOUNDARY LAYER PRESSURE SPECTRA MEASURED ON
WALL OF 7' x 10' TUNNEL TEST SECTION
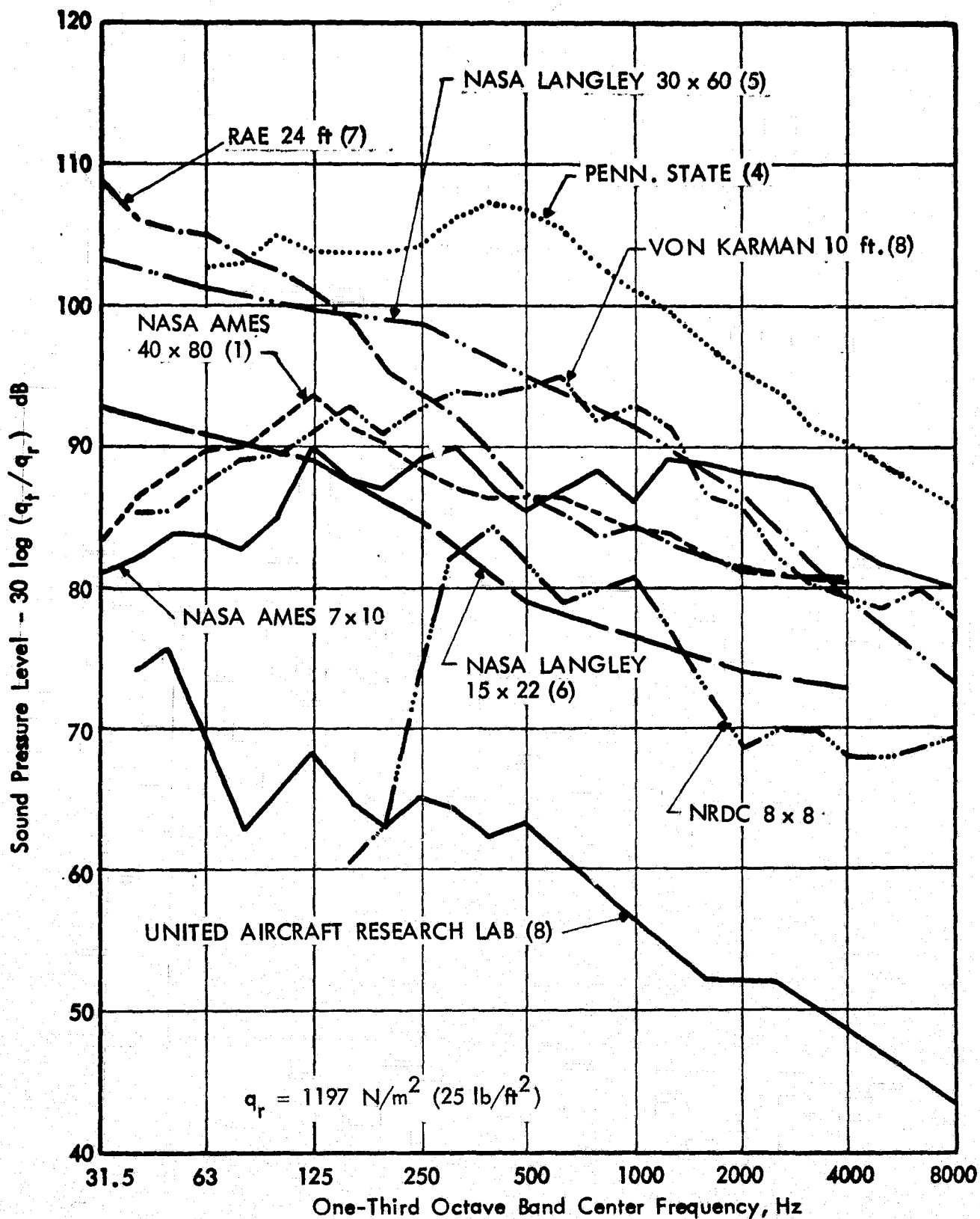
FIGURE 47   COMPARISON OF NORMALIZED NOISE LEVELS
MEASURED IN SEVERAL TUNNEL TEST SECTIONS
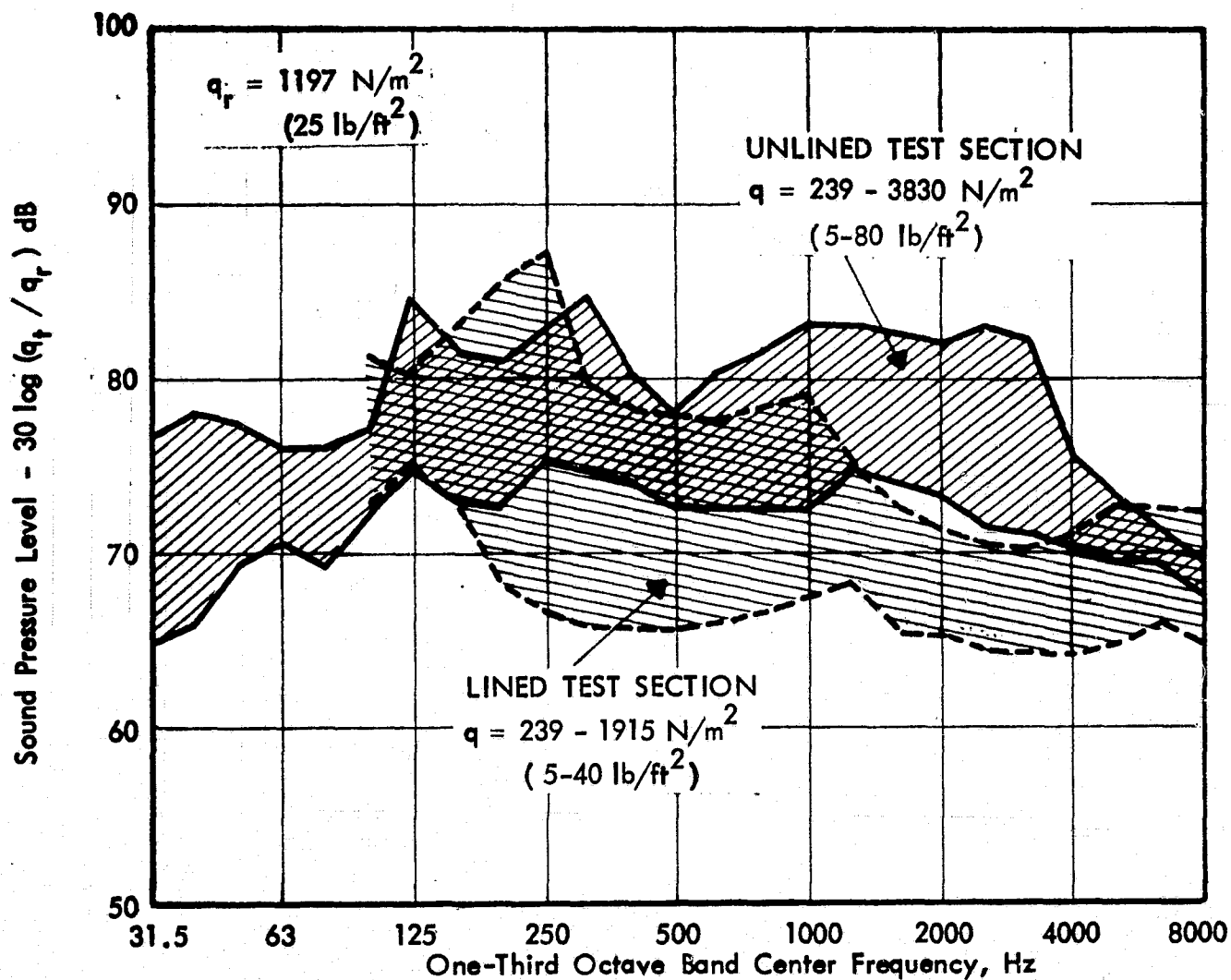
FIGURE 48   NOISE LEVELS IN LINED AND UNLINED TEST SECTION
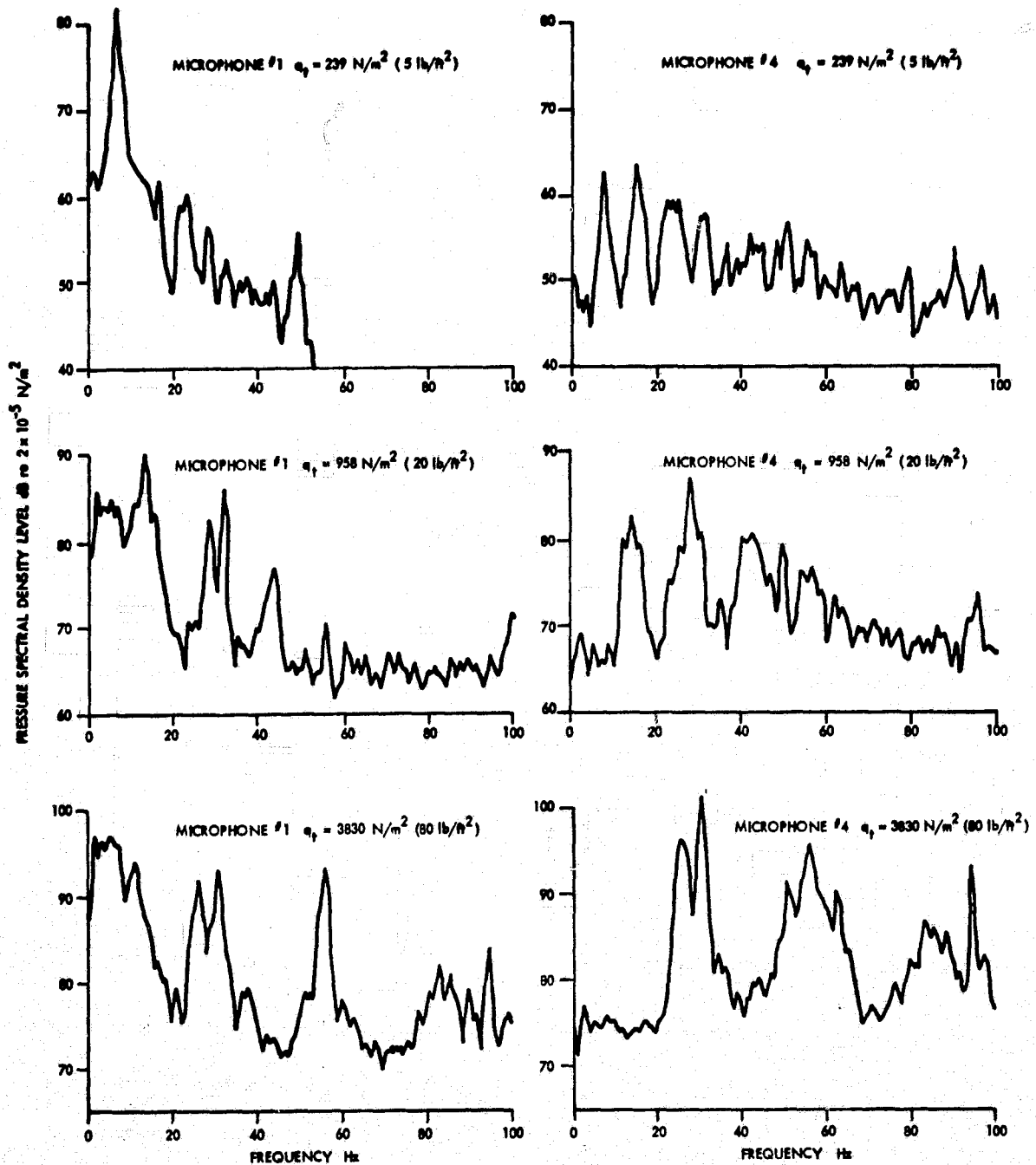
FIGURE 49   NARROWBAND SPECTRA OF FAN NOISE IN
              TEST SECTION (FILTER BANDWIDTH 0.5Hz)
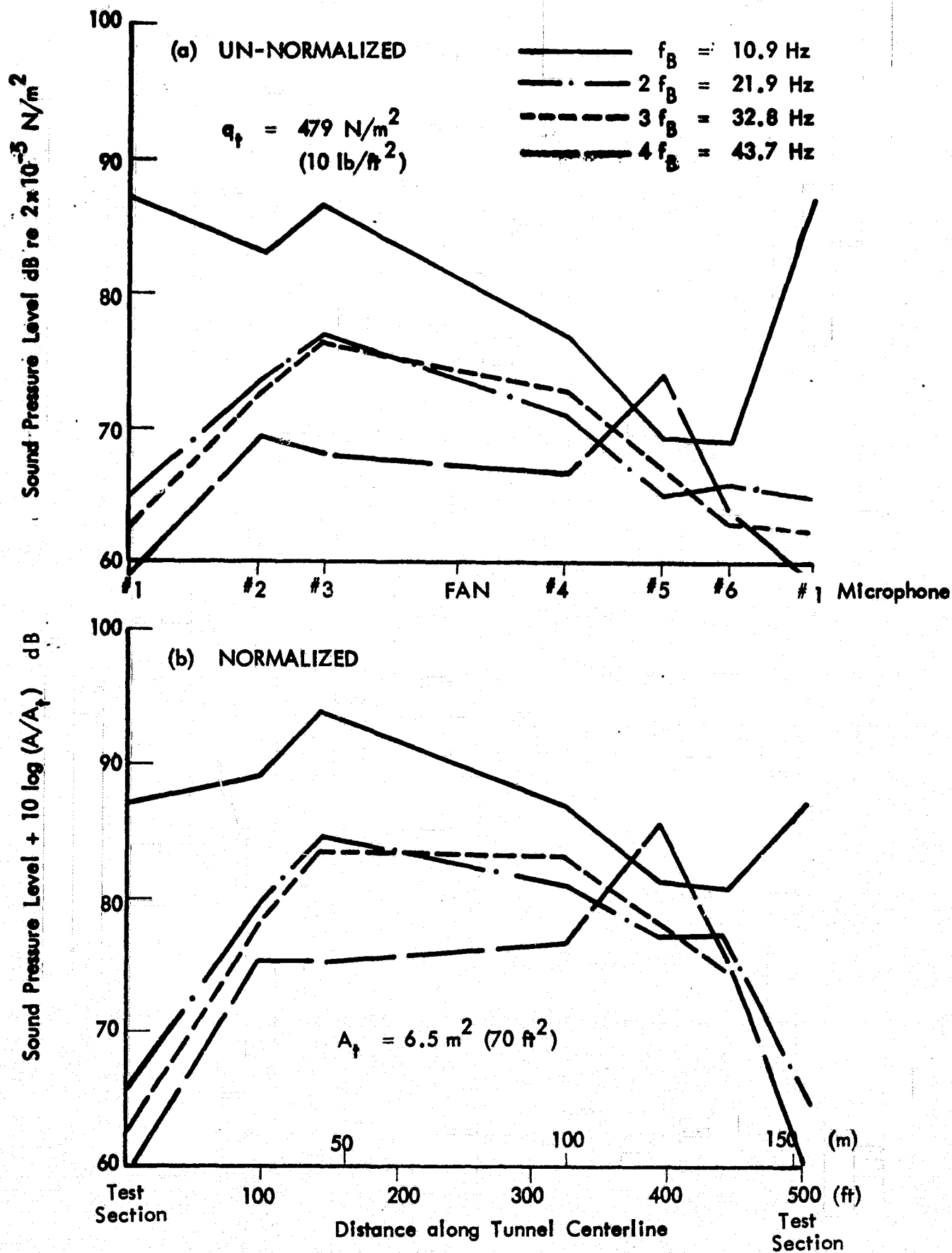
FIGURE 50   SPATIAL DISTRIBUTION OF FAN TONE SOUND
LEVELS (q = 479 N/m^2) (FILTER BANDWIDTH 0.5Hz)
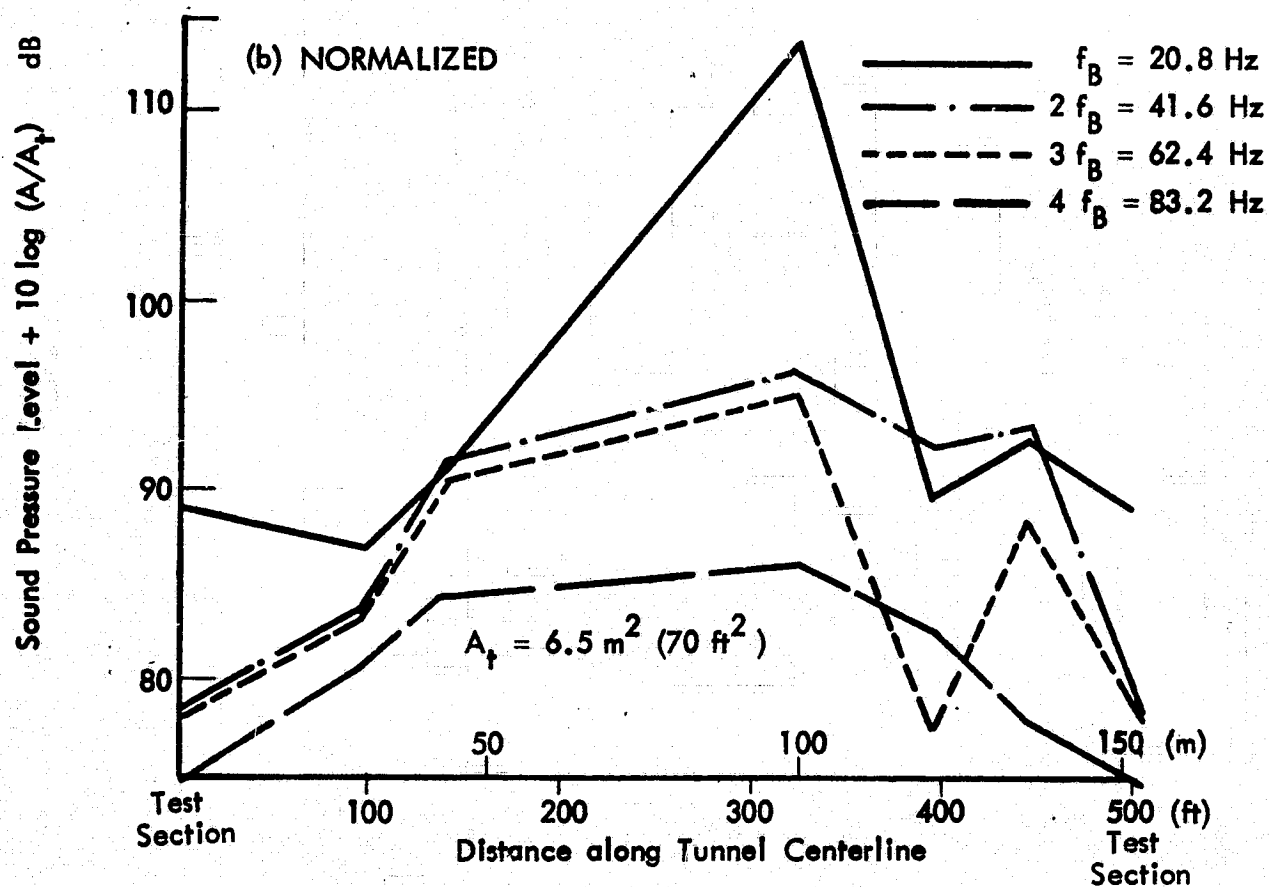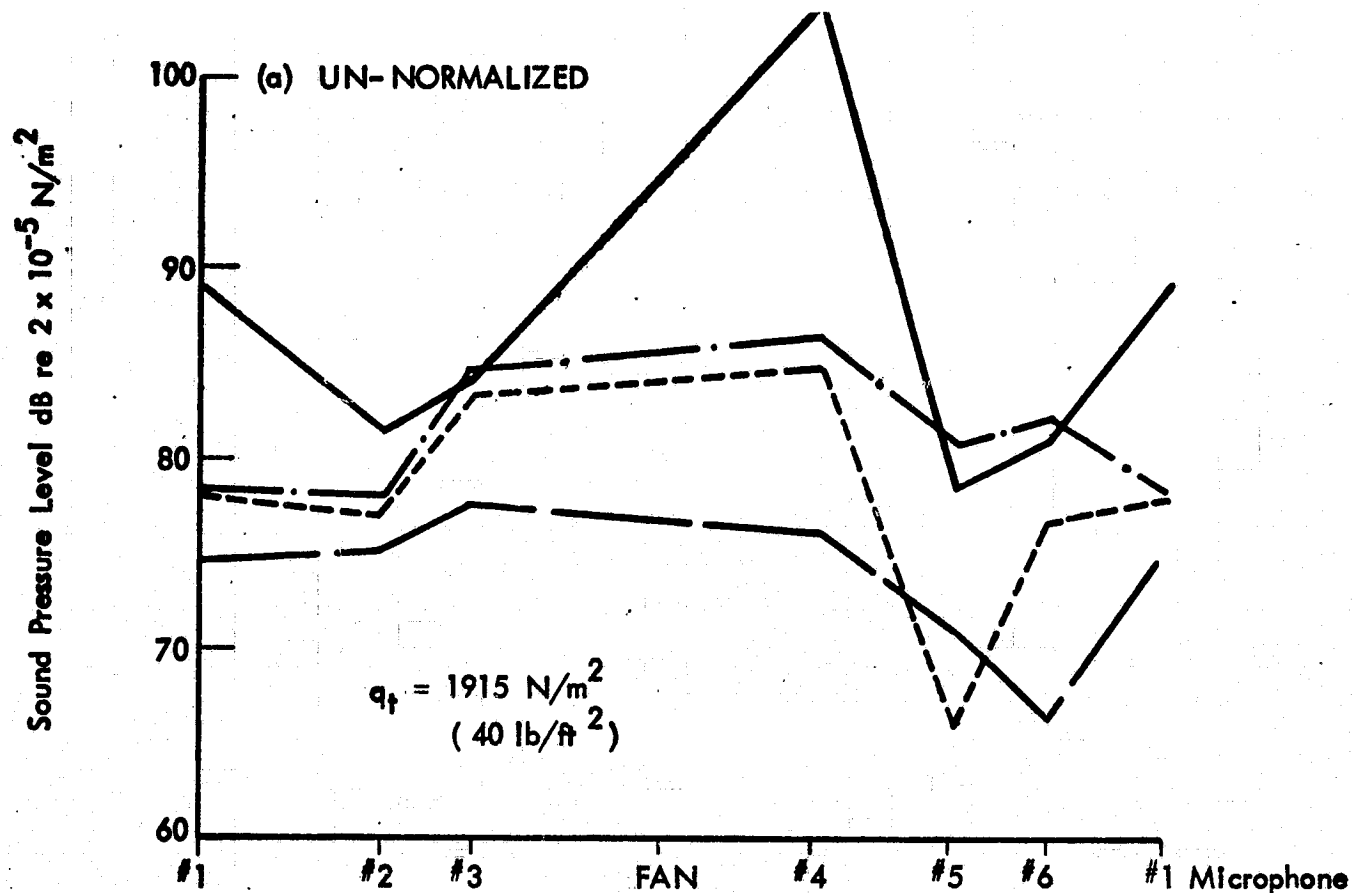
FIGURE 51   SPATIAL DISTRIBUTION OF FAN TONE SOUND
LEVELS (q = 1915 N/m^2)(FILTER BANDWIDTH 0.5Hz)
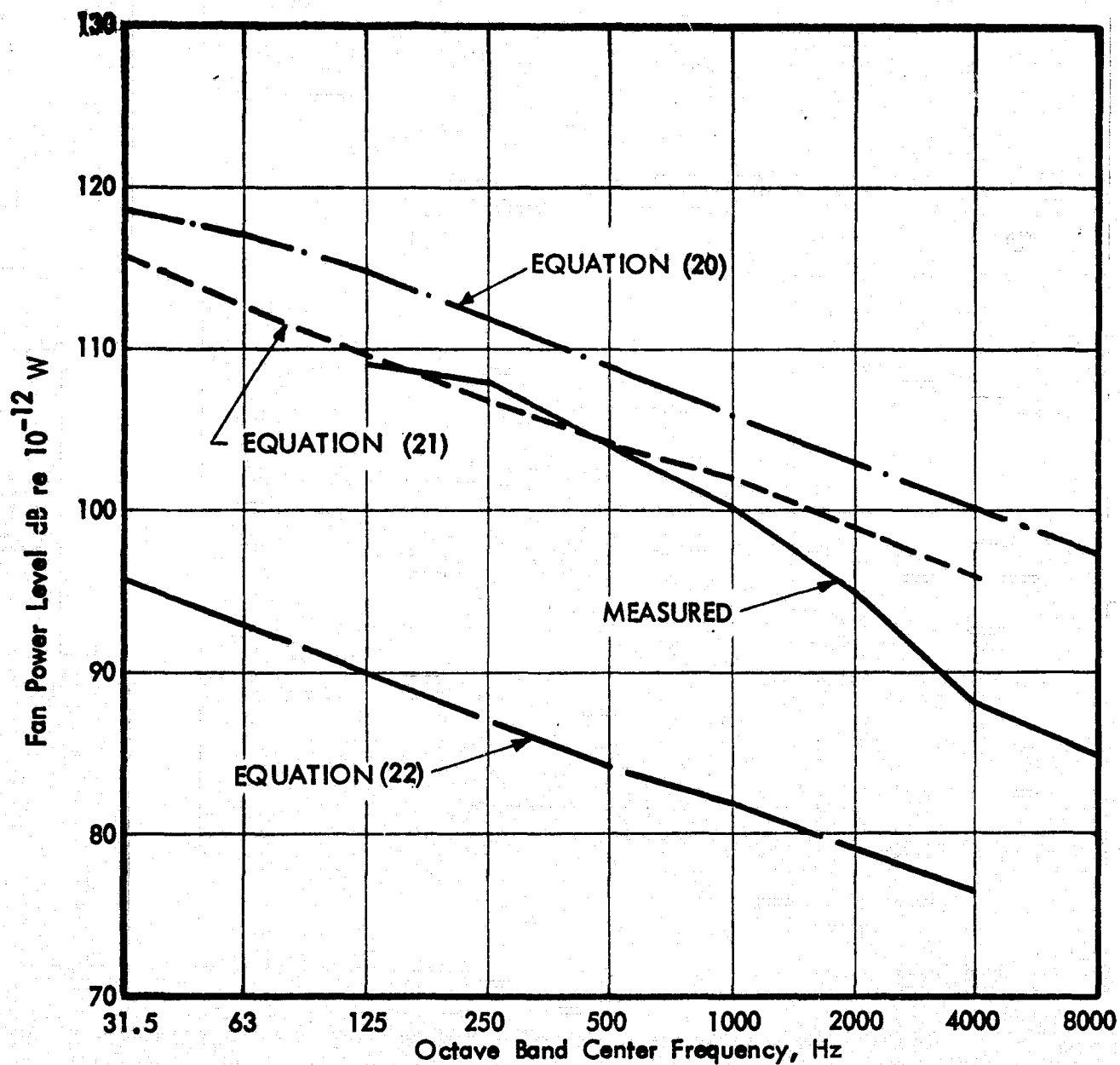
FIGURE 52 COMPARISON OF MEASURED AND PREDICTED SOUND POWER LEVELS FOR DRIVE FAN
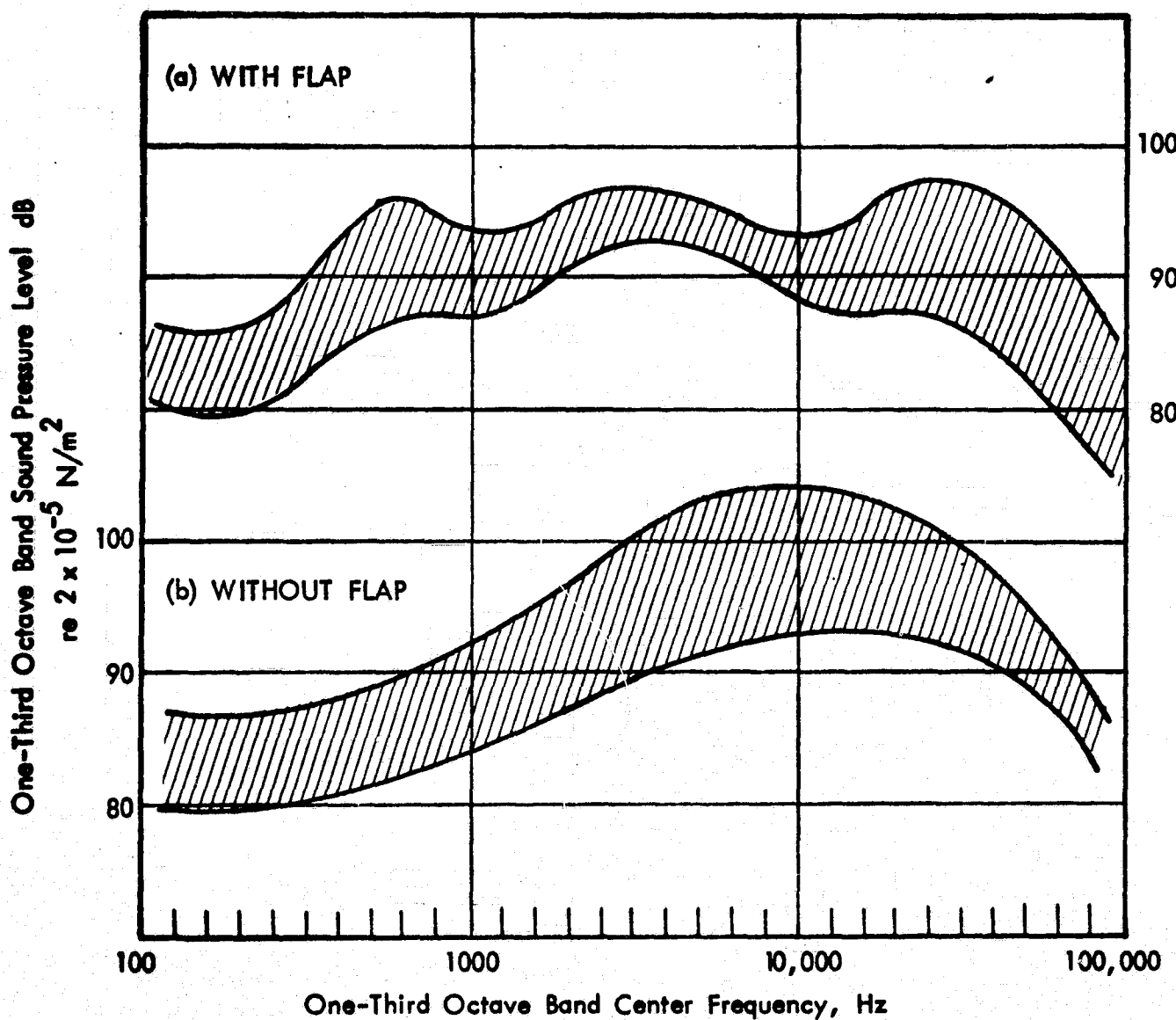
FIGURE 53   NOISE FROM AUGMENTOR WING WITH AND
WITHOUT FLAP SYSTEM (P.R. = 1.54)
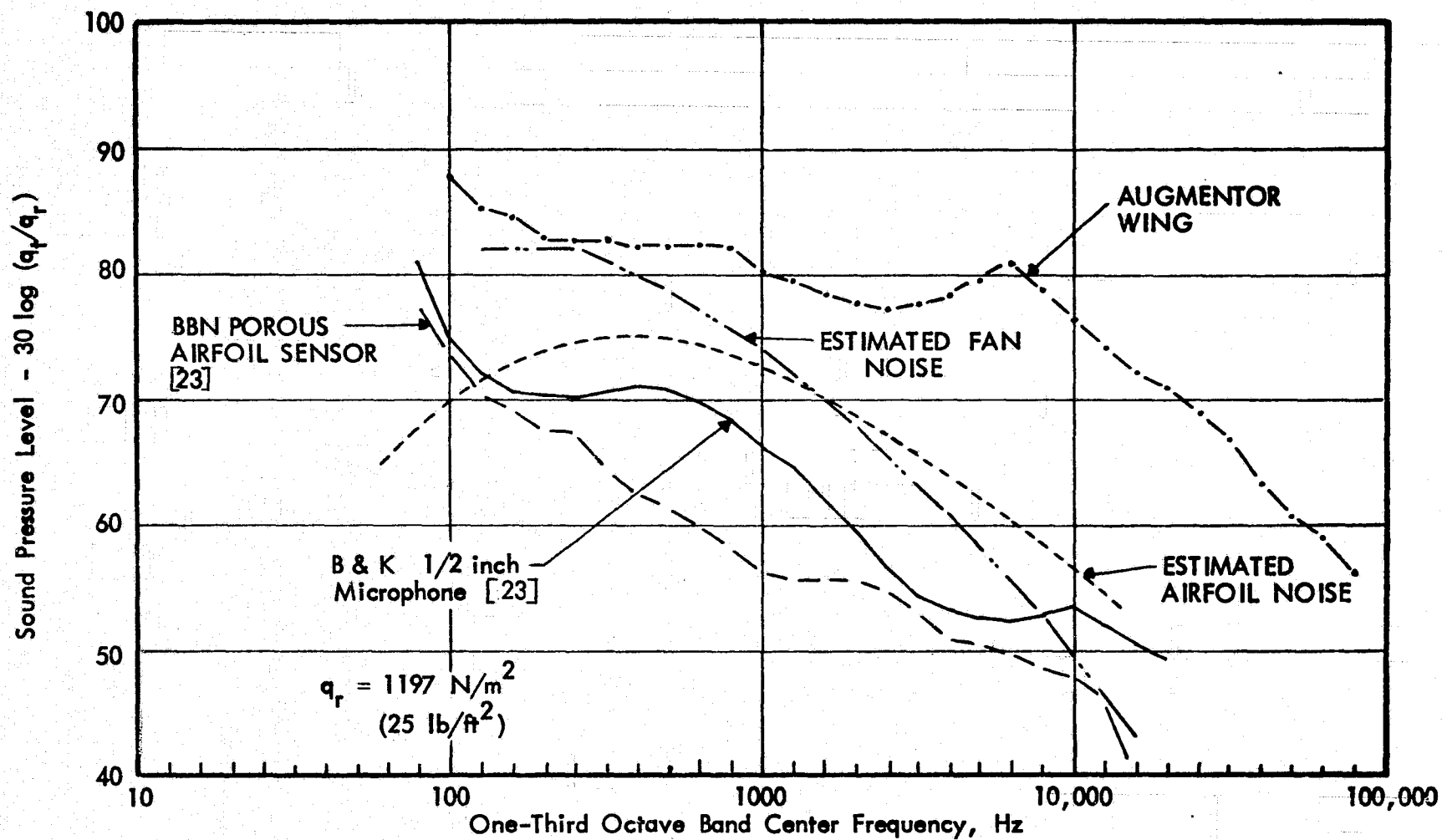
FIGURE 54   COMPARISON OF AIRFRAME, FAN AND MICROPHONE NOISE LEVELS IN TEST SECTION
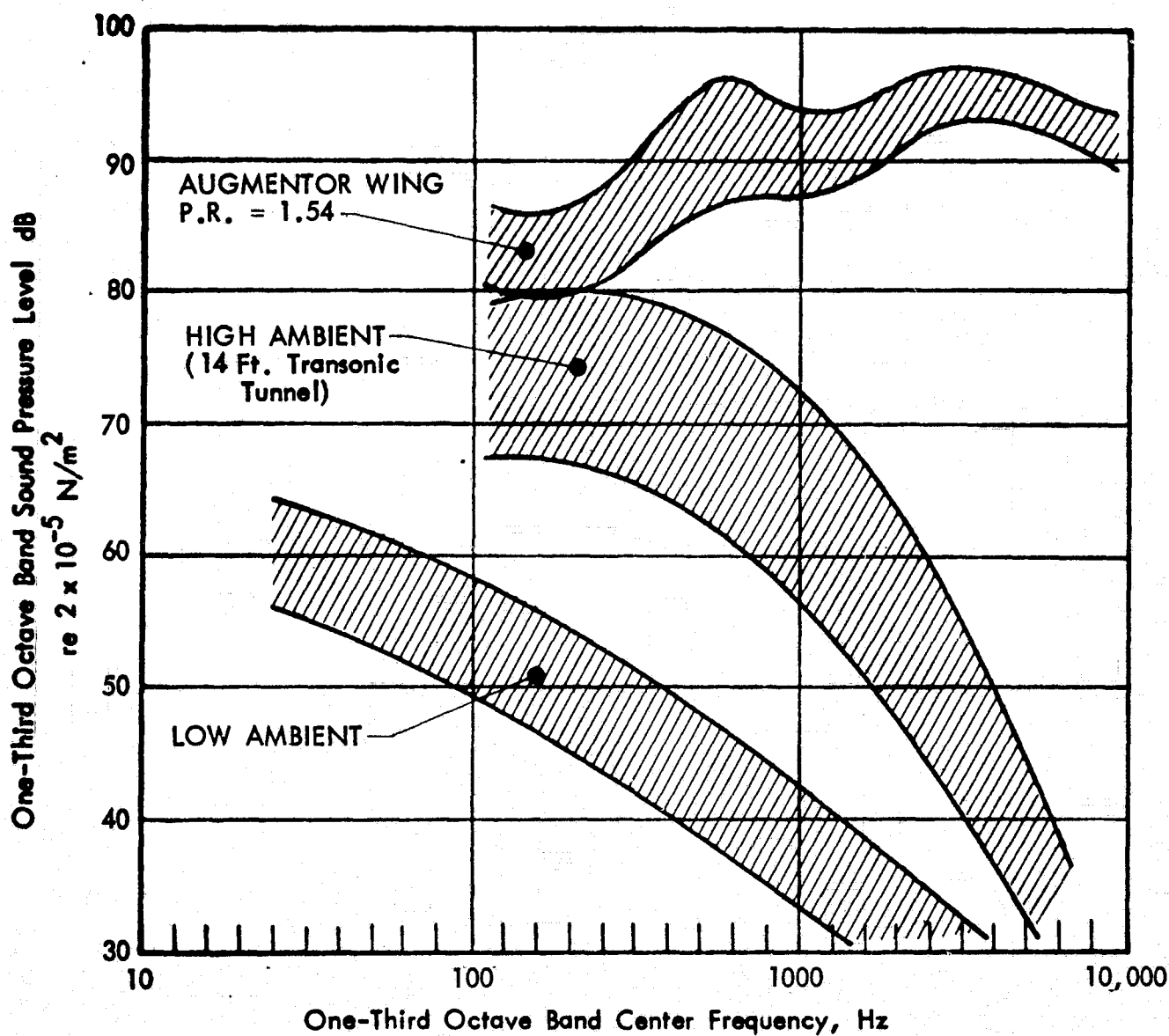
FIGURE 55   COMPARISON OF AUGMENTOR WING AND TEST
SECTION AMBIENT NOISE (NO FLOW)
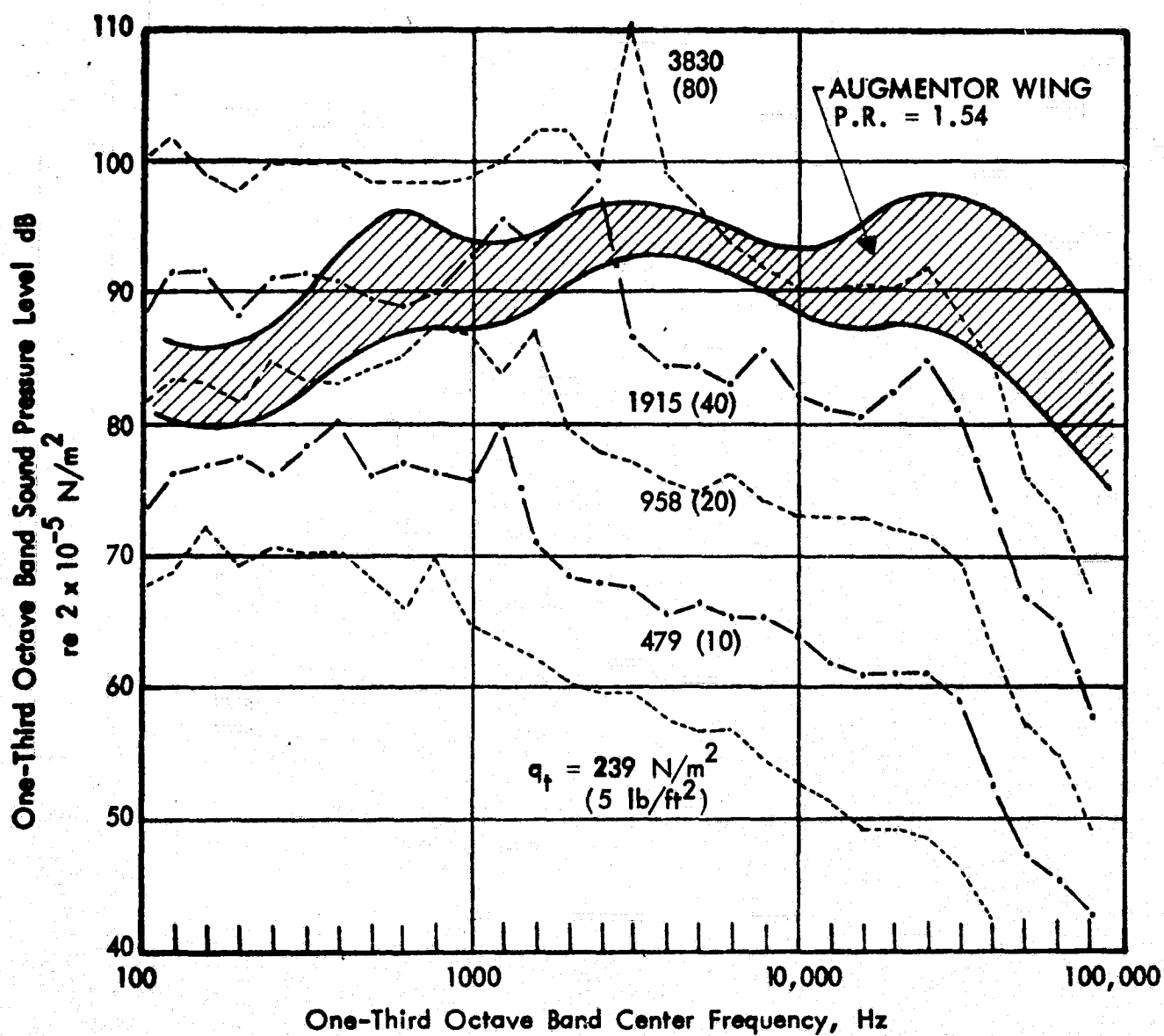
FIGURE 56   COMPARISON OF AUGMENTOR WING AND TUNNEL NOISE
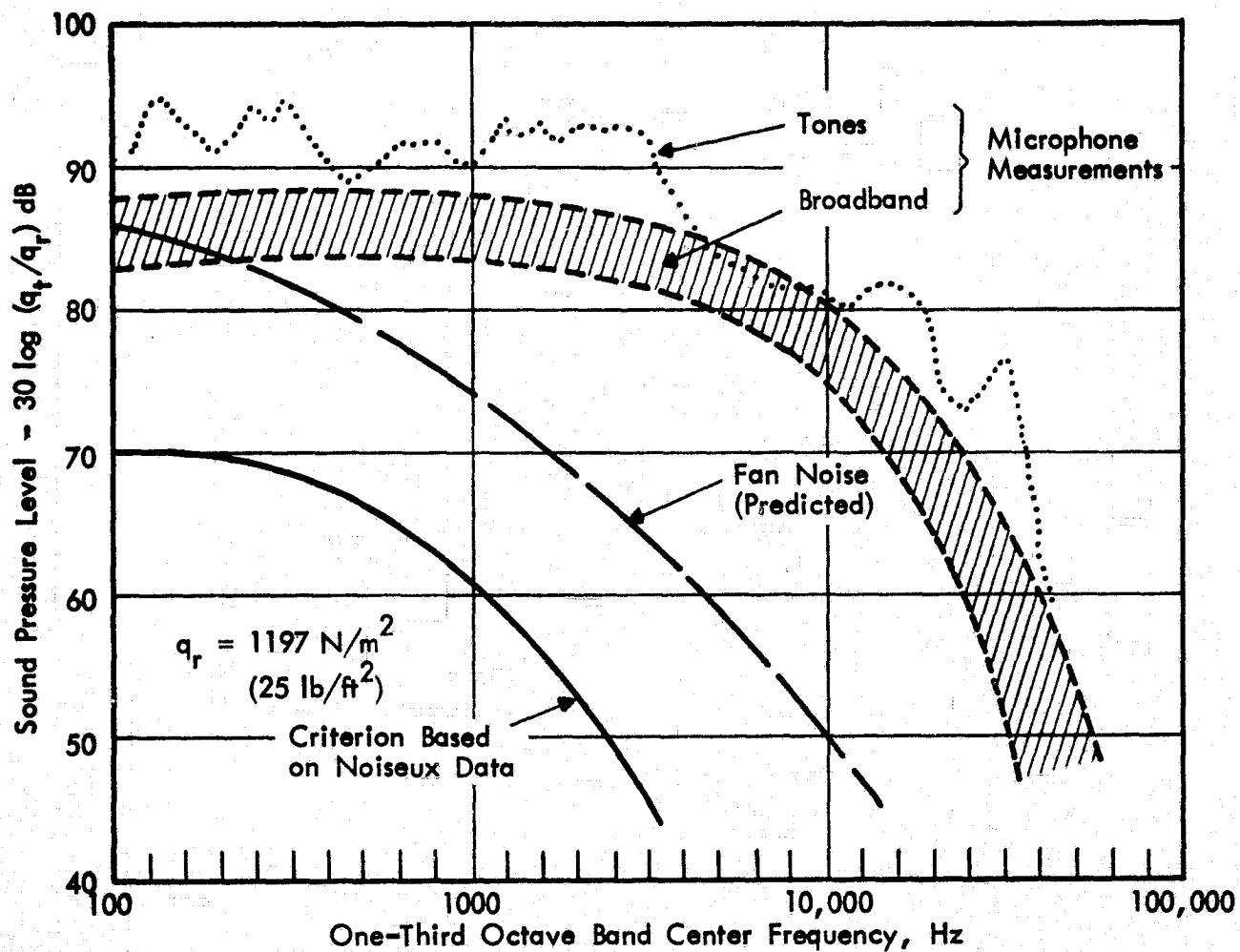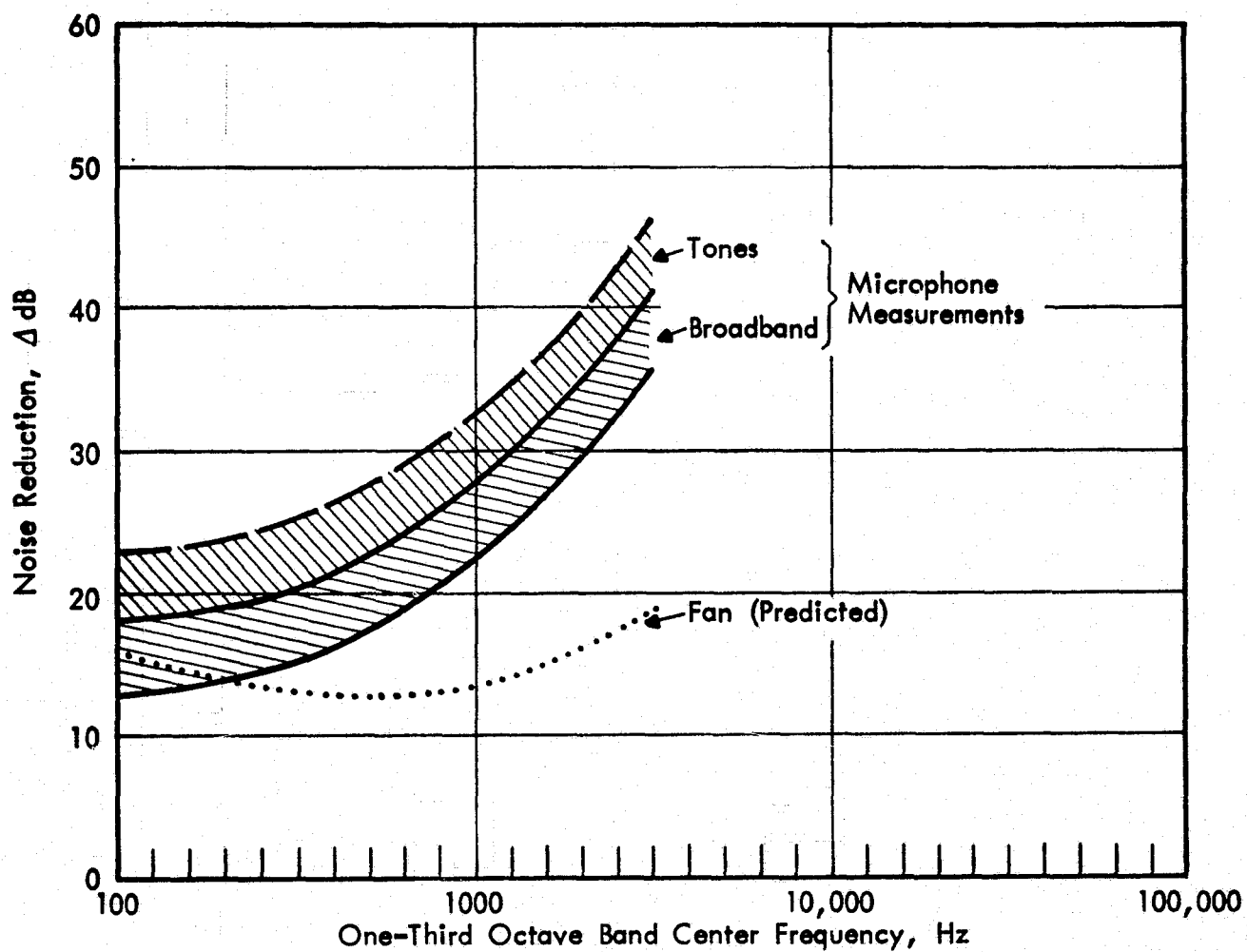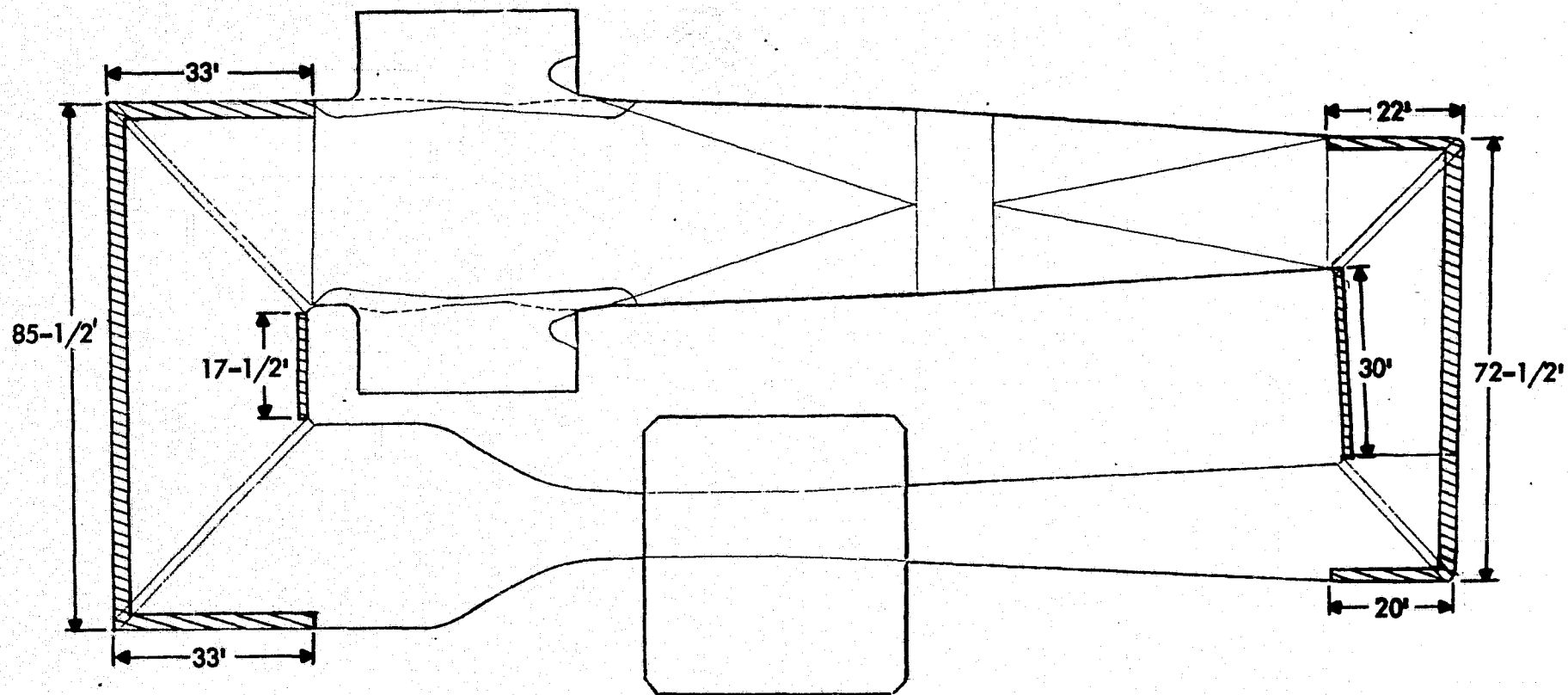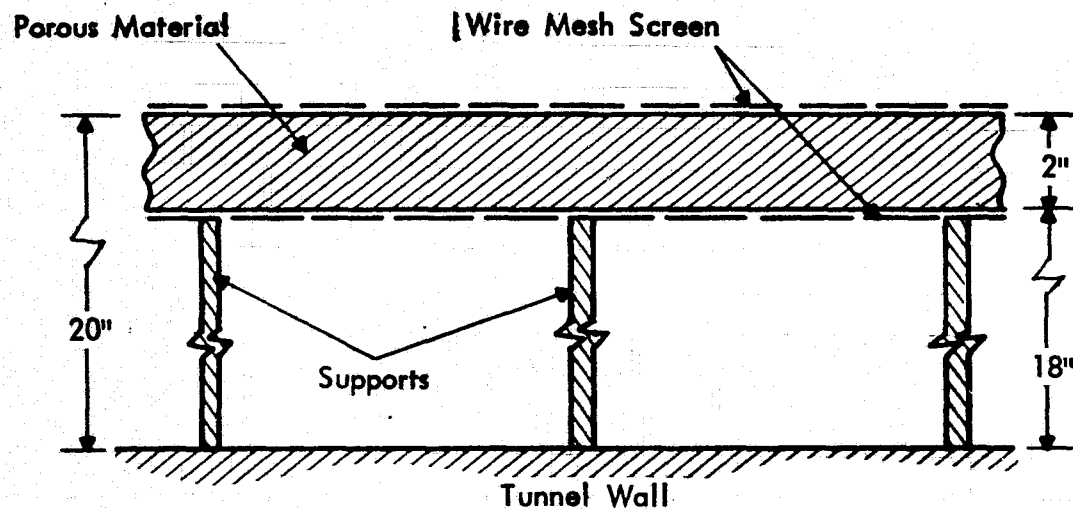
FIGURE 57. NOISE CRITERION FOR TEST SECTION

FIGURE 58. NOISE REDUCTION REQUIRED TO MEET CRITERION

(See Fig 60 for Details of Treatment)

FIGURE 59. ALTERNATIVE A: WALL TREATMENT

Porous Material | Wire Mesh Screen

2"

20"

Supports

18"

Tunnel Wall

The porous material is held between wire mesh
screens with about 50% open area. Spacing
of supports will depend on local air velocity
in tunnel area.

FIGURE 60. DETAILS OF WALL TREATMENT

17-1/2'

45'

Single Splitter

Single Splitter

45'
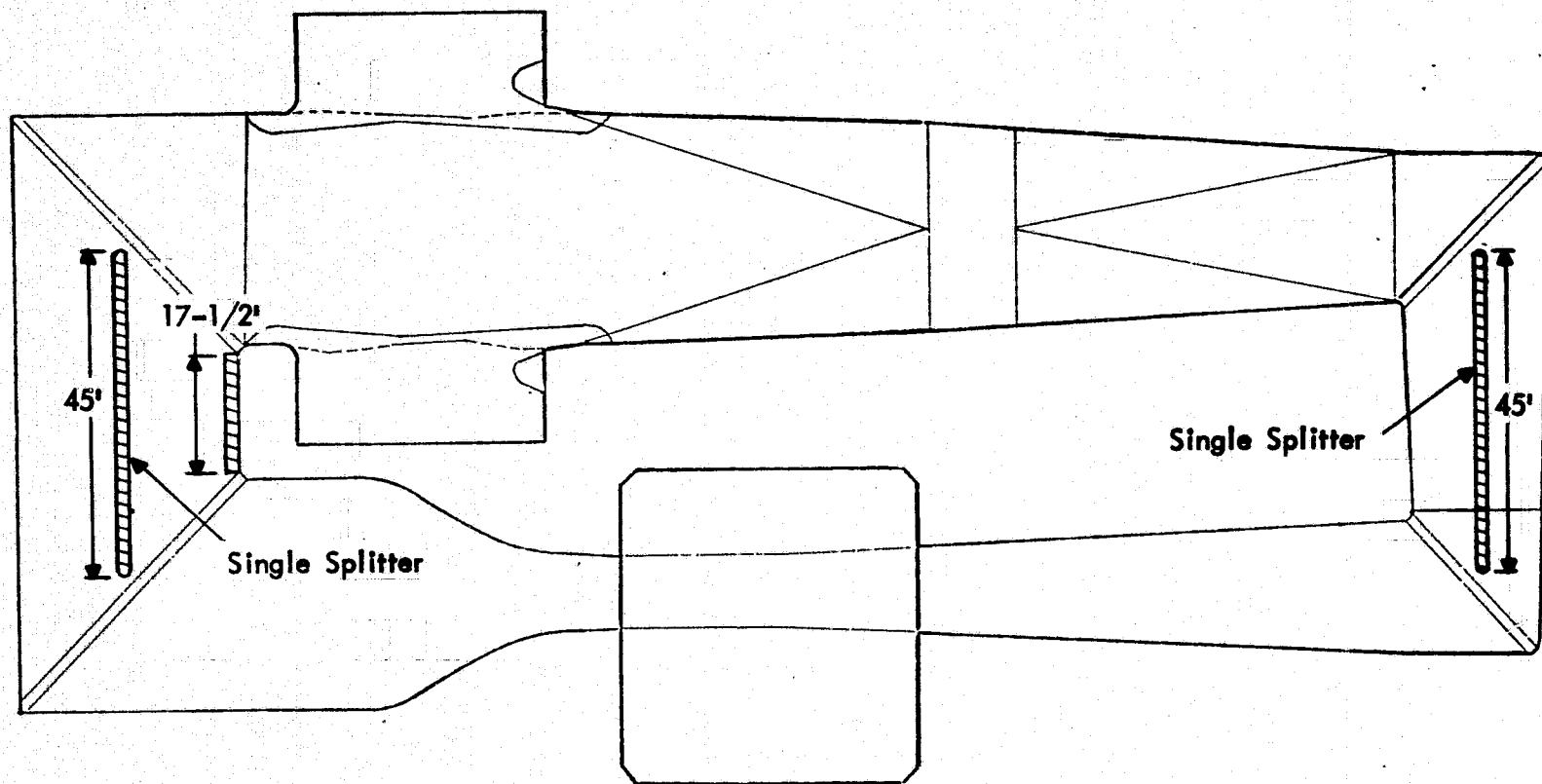
Single Splitter

(See Fig 62 for Details of Splitter)

FIGURE 61.   ALTERNATIVE B: SINGLE SPLITTER
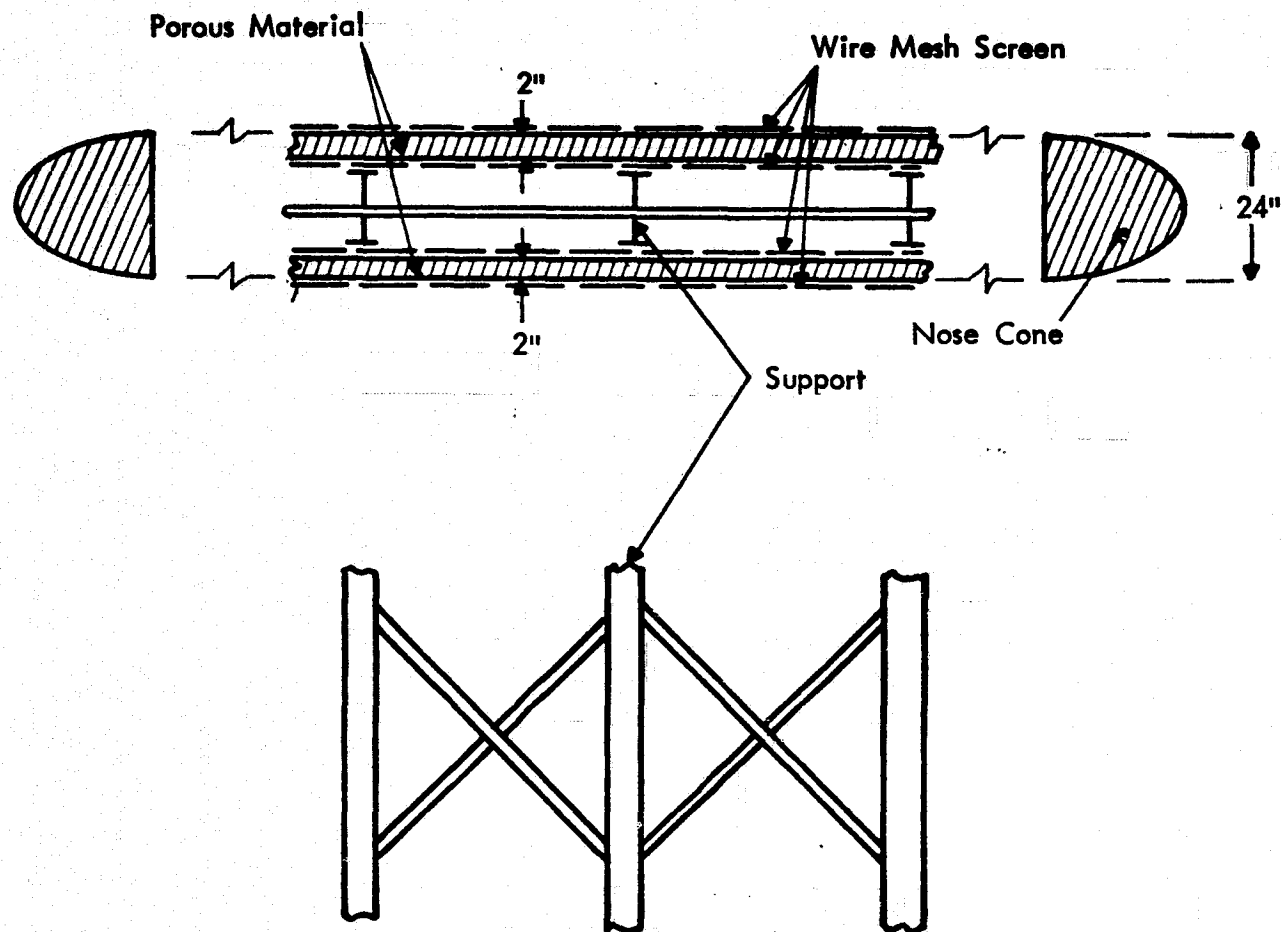
Porous Material

Wire Mesh Screen

2"

24"

2"

Nose Cone

Support

FIGURE 62.   DETAILS OF SPLITTER